Evaluation of the Coxsackievirus and Adenovirus Receptor (CAR) as a therapeutic target in cardiac disease

Dissertation
zur Erlangung des akademischen Grades
doctor rerum naturalium
(Dr. rer. nat.)
im Fach Biologie
eingereicht an der

Mathematisch-Naturwissenschaftliche Fakultät I
der Humboldt-Universität zu Berlin

von
M. Sc. Chen Chen
Geb. am 15.11.1979, Zhejiang, China

Präsident der Humboldt-Universität zu Berlin
Prof. Dr. Dr. h.c. Christoph Markschies

Dekan der Mathematisch-Naturwissenschaftlichen Fakultät I
Prof. Dr. Lutz-Helmut Schön

Gutachter: 1. Prof. Dr. Michael Gotthardt

2. Prof. Dr. Harald Saumweber

3. Prof. Dr. Michael Bader

Datum der Einreichung: 27.03.2009

Datum der Promotion: 09.07.2009

Table of Contents

Zusammenfassung

Der Coxsackievirus- und Adenovirusrezeptor (CAR) ist ein Typ I Transmembranprotein, das an der Adsorption von Viren und der Aufrechterhaltung von Zell-Zellkontakten beteiligt ist. Er wird hauptsächlich im sich entwickelnden Gehirn und Herzen exprimiert, sowie bei Herzkerkrankungen, die zu strukturellen Veränderungen führen. Coxsackievirus B3 (CVB3) Infektionen sind eine häufige Ursache für akute Myokarditis, die bei Patienten häufig zu chronischer Kardiomyopathie mit Fibrose und reduzierter Kontraktilität des Herzens bis zur Herzinsuffizienz führen können. CAR ist für die Aufnahme von Viren in unterschiedliche Zelltypen verantwortlich und damit ein potentielles Ziel bei der Therapie und Prävention von CVB3-Infektionen. Um die Rolle von CAR in der Pathogenese von inflammatorischen Herzerkrankungen zu verstehen, wurde eine konditionelle Knockout-Strategie verwendent. Der resultierende herzspezifisch induzierbare und komplette Knockout des Gens erlaubt die Untersuchung von CAR in der Embryonalentwicklung und im erwachsenen Herzen.

Der komplette Knockout von CAR ist embryonal letal (E11.5). Die betroffenen Embryonen zeigten Missbildungen des Herzens mit verstärker Einlagerung von Apoliproteinen. Dies deutet auf eine Rolle von CAR in der Aufnahme von Lipiden. Weiterhin konnte eine reduzierte Expression von Connexinen im Knockout beobachtet werden – ein mögliches Zeichen gestörter interzellulärer Kommunikation.

Mit Hilfe des MerCreMer Transgens konnten wir Tiere züchten, die nach Induktion mit Tamoxifen eine reduzierte Expression von CAR im Herzen aufwiesen. In diesen Tieren führte die Infektion mit CVB3 im Gegensatz zu CVB3-infizierten Wildtyp Kontrolltieren zu keinen pathologischen Veränderungen wie z.B. Infiltration mit Mononukleären Zellen und Fibrose oder eine Erhöhung von Entzündungsmarkern. Zudem war − anders als in

Kontrolltieren − die kontraktile Funktion des CVB3-infizierten Knockout Herzen erhalten.

Um mögliche unerwünschte Konsequenzen aus dem Verlust von CAR zu untersuchen, wurde eine umfassende kardiale Phänotypisierung durchgeführt, die eine elektrische Reizleitunsstörung (AV-block) im Knockout-Herzen zeigte. Der zugrunde liegende Mechanismus betrifft die Interaktion von Tight- und Gap-Junctions mit veränderter Expression und Lokalisierung von Connexinen, sowie die interzelluläre Kommunikation zwischen CAR-Knockout Kardiomyzeten.

CAR ist essentiell für eine normale Embryonalentwicklung und kardiale Funktion. Das CAR-Knockout-Modell bietet einerseits den ersten genetischen Hinweis für eine Rolle von CAR als Virusrezeptor *in vivo* und belegt andererseits die Relevanz von direkter Virus-vermittelter Symptomatik gegenüber einer sekundären autoimmun- Komponente in CVB3-induzierten Herzerkrankungen. Damit ist CAR ein potentielles therapeutisches Target in der Prävention und Behandlung von viraler Myokarditis.

Schlagwörter:

Knockout, Entwicklung des Herzens, Myokarditis, Virus, Zelladhäsionsmolekül (CAM), Rezeptor, Arrhytmie, Reizleitungssystem

Abstract

The coxsackievirus and adenovirus receptor (CAR) is a type I transmembrane protein involved in virus uptake and the maintenance of cell-cell contacts. It is predominantly expressed in the developing brain and heart, and re-induced upon cardiac remodeling in heart disease.

Coxsackievirus B3 (CVB3) infections are frequent causes of human acute myocarditis, often resulting in chronic cardiomyopathy with fibrosis and reduced contractile function that may progress into terminal heart failure. The coxsackievirus and adenovirus receptor (CAR) is involved in virus uptake into various cell types and has therefore been suggested as a therapeutic target to prevent or treat CVB3 induced diseases such as myocarditis and cardiomyopathy. To understand the role of CAR in the pathogenesis of inflammatory heart disease we used conditional knockout approach. The inducible heart-specific and the complete knockout model enabled us to study CAR's role in embryonic development and in the adult animal heart.

The complete CAR-knockout was embryonic lethal at midgestation (E11.5) with cardiac malformation such as ventricular hypertrophy and atrial dilation. Apolipoproteins were accumulated in the knockout heart, indicating a role for CAR in lipid uptake. Connexin expression was decreased in the knockout, suggesting an abnormal cell-cell communication secondary to the loss of CAR.

Using the MerCreMer transgene we were able to obtain adult animals that can be induced with tamoxifen to progressively lose CAR expression in the heart. The role of CAR in murine viral myocarditis was investigated using the inducible CAR-knockout infected with CVB3. Unlike control animals exposed to CVB3, the cardiac inducible knockout mice did not exhibit structural changes such as monocyte infiltration and fibrosis following CVB3 infection, or increased production of markers of inflammation. While CVB3 infection resulted in severe con-

tractile dysfunction in the hearts of animals that express wildtype CAR, the CAR deficient hearts were essentially normal.

To evaluate possible adverse effects that might result from CAR deficiency, we implemented a detailed cardiac phenotyping protocol and found that CAR deficient animals developed a conduction defect (AV nodal block). The underlying mechanism relates to the crosstalk of tight and gap junctions with altered expression and localization of connexins that affect the communication between CAR knockout cardiomyocytes.

Thus, CAR is essential for embryonic development and normal cardiac function. The CAR-knockout does not only provide the first genetic evidence to establish CAR as the CVB3 receptor *in vivo*, but furthermore demonstrates the relevance of direct virus-mediated pathology versus a secondary autoimmune component in CVB3 induced heart disease. Our data suggest that CAR is a suitable target to help prevent and treat viral myocarditis.

Keywords:

Knockout, cardiac development, myocarditis, viruses, cell adhesion molecules, receptors, arrhythmia, conduction

1 Introduction

The initiation of virus entry is triggered by the attachment of viruses to receptors on the cell surface. Expression of specific receptors can be an important determinant of a cell's susceptibility to infection and of virus tropism for particular tissues. The long sought coxsackievirus and adenovirus receptor (CAR), was first identified as a coxsackievirus B (CVB) receptor and later found to mediate uptake adenoviruses by binding fiber knob proteins (Carson et al., 1997; Tomko et al., 1997; Bergelson et al., 1997). Due to widespread interest in utilizing adenoviruses as vectors for therapeutic gene delivery, considerable attention has been paid to the roles of CAR in virus tropism, and to its structural features important for virus attachment. CAR belongs to a growing subfamily of immunoglobulin-like surface molecules, many of which have been localized to sites of cell-cell contacts and appear to function in cell adhesion or intercellular recognition. CAR mediates homotypic cell-cell interactions and functions as a transmembrane component of the epithelial cell tight junction (Cohen et al., 2001b).

1.1 The Coxsackievirus and Adenovirus Receptor (CAR)

The coxsackievirus and adenovirus receptor (CAR) cDNA was cloned independently by two groups using different techniques (Tomko et al., 1997; Bergelson et al., 1997) and the CAR protein was isolated and partially sequenced by another group concurrently in the year 1997 (Carson et al., 1997). CAR is a highly conserved type I transmembrane protein of the tight junction. The extracellular Ig-domains can mediate homotypic cell adhesion and uptake of adenovirus and coxsackievirus B (CVB). The cytoplasmic tail is alternatively spliced and interacts with various adaptor proteins that link to signal transduction and endocytosis (Cohen et al., 2001b; Chung et al., 2005; Sollerbrant et al., 2003; Coyne et al., 2004).

CAR is ubiquitously expressed, predominantly in the developing brain and heart (Tomko et al., 1997). It has been found that CAR is re-induced upon cardiac remodeling such as in experimental autoimmune myocarditis (Ito et al., 2000), in human dilated cardiomyopathy (Noutsias et al., 2001), and in myocardial infarction (MI) in the rat (Fechner et al., 2003).

CAR deficiency results in mid-embryonic lethality with pericardial edema. The underlying molecular changes relate to CAR's role in cell-cell contact formation with altered organization of the myofibrils as well as increased proliferation of cardiomyocytes (Dorner et al., 2005; Chen et al., 2006). The weak expression of CAR on cardiomyocytes of the adult and healthy heart in contrast to the strong expression of CAR in cardiomyocytes of the developing and diseased heart may suggest a role of CAR during the formation of a functional myocardium and cardiac remodeling.

1.1.1 CAR gene and splice isoforms

The gene encoding human CAR is located on chromosome 21q11.2 and composed of seven exons and the transcription unit is around 57kb (Bowles et al., 1999). The murine CAR gene is located on mouse chromosome 16 (human chromosome 21) and at least eight exons have been identified (Chen et al., 2003). The mouse transcript contains an additional splice site 27kb downstream of exon 7. The transcription initiation site and the promoter elements have been mapped at approximately 150bp before the ATG translation start site. A number of mRNAs corresponding to alternative splice variants have been characterized and the longer form is predominant (Bergelson et al., 1998; Dorner et al., 2004; Thoelen et al., 2001b). Several of these would encode transmembrane proteins with an intact extracellular domain, but with modifications of the cytoplasmic domain. RNA encoding CAR2 has been found in a number of tissues (Fechner et al., 2003; Bergelson et al., 1998), but expression of CAR3 appears to be restricted to the murine heart. In addition, at least three other transcripts have also been identified, all lacking the transmem-

brane domain. Two longer forms, called CAR4/7 and CAR3/7) contain an intact D1 domain. A soluble form of CAR (CAR2/7) has been detected in human pleural fluid and in mouse serum, and has been shown to interfere with adenoviurs-mediated gene delivery (Bernal et al., 2002) and coxsackievirus infection (Dorner et al., 2004), and CAR expressing vesicles are shed into the medium of cultured cells (Carson, 2004). It is not clear which of them are produced *in vivo*, and their individual functions are poorly understood. It is not known whether this soluble CAR results from alternative splicing or from proteolysis.

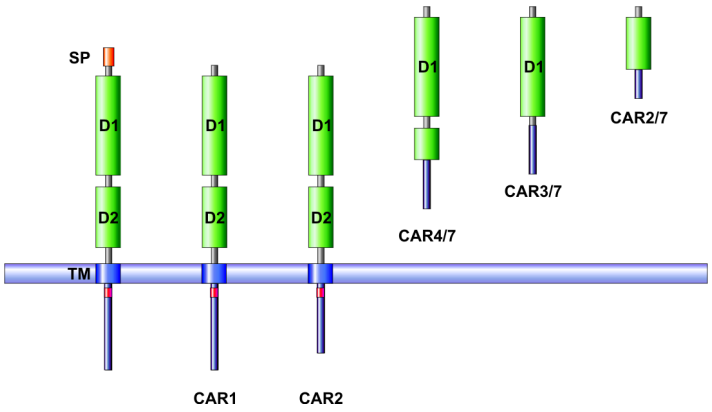

Figure 1: CAR structure and splicing variants. CAR1 and CAR2 contain a cytoplasmic domain. CAR4/7 and CAR3/7 contain only the D1 domain, CAR 2/7 has an incomplete D1 domain. SP: signal peptide, TM: transmembrane domain, D1: Ig-like domain 1, D2: Ig-like domain 2.

1.1.2 CAR protein domain structure and function

CAR cDNA encodes a 365 amino acid protein; cleavage of a 19-residue signal peptide results in a mature protein of 346 amino acids. CAR contains a single 23 amino acids membrane-spanning domain that separates an extracellular domain of 216 residues from a 107 or 94 residue intercellular domain dependent on alternative splicing (Fig. 1). Those two splice isoforms are referred to as mCAR1 and mCAR2 for the mouse and hCAR1 and hCAR2 for the human. The extracellular domain is composed of two immunoglobulin (Ig)-like domains D1 and D2. Both CVB and Adenovirus bind to the N-terminal D1

domain, but the two viruses recognize different specific sites within D1 (Fig. 2) (He et al., 2001; Bewley et al., 1999). Two membrane-proximal cytoplasmic cysteines are subject to fatty acid acylation (van't Hof and Crystal, 2002). The cytoplasmic part also contains potential sites for phosphorylation and furin cleavage, and an extreme C-terminal hydrophobic peptide motif that interacts with PDZ-domain proteins (Xie et al., 2001). The predicted molecular weight of CAR is approximately 38kDa, but it migrates at 46kDa on SDS polyacrylamide gels, due to two N-linked glycans (Asn 106 and Asn 201).

The predicted CAR structural model is supported and confirmed in biochemical and structural studies. The crystal structure of CAR D1 shows a β-sandwich fold characteristic of Ig variable domains (Bewley et al., 1999; van Raaij et al., 2000; Jiang et al., 2004). The structural analysis of CAR D1 supports the proposed function which CAR mediates homotypic cell adhesion (Cohen et al., 2001b; Honda et al., 2000; Okegawa et al., 2001). It is speculated that D1 homodimerization explains CAR's adhesive function. Within the crystal, D1 forms a homodimer; residues involved in dimerization are highly conserved in evolution, suggesting that the potential to dimerize is conserved and may be functionally important. D1 homodimers also form in solution; the measured dissociation constant of 16 μM (van Raaij et al., 2000) is consistent with those measured for other cell adhesion molecules (Atkins et al., 1999; van der Merwe and Barclay, 1994; van der Merwe et al., 1994). Furthermore, the dimerization is pH sensitive and ion pairing plays an important role in CAR D1 homodimer stabilization. However, there is no direct evidence that the dimers observed in the crystal are identical to those seen in solution, and it is not clear whether D1 dimerization is the mechanism of cell adhesion, or whether it represents an interaction that occurs between molecules side-by-side on a single cell surface. The crystal structures of murine (Kostrewa et al., 2001) and human junctional adhesion molecule (JAM) (Prota et al., 2003), another tight junction protein, reveal a D1 dimer interface similar to that observed for CAR. However, it is not clear whether the JAM homodimer is

formed by pairs of molecules on the surface of a single cell, or whether it occurs between JAM molecules engaged across the intercellular junction.

CAR D2 does not exhibit a high degree of sequence identity to other immunoglobulin domains, although it is also a member of the Ig superfamily. CAR D2 is shown to be a β-sandwich motif comprised of two β-sheets, which are stabilized by two disulfide bonds by NMR spectroscopy. A lone helix encompassing residues 185-192 (referred as helix D) is found in the position of β-strand D of the c-type immunoglobulin fold. The surface of helix D is relatively hydrophobic, and offers a potential interaction site for the cellular partners of CAR (Jiang and Caffrey, 2007).

Adenovirus interaction with CAR is mediated by fiber knob, an elongated fiber protein projecting from the virus capsid (Fig. 2C). adenovirus fiber binds to CAR with high affinity (1nM) (Wickham et al., 1993) at a site similar to that involved in dimerization (Bewley et al., 1999; van Raaij et al., 2000); fiber interaction with CAR might thus disrupt the low-affinity D1-D1 association. In fact, adenovirus fiber has been shown to dissociate CAR-mediated epithelial cell junctions (Walters et al., 2002), although the mechanism is not certain. The adenovirus fiber knob is a trimer, with globular knob domains arranged in a trefoil at its tip. The crystal structure of CAR D1 in association with the fiber knob reveals that three D1 domains bind to the outside of the knob (Bewley et al., 1999). In contrast, CVB attachment to CAR involves insertion of the D1 domain into a canyon on the virus surface, formed by VP1, VP2 and VP3 (He et al., 2001). VP1 dominates the interaction with CAR D1. Thus whereas the D1 residues involved in Adenovirus interaction are clustered on one face of the domain, residues in contact with coxsackievirus are more widely distributed. The residues critical for CAR D1 homodimerization and for interactions with Adenovirus and CVB3 are shown in figure 2. The surfaces of CAR D1 bind to CVB3, fiber knob, and CAR D1 itself are partially overlapped, possibly accounting for the competition of Adenovirus and CVB3 for identical binding sites on the plasma mem-

brane. Full-length CAR protein has higher affinity and stability than CAR D1 or CAR D1+D2 extracellular fragments, regarding to the binding to CVB3 (He et al., 2001). The cryoEM reconstruction of full-length CAR-CVB3 complexes shows that adjacent CAR molecules, which related by icosahedral two-fold axes, share common density in the external transmembrane and cytoplasmic regions. This bivalent association of the adjacent receptors might stabilize the complex with CVB3 or increase the possibility of forming saturated complexes.

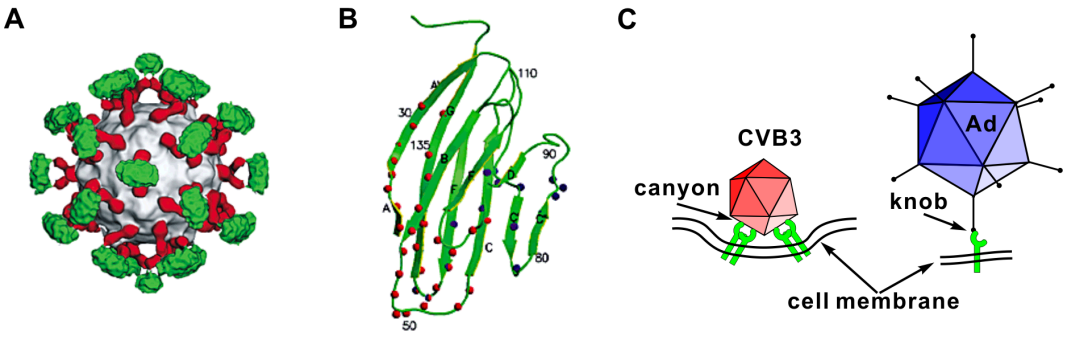

Figure 2: A) Stereo view of full length CAR bound to CVB3. The virus is represented as a grayscale surface. Domains D1 and D2 of CAR are colored red, and the transmembrane and cytoplasmic regions are green. B) Stereo diagrams of the CAR D1 domain. The β-strands are labeled A–G. The amino acids identified as being in the virus–receptor interface are indicated by spheres. CAR with adenovirus knob in blue and CAR with CVB3 in red. C) Schematic diagram of the modes by which CAR (green) binds to CVB3 (red) and adenovirus19 (blue). The suggested membrane curvature is speculative. CVB3: coxsackievirus B3, Ad: adenovirus. Figure adapted from (He et al., 2001).

The cytoplasmic tail of CAR seems to be unnecessary for either CVB or adenovirus infection (Wang and Bergelson, 1999), but it may be important for functions in cell signaling, growth and correct subcellular localization. Apparently, the CAR cytoplasmic domain has a role in tumor cell growth, but the nature of the effect varies among reports using different cell types (Okegawa et al., 2001; Bruning et al., 2005). Binding of Adenovirus fiber knob to CAR on respiratory cells stimulates production of inflammatory products (Tamanini et al., 2006). Since inflammation is a key component of CVB-associated pathology, CAR-mediated signaling may prove to be very important in CVB-associated

diseases. In addition to signaling, the cytoplasmic domain also influences CAR distribution within the cell (Cohen et al., 2001a; van't Hof and Crystal, 2002), and the carboxyl-terminal PDZ-binding motif(s) association with PDZ-domain proteins has been established. The absence of the intercellular tail results in the loss of targeting of CAR to tight junctions *in vivo* (Raschperger et al., 2006).

The glycosylation of CAR does not alter cell surface levels or junctional localization, it affects both adhesion and adenovirus infection in unique ways. CAR-mediated adhesion appears to require at least one site of glycosylation. Glycosylation of the D2 domain is required for adenovirus cooperative binding, it has a negative consequence upon infection (Excoffon et al., 2007).

1.1.3 Evolutionary conservation

CAR has been identified in a variety of mammalian species (Noutsias et al., 2001; Tomko et al., 1997; Bergelson et al., 1998; Thoelen et al., 2001a), as well as in non-mammalian vertebrates such as fish and frog (Petrella et al., 2002), but no obvious CAR homologues could be found in Drosophila or nematodes. The overall homology between human, mouse, rat, dog, and pig CAR is about 90%. The D1 domain is more conserved (over 90%) than the D2 domain, whereas the cytoplasmic tail is about 95% identical among these species. The transmembrane domain is less conserved and 77% identical between human and mouse. Zebrafish and human CAR are 44% identical over all. More extensive conservation within the cytoplasmic domain (66% identity) may suggest that this portion of the molecule participates in intercellular interactions that are also conserved.

CAR belongs to a subfamily of proteins of which the original member is CTX, a putative receptor expressed on the surface of frog thymocytes (Chretien et al., 1996; Chretien et al., 1998). Proteins of the CTX family consist of two homolog extracellular Ig-loops of the V and C2 type (D1 and D2 domain), with an extra disulfide link in the C2-type do-

main, a transmembrane region, and a cytoplasmic tail of variable length. A subfamily of the CTX proteins also shows sequence conservation within the cytoplasmic domain. In particular, a 21-residue C-terminal peptide is extensively conserved. It is suspected that this peptide motif is responsible for interaction with some unidentified intracellular ligands (Coyne and Bergelson, 2005).

Many of the CTX family members have been found to promote cell adhesion, and a number of family members have been localized to tight junctions. The best characterized among them is JAM. Four JAM isoforms mediate cell adhesion and localize to the tight junction, and JAM specific antibodies inhibit tight junction formation (Hirabayashi et al., 2003; Cunningham et al., 2000; Aurrand-Lions et al., 2001; Liu et al., 2000). ESAM, an endothelial cell specific adhesion molecule, is expressed at endothelial cell junctions and appears to function in the vascular proliferation required for tumor growth (Hirata et al., 2001; Ishida et al., 2003). The CAR like membrane protein CLMP, promotes homotypic cell adhesion and is expressed at the epithelial tight junction like JAM and CAR (Raschperger et al., 2004). Other CTX family members include A33, an antigen expressed in colon carcinomas (Welt et al., 2003), a brain and testis specific Ig family member BT-IgS (Suzu et al., 2002), and a less well characterized Ig superfamily member 11 (IgSF11) expressed on intestinal cancer cells (Katoh and Katoh, 2003). Of these proteins, only CAR and JAM-A, a receptor for reovirus, have so far been identified as virus receptors.

1.1.4 CAR expression

1.1.4.1 CAR expression pattern in various tissues

CAR is abundantly expressed in the mouse embryo with a preference for the nervous system, including all neuroepithelial cells, in ganglions, and peripheral nerves (Tomko et al., 2000). The developing brain expresses increased CAR compared to the adult brain, and

the highest mRNA level is detected near birth and diminishing thereafter, though the timing of peak expression varied between regions of the brain (Honda et al., 2000).

Detailed analysis of CAR protein expression has been facilitated by CAR specific antibodies used in immunohistochemistry. A systematic survey of mouse tissues has been reported (Raschperger et al., 2006). CAR can be detected in epithelial cells of embryonic liver, lung, heart, eye, pancreas, kidney, and the submandibular glands. In digestive and respiratory system, CAR specifically co-localizes with the tight junction protein ZO-1 and occludin. CAR has also been detected in trachea and bronchi but is absent from alveoli of adult animals. CAR is not detectable in connective tissue, smooth muscle cells, or endothelial cells of the vasculature, including brain capillaries. In the adult rat, CAR protein is reportedly expressed primarily on epithelial derived cells in the liver, intestines, and lung (Tomko et al., 2000).

In cultures of polarized epithelial cells, CAR is preferentially expressed at the basolateral side of the tight junctions, where it may be sequestered and inaccessible to virus, especially from the apical side (Cohen et al., 2001b; Walters et al., 2001). Although CAR may function as a homophilic cell adhesion molecule, it should be noted that CAR also has been detected on membrane regions other than tight junctions, for example on the luminal (apical) surface of the prostate epithelium (Bao et al., 2005; Rauen et al., 2002). In addition, CAR is detected in other cells of epithelial origin, such as renal podocytes and liver hepatocytes. The expression of CAR mRNA is prominent in the liver (Raschperger et al., 2006). These alternate cellular locations for CAR, its apparent capacity to form heterophilic associations (e.g., with JAML), and its potential role in cell signaling indicate that CAR can serve other functions in addition to homophilic cell adhesion.

Although CAR is not detected in endothelial or mesenchymal cells in the adult mouse (Raschperger et al., 2006), it has been detected in cultured human umbilical vein endo-

thelial cells, where expression is related to cell density and could be downregulated by treatment with cytokines (Carson et al., 1999; Vincent et al., 2004). CAR is detected in CD31+ cells in damaged areas of the heart, but not in the endothelium of vessels in undamaged tissue (Fechner et al., 2003), suggesting that endothelial CAR expression *in vivo* may be restricted to regions of vessel growth or tissue repair.

In numerous studies of adenovirus mediated gene delivery, CAR expression has been identified as important for adenovirus tropism, and expression of CAR in refractory cell lines has enhanced their susceptibility to virus entry (Ross et al., 2003; Kim et al., 2002; Miller et al., 1998; Qin et al., 2003; Hemmi et al., 1998; Pearson et al., 1999). Nonetheless, it is not clear that the marked adenovirus tropism for mouse liver observed in gene therapy experiments reflects CAR expression or other factors, as modified adenovirus vectors unable to bind CAR still infect the liver (Mizuguchi et al., 2002).

Adult human CAR RNA levels are highest in the heart, brain, and pancreas, with significant levels in the liver, testis and prostate (Tomko et al., 1997; Bergelson et al., 1998). This RNA expression pattern is consistent with the tropism of coxsackievirus B3, which infects via the GI tract, and causes myocarditis, cardiomyopathy, meningoencephalitis, and pancreatitis. CAR-binding adenoviruses primarily infect the respiratory tract, although these adenoviruses are also a major cause of cardiac inflammation like CVB (Bowles et al., 2003).

Very little CAR is detected on healthy adult skeletal muscle and on lymphocytes (Tomko et al., 1997; Bergelson et al., 1998; Fechner et al., 1999). The paucity of CAR expression appears to be an important limitation for adenovirus-mediated transduction: lymphocyte- and skeletal myocyte-specific CAR expression in transgenic mice notably increases the susceptibility of normally resistant tissues. In addition, transgenic mice with ubiquitous CAR expression show increased susceptibility to Adenovirus transduction in several tis-

sues (Wan et al., 2000; Tallone et al., 2001; Nalbantoglu et al., 2001; Hurez et al., 2002; Schmidt et al., 2000).

1.1.4.2 CAR expression in embryonic development

The heart is the first organ to form during embryonic development in vertebrates. It arises through a complex series of morphogenetic interactions involving cells from several embryonic origins (Olson and Srivastava, 1996; MacLellan and Schneider, 2000). The early heart developmental process includes formation of the primitive cardiac tube, looping of the cardiac tube to the right, and chamber specification and formation. Then, during maturation of the fetal heart, cardiomyocytes exhibit two related but distinct modes of growth that are highly regulated. The ventricular mass of the fetal heart is augmented by cardiomyocyte proliferation, also termed hyperplasia, which decreases progressively in late gestation and ceases soon after birth. Increases in cardiac mass postnatally are achieved preponderantly through increased cell volume, termed hypertrophy, and not by cell proliferation, since the cardiomyocytes have permanently exited the cell cycle. These complicated cardiac morphogenetic events must be coordinated by many fine-tuned, as yet unidentified factors. Changes in these homeostatic factors may contribute to developmental anomalies of the heart.

CAR expression levels change dramatically during development. A rapid downregulation of CAR occurs at birth, after which CAR is only sparsely detected in most of these tissues. In the mouse embryo, CAR expression is prominent in the brain, but expression levels drop significantly within the first month of life (Honda et al., 2000; Hotta et al., 2003; Xu and Crowell, 1996). High levels of CAR expression in the new born brain may account for the unique susceptibility of new born, but not adult, mice to encephalitis caused by CVB (Feuer et al., 2003). In the nervous system of the adult mouse, expression appears restricted to cells close to the ependymal region lining the ventricular system,

which is consistent with adenovirus infection from the lateral ventricles (Tomko et al., 2000).

CAR expression in the heart is of particular interest because adenoviruses and coxsackieviruses are the most important causes of viral myocarditis. A variety of evidence suggests that CAR expression is regulated during cardiac development. In the rat, CAR is highly expressed on fetal and newborn but not adult myocardium (Ito et al., 2000), and CAR mRNA levels, which are high in the fetus and newborn, are seen to drop significantly in the adult (Fechner et al., 2003; Kashimura et al., 2004). It is not certain whether all CAR isoforms are regulated in parallel. In the mouse, it is noted that high levels of CAR protein in the embryonic heart, with expression dropping after birth. With a limited number of human autopsy specimens, Bergerson's lab has detected CAR expression in the hearts of human foetuses, but not in hearts of young children or adults, and little or no CAR is seen in most human myocardial biopsy specimens (Coyne and Bergelson, 2005). In immature myocardium, CAR appears diffusedly expressed on the cell surface, but on mature myocardium, CAR is localized to the intercalated discs that connect myocardial cells end-to-end (Petrella et al., 2002; Kashimura et al., 2004). Expression on fetal and regenerating myocytes may account for the susceptibility of these cells, but not adult skeletal muscle, to adenovirus mediated transduction (Nalbantoglu et al., 1999).

The expression in epithelial cells in kidney, intestine, and liver is not downregulated after birth, but the staining in pancreas and the submandibular glands has partially disappeared (Raschperger et al., 2006).

1.1.4.3 CAR expression in disease

1.1.4.3.1 Cardiac disease and altered CAR expression

CAR expression on cultured rat cardiomyocytes is upregulated after exposure to cytokines, and increased expression is seen in the hearts of adult animals suffering from au-

toimmune myocarditis, suggesting that CAR expression is modulated in response to inflammation (Ito et al., 2000). In a rat model of myocardial infarction, CAR protein expression is increased on damaged myocardium during the recovery phase, suggesting a possible role for CAR in tissue remodeling (Fechner et al., 2003).

In humans, CAR expression is increased in patients with dilated cardiomyopathy, and illness of uncertain etiology that sometimes follows viral myocarditis (Noutsias et al., 2001), but CAR gene mutations are not a major host determinant in the development of myocarditis and DCM (Bowles et al., 2002). It is conceivable that some patients are more susceptible to viral infections of the heart because they constitutively express high levels of myocardial CAR; however, no abnormalities within the CAR gene have so far been identified in patients with myocarditis or cardiomyopathy (Bowles et al., 2002). It is also possible that, as in the rat infarction model, CAR expression is induced as part of a remodeling program.

1.1.4.3.2 CAR expression is differed in various cancers

A number of investigators have been interested in using adenovirus vectors in therapeutic approaches to cancer. As a result, many tumor samples have been examined for CAR expression, which has generally been found to correlate with susceptibility to transduction (Okegawa et al., 2001; Pearson et al., 1999; Kawashima et al., 2003; Kim et al., 2003; Qin et al., 2003; Sachs et al., 2002; Gu et al., 2004; Wang et al., 2006; Korn et al., 2006; Abdolazimi et al., 2007; Okegawa et al., 2000). CAR mRNA was expressed at high levels in osteosarcoma, Ewing's sarcoma, neurofibroma, schwannoma, squamous cell carcinoma lung cancers, small cell lung cancers; at intermediate levels in exostosis, giant cell tumor, liposarcoma, synovial sarcoma, malignant peripheral nerve sheath tumor, and hemangioma; at low levels in alveolar soft part sarcoma and desmoids; and inconsistent in adenocarcinoma lung cancers (Kawashima et al., 2003; Gu et al., 2004; Wang et al., 2006).

Of greater interest are reports that in several human cancers, including bladder and prostate carcinoma, and glioblastoma-multiform, CAR expression is down regulated during the progression to malignancy (Okegawa et al., 2001; Kim et al., 2003; Sachs et al., 2002; Fuxe et al., 2003). In CAR deficient prostate tumor lines, expression of transfected CAR results in inhibition of cell proliferation and decreased tumorogenicity in animals (Kim et al., 2003; Okegawa et al., 2000). Similar results have been reported for malignant glioma cells (Kim et al., 2003). In bladder cancer cells, CAR expression inhibits proliferation, and is related to modulations in the activity of the cell cycle regulators p21-CIP and Rb. CAR dependent growth inhibition requires the presence of the CAR cytoplasmic domain, and is inhibited by a CAR specific antibody that blocks homotypic adhesion. One interpretation of these results is that CAR dependent intercellular recognition results in transmission of a signal that regulates Rb and CIP and results in growth inhibition. In GI malignancies (esophageal, pancreatic, colorectal and liver cancer), loss of CAR expression at cell-cell junction was evident in many tumor samples. A significant correlation between CAR expression and histological grade was found, with moderately to poorly differentiated tumors most frequently demonstrating loss or reduction of CAR expression (Korn et al., 2006).

Given CAR's importance for adenovirus targeting, and its possible function as a tumor suppressor in some tumor types, there has been interest in identifying pharmacological agents that will upregulate CAR expression. In a variety of carcinoma cell lines, CAR expression is increased by inhibitors of MEK activity, and decreased by Raf activation, suggesting that CAR downregulation is controlled through the Raf-MEK-ERK signaling pathway (Anders et al., 2003). The activation of the CAR gene promoter is modulated by histone acetylation, but not by DNA methylation, in urogenital cancer cells (Pong et al., 2003). The histone deacetylase inhibitor FR901228 also enhances CAR expression, and increases transduction efficiency in a variety of carcinoma cell lines (Goldsmith et al.,

2003; Kitazono et al., 2001). In a recent study, proteasome inhibitor MG-132 can enhance CAR expression in the colon carcinoma cell line lovo (Zhang et al., 2008). In addition, CAR expression is increased in cells treated with the chemotherapeutic agents *cis*-platinum and etoposide (Hemminki et al., 2003).

1.1.5 CAR knockout models

Various CAR deficient animal models have been generated to gain additional insight into its physiological functions.

A zebrafish model was generated by injection of morpholino antisense oligonucleotides. A requirement for CAR in the terminal differentiation of glomerular podocytes and pronephric tubular epithelia was identified. Podocytes differentiate in CAR morphants but are not able to elaborate a regularly patterned architecture of foot processes. In the tubules, CAR was required for the apposition of plasma membranes from adjacent epithelial cells but did not appear to be necessary for the formation of tight junctions. Additionally, tubular epithelia lacking CAR were not able to elaborate apical brush border microvilli. These results establish a requirement for CAR in the terminal differentiation of renal glomerular and tubular cell types (Raschperger et al., 2008).

The first CAR murine KO model was established by targeting exon 2 and documented that CAR deficiency resulted in embryonic lethality associated with cardiac defects. Specifically, commencing E10.5, $CAR^{-/-}$ cardiomyocytes exhibited regional apoptosis documented by both histopathologic features of cell death and positive staining for the apoptotic marker cleaved caspase 3. $CAR^{-/-}$ fetuses invariably suffered from degeneration of the myocardial wall and thoracic hemorrhaging, leading to death by E11.5 (Asher et al., 2005b).

In a similar CAR deficient mouse model targeting exon 1, embryonic lethality occurred at E11.5 and E13.5 of embryonic development with disorientation and reduced density of myofibrils. In addition, mitochondria were enlarged and glycogen storage strongly enriched. In line with these defects, pericardial edema as a clear sign of insufficient cardiac function was observed. Developmental abnormalities likely to be secondary effects of gene ablation were the persistent singular cardial atrio-ventricular canal and dilatation of larger blood vessels such as the cardinal veins. The secondary nature of these defects was supported by the fact that CAR was not expressed on cells of the vascular wall. No obvious signs for alterations of the histological organization of the placenta were observed. Thus, CAR is required for embryonic heart development, most likely due to its function during the organization of myofibrils in cardiomyocytes (Dorner et al., 2005).

Chen et al. used conditional gene targeting strategies, generated mice with both germline and tissue-specific defects in CAR expression. Homozygous germline deletion of CAR exon 2 or cardiomyocyte-specific gene deletion at E10 mediated by Cre recombinase expressed under the control of the cardiac troponin T promoter resulted in death by E12.5. Embryos showed marked cardiac abnormalities by E10.5, with hyperplasia of the left ventricular myocardium, distention of the cardinal veins, and abnormalities of sinuatrial valves. Within the hyperplastic left ventricle, increased numbers of proliferating cells were evident; proliferating cardiomyocytes had failed to differentiate and form normal trabeculae. The intercellular junctions of CAR-deficient cardiomyocytes were ill formed or absent; myofibrils were also poorly organized. When cardiomyocyte-specific deletion occurred by E11, mediated by Cre under control of the α-myosin heavy chain promoter, animals survived to adulthood and did not have evident cardiac abnormalities. These results indicate that during a specific temporal window, CAR expression on cardiomyocytes is essential for normal cardiac development (Chen et al., 2006).

Cardiac specific CAR deletion early in embryonic life leads to severe cardiac abnormalities and death in utero. Two independent knockouts targeting either exon 1 or 2 demonstrated atrioventricular (AV) conduction block developed in the absence of CAR in the adult mouse heart separately (Lim et al., 2008; Lisewski et al., 2008). Lim et al. showed the prolongation of AV conduction occurred in the embryonic heart of the global CAR KO mouse. In the cardiac-specific CAR KO (CAR-cKO) mouse, the loss of connexin 45 localization to the cell-cell junctions of the AV node but preservation of connexins 40 and 43 in contracting myocardial cells and connexin 30.2 in the AV node was observed. There was a marked decrease in β-catenin and zonula occludens-1 (ZO-1) localization to the intercalated discs of CAR-cKO mouse hearts at 8 weeks before the mice developed cardiomyopathy at 21 weeks of age. CAR formed a complex with connexin 45 via its PSD-95/DigA/ZO-1–binding (PDZ-binding) motifs. They concluded that CAR expression is required for normal AV-node conduction and cardiac function. Furthermore, localization of connexin 45 at the AV-node cell-cell junction and of β-catenin and ZO-1 at the ventricular intercalated disc are dependent on CAR (Lim et al., 2008).

1.2 CAR is a tight junction protein

Tight junctions between epithelial cells regulate the selective diffusion of ions, solutes and macromolecules across the intact epithelium and serve to divide the apical and basolateral membrane compartments, such as restrict apical/basolateral intermembrane diffusion of lipids. A variety of researches provide evidences that CAR is a component of the tight junction (Cohen et al., 2001b). In polarized epithelial cell lines, and in primary human airway epithelial cells, CAR can be seen both by confocal microscopy and thin section electron microscopy, at the apical pole of the lateral membrane, where it co-localizes with the cytoplasmic plaque tight junction protein zonula occludens-1 (ZO-1), a PDZ-domain protein, although the direct complex formation has not been established. CAR expression in transfected cells inhibits transepithelial passage of both ions and large mo-

lecules, and both soluble CAR (Cohen et al., 2001b) and anti-CAR antibodies (Walters et al., 2002) disrupt tight junction formation. In addition, CAR precipitates with ZO-1 (Cohen et al., 2001b) and other tight junction proteins from lysates of polarized epithelial cells. In non-polarized cells, CAR is also localized to sites of intercellular contact, but not to tight junctions per se: for example, CAR is present in the intercalated discs of cardiomyocytes (Noutsias et al., 2001) and, under some conditions, it may be present in the adherens junctions of epithelial cells (Walters et al., 2002).

The central structure in the tight junctions is a series of intramembranous strands that are believed to provide the occlusive contacts that regulate paracellular ion and solute flow (Staehelin, 1973; Sasaki et al., 2003). Freeze fracture splites the leaflets of the cell membrane, allowing an enface view of tight junction strands. Although the precise composition of the strands remains uncertain, SDS freeze fracture replica labeling (SDS-FRL) permits one to demonstrate a close association between specific transmembrane proteins (such as occludin and claudins) and the intramembranous tight junction strands (Morita et al., 1999; Fujimoto, 1995). Using SDS-FRL, it was demonstrated that CAR is localized specifically to the tight junctions of primary airway epithelial cells. These data provide additional evidence that CAR is a component of the tight junction.

CAR's hydrophobic C-terminal peptide resembles peptide motifs known to interact with PDZ protein domains, such as those contained within ZO-1 and other membrane associated guanylate kinase (MAGUK) proteins (Gonzalez-Mariscal et al., 2000). ZO-1, the central structural protein of the tight junction, serves as intracellular scaffold, linking transmembrane receptor proteins, cytoskeletal components, and intracellular signaling molecules (Cohen et al., 2001b; Itoh et al., 1999; Fanning et al., 1998; Bazzoni et al., 2000; Fanning et al., 2002). Within the tight junction, ZO-1 is known to interact directly with the transmembrane proteins occluding and claudins, as well as with JAM (Ebnet et al., 2000). CAR associates with ZO-1, as demonstrated by coprecipitation and relocaliza-

tion of ZO-1 that occurs in CAR-transfected CHO cells (Cohen et al., 2001b); however, it is not yet know whether the association between CAR and ZO-1 is direct, or whether it involves an unidentified intermediary protein.

People have used yeast two-hybrid analysis to identify proteins that interact directly with the CAR cytoplasmic domain, and have observed possible interactions with several PDZ proteins (Sollerbrant et al., 2003; Coyne et al., 2004; Excoffon et al., 2004). A direct interaction between CAR and multi-PDZ containing protein MUPP1 was found. MUPP1 is a tight junction associated molecule known to interact with claudins, JAM and TAPP1 (Hamazaki et al., 2002; Jeansonne et al., 2003; Kimber et al., 2002). TAPP1 is a protein implicated in phospatidylinositol signaling. In the vicinity of synpases, MUPP1 binds Tech, a RhoA guanine nucleotide exchange factor (GEF), suggested that it also regulates RhoA signaling pathways (Estevez et al., 2008). CAR has also been reported to associate with a MAGI-1 (Excoffon et al., 2004), a tight junction associated MAGUK known to interact with molecules such as β-catenin, RapGEP, synaptopodin, α-actinin 4 and JAM4 (Dobrosotskaya and James, 2000; Hirabayashi et al., 2003; Ide et al., 1999; Mino et al., 2000; Patrie et al., 2002). In addition, the C-terminus of both CAR splice isoforms interact with ligand of Numb-X (LNX) (Sollerbrant et al., 2003), a PDZ protein believed to regulate proteolysis in the Notch signaling pathway in the CNS; however, LNXs have not been identified as tight junction proteins (Dho et al., 1998). CAR is also able to interact with several other proteins, such as harmonin, MAGI-1b, PICK 1 and PSD-95 (Excoffon et al., 2004).

1.3 CAR mediates virus uptake

Tight junctions are important in the natural defense against invasion by microbial pathogens. In order to initiate infection, many pathogens must breach the epithelial barrier to gain access to the body.

Unsuccessful efforts to use viral vectors for therapeutic gene delivery to airway epithelium have led to the recognition that intact epithelium is highly resistant to adenovirus infection and adenovirus mediated gene transfer. Efficient gene delivery to epithelium *in vivo*, and to epithelial monolayers in culture, depends on disruptions of intercellular junctions, at least in part because the virus is unable to attach to the epithelial surface receptors when junctions are intact. The importance of receptor accessibility is demonstrated by the increased efficiency of infections noted in epithelial cultures engineered to express CAR on the apical surface (Davis et al., 2004; Pickles et al., 2000; Walters et al., 2001). Nonetheless, many viruses are known to infect by crossing the airway or intestinal epithelium.

At least three viruses are now known to initiate infection by attaching to receptors within the tight junction: both coxsackieviruses and adenoviruses bind to CAR, reoviruses attach to JAM (Barton et al., 2001). Because CAR and JAM are normally sequestered within junctions, and thus not readily available to viruses at the apical cell surface, it is not clear how interaction with CAR and JAM can promote virus infection of epithelial surfaces. Viruses may attach to CAR and JAM when intercellular contacts are opened, the receptor molecules may sometimes be exposed on the apical membrane, or alternative receptors may be required for infection of intact epithelium. It is also possible that viruses cross the epithelium by alternative mechanisms, such as transport through intestinal M-cells, which do not require infection of the epithelial cells themselves (Clark and Jepson, 2003).

The crystal structure of the reovirus σ1 protein (the attachment protein responsible for interaction with JAM) reveals striking similarity between σ1 and the adenovirus fiber knob (Chappell et al., 2002). The structures of the JAM N-terminal domain and of CAR D1 (including the surfaces involved in receptor dimerization and virus attachment) are also strikingly similar. Because viruses bind with high affinity to these receptors, it is conceivable that virus attachment proteins could disrupt the low affinity dimers responsi-

ble for junction formation as described in 1.1.2 (although this would require that attachment proteins gain physical access to the sequestered receptors).

It is reported that adenovirus fibers applied to the basal surface of a polarized epithelial monolayer can disrupt intercellular junctions (Walters et al., 2002). Based on this observation, a model has been proposed in which excess production of adenovirus fiber knob leads to the disruption of cellular junctions, thus contributing to virus spread into the airway lumen. It is not yet known whether the junctional rearrangements induced by fiber knob result directly from interference with CAR dimerization, or whether fiber knob triggers signals that lead to junctional reorganization, which occurs only after 24 hours. Inflammatory cytokines have marked effects on the integrity of airway tight junctions, and it is possible that adenovirus or soluble fiber may disrupt cell-cell junctions by triggering a cytokine response (Coyne et al., 2002).

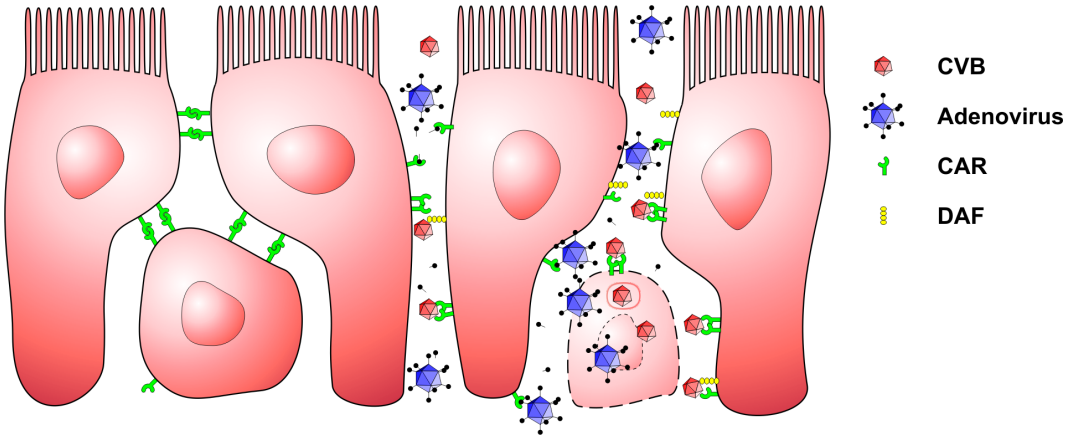

Figure 3: Model of adenovirus and coxsackivirus escape from airway epithelia. CAR does not only mediate cell-cell junction via its extracellular Ig domain homodimerization, but also uptakes adenovirus and coxsackievirus. CAR (green) is localized on the basolateral membrane below the level of the tight junction seal and on basal cells. Once infection is established, adenovirus (blue) and fiber protein (black) are released basolaterally. Fiber increases paracellular permeability by competing CAR-mediated cell-cell adhesion. This allows adenovirus escape to the apical surface.. Independent from or together with its co-receptor DAF (decay accelerating factor/CD55) (yellow), CAR mediates coxsackievirus binding and uptake and escape from the infected cells. Figure modified from (Walters et al., 2002), according to the results from (Meier et al., 2005) and (Chung et al., 2005).

Like adenoviruses, coxsackieviruses also appear limited in their capacity to infect polarized epithelium when the CAR receptor is engaged in intercellular contacts. The CVB susceptibility of cells in vitro is clearly related to the measurable presence of CAR (Shafren et al., 1997), so it has been presumed that the tissue tropism of CVB in vivo is related to differential expression of the receptor among cell types. The exceptions, however, suggest that the situation is more complicated in vivo. Some tissues, such as liver, with readily measurable CAR are not associated with significant CVB pathology (Wessely et al., 2001), and cytoplasmic host proteins may inhibit the ability of CVB to replicate in some cells (Cheung et al., 2005). In contrast, CVBs have been documented in cells of some organs that have not been reported to express CAR at readily detectable levels (Anderson et al., 1996; Mena et al., 1999). However, some coxsackievirus isolates bind to an additional receptor, the complement regulatory protein decay acceleration factor (DAF/CD55) (Shafren et al., 1995). Because of its glycosyl-phosphatidylinositol-linked membrane anchor, DAF is sorted to the apical surface of polarized cells, and is thus likely to be accessible to pathogens in the airway or intestinal lumen. DAF-binding CVB isolates, unlike those that interact only with CAR, are capable of infecting polarized epithelial monolayers; thus, the capacity to bind to DAF may provide these viruses with a mechanism by which to cross the epithelium despite the inaccessibility of CAR (Shieh and Bergelson, 2002).

1.4 Aim of the study

CAR is a type I transmembrane protein of the tight junction and intercalated discs, where it mediates virus uptake and homotypic cell adhesion through its extracellular Ig-domains. The cytoplasmic tail is alternatively spliced and interacts with various adaptor proteins that link to signal transduction and endocytosis (Chung et al., 2005; Sollerbrant et al., 2003; Coyne et al., 2004; Cohen et al., 2001b).

Coxsackievirus B3 (CVB3) infections are frequent causes of human acute myocarditis, often resulting in chronic cardiomyopathy with fibrosis and reduced contractile function that may progress into terminal heart failure. It has therefore been suggested as a therapeutic target to prevent or treat CVB3 induced diseases such as myocarditis and cardiomyopathy. So far, the contribution of CAR-mediated virus update to the pathology associated with myocarditis and the underlying pathomechanism has not been investigated *in vivo*. In this work, a heart specific knockout mouse model was generated to study the role of CAR in viral myocarditis. This also includes the evaluation of the molecular mechanism and potential side effects secondary to the loss of CAR.

In addition to its role as a gateway for viruses to enter their target cells, it is important to understand the physiological functions of CAR. Thus, various CAR deficient animal models have been generated to gain additional insight into its role in cell-cell contact formation and remodeling (Dorner et al., 2005; Asher et al., 2005b; Chen et al., 2006; Lisewski et al., 2008; Anderson et al., 1996; Mena et al., 1999). Although targeting either exon 1 or 2 results in cardiac malformation, degeneration, and lethality in mid-gestation of the conventional knockouts, the mechanism lead to those defects and physiological changes has been remained elusive. With our converted CAR knockout that resulted in the complete deletion of CAR in all cells of the organism, we were able to obtain additional insight into the molecular basis of the embryonic phenotype.

2 Materials

2.1 Chemicals and reagents

If not specified otherwise, all chemicals were purchased from GE Healthcare, Fluka, Invitrogen, Merck, Roth, and Sigma-Aldrich. Taq Polymerases, nucleic acids (kb ladders) were ordered from GE Healthcare, Fermentas GmbH, Invitek, Invitrogen, and Roche.

2.2 Kits

Table 1: List of kits used in this thesis

Kit	Producer
ABI Prism Big Dye Terminator Kit 3.1	Applied Biosystems
BCA Protein Assay Kit	Pierce
Bradford Protein Assay	Bio-Rad
Easy Pure DNA Purification Kit	Biozym
ENZA Plasmid Mini Prep Kit I	Paqlab
Invisorb Spin Plasmid Mini Kit	Invitek
Nucleo Bond BAC 100	Macherey Nagel
Prime-It Random Primer Labeling Kit	Stratagene
qPCR MasterMix Plus	Eurogentec GmbH
RNase-Free DNase Set	Qiagen
RNeasy Mini Kit	Qiagen
RNeasy total RNA isolation kit	Qiagen
Supersignal West Femto Maximun Sensitivity Substrate	Pierce
Supersignal West Pico Chemiluminescent Substrate	Pierce
Thermoscript First-Strand Synthesis System	Invitrogen

2.3 Solutions

Table 2: Buffers

Solution	Contents
10× FA gel buffer	200 mM 3-[N-morpholino] propanesulfonic acid (MOPS), 50 mM sodium acetate, 10 mM EDTA, pH 7.0
1× FA running buffer	1/10 volume 10× FA gel buffer, 250 mM formaldehyde
1× TAE	10 mM sodium acetate, 1 mM Na_2EDTA, 40 mM Tris/HCl, pH 8.0
1× TE	10 mM Tris/HCl, 1 mM EDTA, pH 8.0
20× SSC	3 M NaCl, 0,3 M sodiumcitrat pH 7.0
Agarose loading buffer	50% (v/v) glycerol, 1 mM Na_2EDTA,0.1% (v/v) Xylencyanol, 0.1% (v/v) orange G
Blocking solution	5% (w/v) skim milk, 0.1% (v/v) Tween 20 in PBS
Embryo lysis buffer	50 mM KCl, 3 mM $MgCl_2$, 10 mM Tris/HCl, pH 8.9, 0.01% (w/v) gelatine, 0.45% (v/v) NP-40,0.45% (v/v) Tween 20
Fixation solution	4% (w/v) paraformaldehyde in PBS, pH 7.4
Gitschier buffer 10×	166 mM $(NH_4)_2SO_4$, 670 mM Tris pH8.8, 67 mM $MgCl_2$, 50 mM β-Mercaptoethanol, 67 mM EDTA
HAB lysis buffer	6 M urea, 2% (w/v) CHAPS, 1 mM DTT

Solution	Contents
HBSS	5.4 mM KCl, 0.3 mM Na_2HPO_4, 0.4 mM KH_2PO_4,4.2 mM Na-HCO_3, 1.3 mM $CaCl_2$, 0.5 mM $MgCl_2$, 0.6 mM $MgSO_4$, 137 mM NaCl, 5.6 mM glucose, pH 7.4
HS-PBS	637 mM NaCl, 2.7 mM KCl, 10 mM Na_2HPO_4, 2 mM KH_2PO_4, pH 7.4
Kinexus buffer	20 mM MOPS, pH 7.0 (any other buffer at this pH could be substituted), 2 mM EGTA, 5 mM , 30 mM NaF, 60 mM ß-glycerophosphate, pH 7.2, 20 mM sodium pyrophosphate ($Na_2P_2O_7 \cdot 10H_2O$), 1 mM sodium orthovanadate (Na_3VO_4), 1% Triton X-100 (can be substituted with 1% Nonidet P-40)
Laemmli-buffer	50 mM Tris, 1% (v/v) ß-mercaptoethanol, 2% (w/v) SDS, PBS 137 mM NaCl, 2.7 mM KCl, 4.3 mM Na_2HPO_4, 10% (v/v) glycerine, 0.1% (w/v) bromphenolblue, pH 6.8, 1.4 mM KH_2PO_4, pH 7.4
Low TE	10 mM Tris/HCl, 0.1 mM Na_2EDTA, pH 8.0
PBS	137 mM NaCl, 2.7 mM KCl, 4.3 mM $Na_2HPO_4 \times 2\ H_2O$, 1.4 mM KH_2PO_4
PBST	PBS with 0.1% (v/v) Tween 20
protein lysis buffer	Kinexus buffer, 1% Octyl-ß-D-Glucophyranoside (OGP), 1mM PMSF, proteinase inhibitor cocktail tablet/10 ml
SDS-Buffer	1 % SDS, 10 mM Tris-HCl, pH 7.5, 2 mM EDTA, pH 8.0
SET stock solution	3M NaCl, 0.4M Tris-HCl, pH 7.8, 20 mM EDTA, pH 7.8
SET solution	0.2×SET, 0.2% SDS
Stripping solution	2 % SDS, 62.7 mM Tris-Base, 100mM ß-mercaptoethanol, pH 6.8
TAB lysis buffer	8 M urea, 2 M thiourea, 2% (w/v) SDS, 75 mM DTT, 0.05 M Tris, pH 6.8
Tail buffer	20 mM Tris/HCl, pH 8.0, 5 mM EDTA, pH 8.0, 0.4 M NaCl, 0.2% (w/v) SDS,
TBS	137 mM NaCl, 2.7 mM KCl, 50 mM Tris, pH 7.4
TBST	TBS with 0.05% (v/v) NP-40
Transfer buffer	192 mM Tris, 25 mM glycine, 20% (v/v) methanol, pH 8.3
Trypsin-EDTA (1x)	0.05% (v/v) trypsin, 0.53 mM EDTA
Washing buffer	PBS with 0.02% (v/v) sodium azide

2.4 Cell culture media

Table 3: List of media for cell culture

Solution	Contents
DMEM	With ultraglutamine and 4.5 g/L glucose, From Lonza-Cambrex
DMEM powder	Gibco-Invitrogen
Fetal Bovine Serum	LOT#41Q2155K, from Invitrogen
ESGRO culture medium	Chemicon
DMEM culture medium	10% (v/v) FBS, 1% p/s, 90% (v/v) DMEM
Differentiation solution	20% (v/v) FBS, 1% p/s, 1% NEAA, 0.08mM ß-mercaptoethanol, 80% (v/v) DMEM
ES medium	6.7g DMEM powder, 1.2g $NaHCO_3$, add water to 540ml, 6ml NEAA, 6ml L-Glutamine, 6ml p/s, 4.2µl ß-mercaptoethanol, 80ml FBS, 120µl Lif (ESGRO)
MC perfusion solution	113 mM NaCl, 4,7 mM KCl, 0.6 mM KH_2PO_4, 0.6 mM Na_2HPO_4, 1.2 mM $MgSO_4 \cdot 7H_2O$, 0.032 mM Phenol Red, 12 mM $NaHCO_3$, 10 mM $KHCO_3$, 10 mM HEPES, 30 mM Taurin, 10 mM 2,3-BDM, 5.5 mM Glucose
MC digestion buffer	Perfusion solution with 0.25 mg/ml Liberase Blendzyme 1, 0.14 mg/ml Trypsin, 12,5 µM $CaCl_2$

Solution	Contents
MC stop solution 1	Perfusion solution with 10% FBS, 12,5 µM $CaCl_2$
MC stop solution 2	Perfusion solution with 5% FBS, 12,5 µM $CaCl_2$
MC plating medium	0,9× MEM with Hanks' salts and L-glutamine, 5% FBS, 10 mM BDM, 100 U/ml Pen/Strep, 2 mM L-glutamine
MC culture medium	1× MEM with Hanks' salts and L-glutamine, 5% FBS, 0.1mg/ml BSA, 100 U/ml Pen/Strep, 2 mM L-glutamine

2.5 Antibodies

Table 4: Antibodies and their working dilutions

		Dilution		
Antibody	**Species**	**IF**	**WB**	**Company**
Primary antibody				
α-actin	rabbit		1:1000	Sigma
α-actinin (EA53)	mouse	1:1000		Sigma
α-Tubulin	mouse	1:100	1:1000	Oncogene
ApoA-1	rabbit		1:1000	Biodesign
β-integrin	rabbit		1:1000	Chemicon
CAR	rabbit	1:50	1:1000	Santa Cruz
Connexin 40	rabbit	1:100	1:1000	Lifespan Bioscience
Connexin 43	mouse	1:100	1:1000	Chemicon
Connexin 43	rabbit		1:1000	Sigma
Connexin 45	mouse	1:100	1:1000	Chemicon
Connexin 45	rabbit	1:100	1:1000	Zymed
Cubilin	rabbit		1:500	Santa Cruz
E-Cadherin	rabbit	1:500	1:1000	Abcam
GAPDH	mouse		1:2000	ABR
HCN4	rat	1:200		Abcam
N-Cadherin	mouse	1:500	1:1000	Zymed
Transthyretin	rabbit		1:2000	Proteintech Group, Inc
Vinculin	rabbit		1:500	Upstate
ZO-1	rat	1:100	1:1000	Chemicon
Secondary antibody				
Alexa Fluor 488	goat	1:500		Invitrogen
Alexa Fluor 488	donkey	1:1000		Invitrogen
Alexa Fluor 568	goat	1:1000		Invitrogen
Alexa Fluor 594	donkey	1:1000		Invitrogen
Alexa Fluor 633	goat	1:1000		Invitrogen
Alexa Fluor 647	goat	1:1000		Invitrogen
Cy3	goat	1:1000		Dianova
IgG mouse HRP conjugated			1:2000	Calbiochem
IgG rabbit HRP conjugated			1:5000	GE Healthcare

2.6 Oligonucleotides

Oligonucleotides for genotyping and sequencing were synthesized by BioTez GmbH. Primer and probes for RT-PCR (TaqMan) analysis were ordered from Applied Biosystems as complete gene expression assay or synthesized by BioTez GmbH (sequences listed below). Sequences of primers were provided in 5'→ 3' orientation:

Table 5: Primers for PCR genotyping

Primers	Sequence
ApoE3	CGAAGCCAGCTTGAGTTACAG
ApoEko5	GACTGGGCACAACAGACAATC
ApoEwt5	TATCTAAACAGACTCCACAGC
CAR P1-3 f	CCATGCACAGGGTGATCTG
CAR P1-3 r	TGAGACTAAAAACCAGCAGCTTC
CAR P1-5 f	AACCTAGCCATTCAAAAAGAAGG
CAR P1-5 r	CTCCCTAAACCTTGATCGATACC
CAR SA K f	GGGTACCGCAAAGGCAGCTCTTACAAAATA
GKneo r	CACGAGACTAGTGAGACGTGCTA
Cre1200	GTAGTTATTCGGATCATCAGCTACAC
Cre800	GCTGCCACGACCAAGTGACAGCAATG
FLP1	GTCACTGCAGTTTAAATACAAGACG
FLP2	GTTGCGCTAAAGAAGTATATGTGCC

Table 6: Primers for Southern blot

Primers	Sequence
CAR-Sou-f	CTGTCAATGCTGCCTGACTAAG
CAR-Sou-r	AAGAGCTTAAAGCGTTGGCTAAT

Table 7: Primers and probes for TaqMan Assay

Primers and probes	Sequence
Mouse ANP f	TTCTAGGCGCAGCCCCT
Mouse ANP r	GCAGAGCCCTCAGTTTGCTT
Mouse ANP porbe	6-FAM-ACCCCTCCGATAGATCTGCCCTCTTGAA-TAMRA
18S RNA f	CGCCGCTAGAGGTGAAATTC
18S RNA r	TGGGCAAATGCTTTCGCTC
18S RNA probe	6-FAM-TGGACCGGCGCAAGACGGAC-TAMRA
GAPDH mouse 154f	GGC AAA TTC AAC GGC ACA GT
GAPDH mouse 223r	AGA TGG TGA TGG GCT TCC C
GAPDH probe	6-FAM-AGGCCGAGAATGGGAAGCTTGTCATC-TAMRA
CAR02 f	ACTTTGAACGTGCGCCTCAGA
CAR02 r	TGTAATGCCATCGGTCTTGT
CAR02 probe	6-FAM-CGTACTTGAACTTAGCGGGTGCCA-TAMRA
IL-1beta f	CAACCAACAAGTGATATTCTCCATG
IL-1beta r	GATCCACACTCTCCAGCTGCA
IL-1beta probe	6-FAMGGTGGGTGTGCCGTCTTTCATTACACAG-TAMRA
IL-4 f	CGCCATGCACGGAGATG
IL-4 r	CGAGCTCACTCTCTGTGGTGTT
IL-4 probe	6-FAM-TGCCAAACGTCCTCACAGCAACG-TAMRA
IL-6 f	ACAAGTCGGAGGCTTAATTACACAT
IL-6 r	TTGCCATTGCACAACTCTTTTC
IL-6 probe	6-FAM-TTCTCTGGGAAATCGTGGAAATG-TAMRA
IL-10 f	CCAGAGCCACATGCTCCTAGA
IL-10 r	GGTCCTTTGTTTGAAAGAAAGTCTTC
IL-10 probe	6-FAM-CTGCGGACTGCCTTCAGCCAGG-TAMRA
IL-12a f	ACTAGAGAGACTTCTTCCACAACAAGAG
IL-12a r	GCACAGGGTCATCATCAAAGAC
IL-12a probe	6-FAM-AGCTGCCTGCCCCCACAGAAGA-TAMRA
IL-12b f	CTACAGCACCAGCTTCTTCATCA

Primers and probes	Sequence
IL-12b r	TCAAAGGCTTCATCTGCAAGTTC
IL-12b probe	6-FAMTGGGCGGGTCTGGTTTGATGATG-TAMRA
TNFα-f	CATCTTCTCAAAATTCGAGTGACAA
TNFα-r	CCAGCTGCTCCTCCACTTG
TNFα probe	6-FAM-CCTGTAGCCCACGTCGTAGCAAACCA-TAMRA
IFNγ f	CAGCAACAGCAAGGCGAAA
IFNγ r	CTGGACCTGTGGGTTGTTGAC
IFNγ probe	6-FAM-AGGATGCATTCATGAGTATTGCCAAGTTTGA-TAMRA
TGFb1 f	GCTCTTGTGACAGCAAAGATAACAA
TGFb1 r	CGCCCCGACGTTTGG
TGFb1 probe	6-FAM-CCACGTGGAAATCAACGGGATCAGC-TAMRA
CX30.2 f	GACGCGGTGCAGCTACAGT
CX30.2 r	ATGCGGAAGATCAGCATGATC
CX30.2 probe	6-FAM- CGCTCGTGGGTCGTCTCTGGC-TAMRA
CX37-2008 f	CCCAGGGTGGCCGAAA
CX37-2008 r	ACACATACTGCTTCTTGGATGCA
CX37-2008 probe	6-FAM-CCCCTAGCCGCCCCAACAGCT-TAMRA
CX40 f	CAGCCTGGCTGAACTCTACCA
CX40 r	CTGCCGTGACTTGCCAAAG
CX40 probe	6-FAM-CGCTGTCGGATCTTCTTCCAGCCCAG-TAMRA
HCN4 f	GGGTTAAGTCAGCAGGGTTTTG
HCN4 r	GCATCGTCAGGTCCCAGTAAA
HCN4 probe	6-FAM-ATTATCCACCCCTACAGTGACTTCAGA-TAMRA
myD88 f	CATTGCCAGCGAGCTAATTG
myD88 r	TCTGTAGATAATCGTCAGAAACAACCA
myD88 probe	6-FAM-AAAGGTGTCGCCGCATGGTG-TAMRA
LCK f	CCTTCAACTTCGTGGCGAAA
LCK r	CGTCCTTACGGCTCAGATTCTT
LCK probe	6-FAM-AAACAGCCTGGAGCCTGAACCTTGG-TAMRA
IFNβ1 f	AAAACTGAAGACCTGTCAGTTGATG
IFNβ1 r	CCGCCTCTGATGCTTAAAGG
IFNβ1 probe	6-FAM-CAGAATGAGTGGTGGTTGCAGGCA-TAMRA
Cublin f	CCAGAGCCCGAATGATACCTAT
Cublin r	AAAAACGTGAAGGTAATATGCAGAAC
Cublin probe	6-FAMTGGGTTGTCAGAACCGATGAGGAATAMRA
DAF1 f	CCAACTCCTCAGAAACCTTCCA
DAF1 r	CACCTGTGTTAGGCTCTCCTTTG
DAF1 probe	6-FAM-AGTTAAAGTTTCAGCAACCCAGCATGTACCTGTT-TAMRA

2.7 Appliances

Table 8: Equipment

Equipment	Company and type
Air pump	AgnTho's, Stellar A30
Agarose gel system (Mini)	Cosmo Bio Co., LTD, Mupid-21
Anaesthesia unit	AgnTho's, Univentor 400
Blotting system	Biorad, Mini Trans. Blot Cell
Cell culture incubator	Binder, APT Line CB 150
Centrifuge	Eppendorf, centrifuge 5804
Centrifuge for 96 well Plates	Sigma, 4K15, Rotor: 09100
Centrifuge for falcon tubes	Sigma, 3K12
Chemiluminescence and fluores-cence imaging system	Fujifilm, LAS-1000
Confocal microscope	Leica, TCS SP5/Carl Zeiss, LSM 5 Pascal

Equipment	Company and type
Cryostat	Leica, Cryocut 3000
Desktop centrifuge	Heraeus, Biofuge/Eppendorf, centrifuge 5417R
Fluorescent image analyser	Fujifilm, FLA-3000
Gas Routing Switch	AgnTho's
Gel documentation	Syngene, GENE GENIUS
Glass capillary puller	Sutter Instrument Inc., P-97
Heating plate for mouse	Föhr Medical Instruments, EHE-3501/280/140/11
Homogenizer	IKA®-Werk, Ultra-Turrax T-8
Image eraser	Raytest
Light Source	Carl Zeiss MicroImaging, Inc, KL 1500 LCD
Micro conductance pressure catheter	Millar-Instruments, Inc., ARIA SPR-719
Microplate reader	Bio Tek, Synergy HT
Microscope	Olympus, CK30/Leica, DMI 6000 B
Microtome	MICROM, HM355S
MiniVent Ventilator for Mice	Föhr Medical Instruments , Model 845
Patch clamp amplifier	HEKA Elektronik, EPC-9
Paraffin dispensing unit	Leica, EG 1140 H
PCR Machine	MJ Research, PTC-200/225
Photometer	GE Healthcare, Ultraspec 2100 pro
Pipette	Gilsen/Eppendorf
Power supply	Biometra, 105BIO-LVD
Pumper	Pharmacia, LKB-Pumpe P1
Real-time PCR system	Applied Biosystems, 7900HT
Scintilla counter	Beckman counter, LS6000SC
SDS-PAGE system	GE-Healthcare, Hoefer Small gel unit
Sonicator	Bandelin, HD 2070 / UW 2070
Spectrophotometry	PeqLab, NanoDrop ND-1000
Sterile working bench	BDK
Stereomicroscope	Leica, MZ75
Temperature control module	Föhr Medical Instruments , TKM-0902
Temperature sensor	Föhr Medical Instruments , Pt-100
Thermo shaker	Eppendorf, Thermomixer comfort
Tissue processor	Leica, TP 1020
UV cross linker	Vilber Lourmat
UV light pack	Olympus, U-RFL-T
Water bath	Haake, DC10

2.8 Software

Table 9: List of software used for this thesis

Software	Company
Adobe Acrobat professional 7.0	Adobe Systems Inc.
Aida version 3.51.042	Raytest GmbH
CorelDRAW Graphics Suite 12.0	Corel Corp.
Delta 2D	Decodon
GraphPad Prism 5.0	GraphPad Software, Inc
Image J V1.42d	Wayne Rasband, NIH
LSM 5 Image Browser	Carl Zeiss GmbH
Metamorph 6.2r2	Universal Imaging Corp.
Microsoft Office 2007	Microsoft
Photoshop CS2	Adope Systems Inc.
SeqMan II 4.03	DNAStar Inc.
Sequence Detection System 2.1 software	Applied Biosystems

2.9 Animals

All the mice were maintained according to the procedure approved by the Max-Delbrück-Center (Germany) institutional animal care committee. Mouse strains were maintained on a mixed (C57Black6 and 129 SVJ) background.

3 Methods

3.1 Molecular biology methods

3.1.1 DNA preparation

3.1.1.1 Mouse Tail DNA preparation

Total genomic DNA for genotyping was extracted from tissue of the tail by overnight (o/n) digest with 25µl of 10 µg/ml proteinase K solution in 725µl Tail lysis buffer at 55°C. Proteinase K was inactivated by heat shock at 95°C for 10 min. One volume of phenol/chloroform was added, mixed gently with the sample and centrifuged for 5min at 14,000rpm. The aqueous phase was transferred into a new tube and 2 volumes of 100% ethanol were added. The tube was inverted and swirled to mix and precipitate DNA at -20°C for at least 30min. The DNA was centrifuged down at 14,000rpm for 15 min. The supernatant was aspired and washed once with 70% ethanol. The pellet was briefly air-dried at room temperature (RT) and was then dissolved in 100µl TE buffer.

3.1.1.2 Embryonic DNA preparation

Total genomic DNA for genotyping was extracted from embryonic tissue by o/n digest at 55°C with 50µl embryo lysis buffer (with 5µl of 10µg/ml Proteinase K) solution. Proteinase K was inactivated by heat shock at 95°C for 10 min. Digested tissue was diluted and utilized directly for polymerase chain reaction (PCR) genotyping.

3.1.2 PCR based genotyping

If not mentioned otherwise, all PCR amplification reactions were conducted with the thermostable *Taq* DNA polymerase.

The following PCR reaction mixes and programs were applied to PCR softstrips (Biozym GmbH).

Soriano PCR (WT: 419bp, primer: P1 5 f & P1-3 r; 3rd lox site: 349bp, primer: P1 3 f & P1-3 r; Rec: 251bp, primer: P1 3 f & P1-3 r):

	Final concentration	Volume
Gitschier buffer (10×)	1×	2.5µl
DMSO	10%	2.5µl
dNTP Mix (10 mM)	0.5mM	1.25µl
Primers (10 µM)	0.2µM	0.5µl each
BSA (10mg/ml)	0.08mg/ml	0.2µl
DNA Template	20-50 ng	1-2µl
Taq Polymerase (5 U/µl)	0.025 U/µl	0.125µl
to a final of 25µl with dH_2O		- µl

Program:

step	temperature	time	
1	93°C	3 min	
2	60°C	5 min	
3	65°C	5 min	
4	93°C	30 sec	
5	60°C	1 min	
6	65°C	3 min	step 4-6, 40×
7	65°C	10 min	
8	10°C	∞	

Cre PCR (480bp):

	Final concentration	Volume
PCR buffer (10×)	1×	2.5µl
dNTP Mix (10 mM)	0.5mM	1.25µl
Primer Cre 800 (10 µM)	0.6µM	1.5µl
Primer Cre 1200(10 µM)	0.6µM	1.5µl
$MgCl_2$(50mg/ml)	1.5mg/ml	0.75µl
DNA Template	20-50 ng	1-2µl
Taq Polymerase (5 U/µl)	0.04 U/µl	0.2µl
To a final of 25µl with dH_2O		- µl

Program:

step	temperature	time	
1	94°C	2 min	
2	94°C	15 sec	
3	49°C	15 sec	
4	72°C	45 sec	Setp 1-4, 35×
5	72°C	8 min	
6	4°C	∞	

3.1.3 Agarose gel electrophoresis

After amplification, the PCR reaction mix was loaded with 1/10 volume agarose loading buffer. Depending on the expected product size, it was applied onto a 1 to 2% (w/v) aga-

rose gel to separate PCR products. Agarose gels were prepared with UltraPureTM agarose (Invitrogen), 0.5× TAE, and 0.5µg/ml ethidiumbromide solution. A 1kB DNA ladder was used to determine the size of the PCR product. The separation took place in 0.5× TAE running buffer for 20 min at 100 volts in an agarose gel chamber Mupid®-ex (Eurogentec GmbH). PCR fragments were visualized on a UV unit (U-RFL-T; Olympus) at 312 nm.

3.1.4 Determination of nucleic acid concentration

The concentration of nucleic acid was determined by spectrophotometry (Nanodrop ND-1000), according to the manufacturer's instructions.

3.1.5 Generation of the targeting vector

The targeting vector of CAR KO was generated or converted by Dr. Michael Radke. To generate CAR deficient animals the Cre-lox recombination system was used, flanking CAR exon 1, which contains the ATG, with lox sites (Fig. 4). After homologous recombination blastocyst injection of targeted ES-cells was used to obtain knockout animals. The neomycin/flp resistance cassette was removed by germline expression of the FLP recombinase (Gotthardt et al., 2003).

3.1.6 DNA Sequencing

DNA sequencing is a linear extension reaction initiated at a specific site on the template DNA by using a complementary oligonucleotide. All sequencing reactions were performed according to the chain termination method from Sanger (Sanger et al., 1977) using the standard T7 or Sp6 sequencing primers and the ABI Prism Big Dye Terminator Kit v3.1 (Applied Biosystems). These reagents are suitable for fluorescence-based cycle sequencing reactions on single-stranded or double-stranded DNA templates and on polymerase chain reaction fragments. The following PCR sequencing reaction mix was used in softstrips (Biozym GmbH) on the PTC-200 (MJ Research):

BigDye Terminator v1.1/3.1 Seq. Buffer (5×)	2.0µl
Big Dye	1µl
Primer (10 µM)	0.25µl
DNA Template	5ng/ 100bp
to a final of 10µl with dH2O	- µl

Program:

step	temperature	time	
1	95°C	10 sec	
2	50°C	5 sec	
3	60°C	4 min	Setp 1-3, 30×
4	10°C	∞	

The ABI PRISM® 377 DNA Sequencer (Applied Biosystems) automatically analyzed DNA molecules labeled with fluorescent dyes. After samples were loaded onto the system's vertical gel, they underwent electrophoresis, laser detection, and computer analysis. Sequences were analyzed with SeqMan II version 4.03 (DNASTAR Inc.).

3.1.7 Southern blot with genomic DNA

10-20 µg of genomic DNA were digested with 30 U of restriction enzyme BamHI) in 40µl total volume overnight at 37°C. The genomic DNA digests were run on a 14×11cm 0.8% agarose gel with 1× TAE and electrophoresised at 70 volts for approximately 4.5-5 hours. After photographing the ethidium bromide stained gel beside a fluorescent ruler, the gel was depurinated by soaking for 20 min in 0.25N HCl and then denatured in denaturing solution (1.5M NaCl, 0.5M NaOH) for 20 min with gentle rocking. The Hybond N+ membrane (GE Healthcare) was prewet in deionized water for 20 min. Membrane and Whatman paper were shortly soaked in neutralization solution (1.5M NaCl, 0.5M Tris-HCl - pH 7.0). DNA was transferred to the membrane by traditional capillary blotting o/n. The gel/membrane sandwich was disassembled and the membrane was washed in neutralization solution for 5-10 min. The blot was slightly air dried for approximately 30 seconds to dampness. The blot was UV crosslinked with 120 Joules twice in a UV crosslinker (Vilber Lourmat). The membrane was checked under UV light for the transfer efficiency. The crosslinked membrane was prehybridized in 10 ml PreHyb Buffer (GE

Healthcare) at 65°C for 1-4 hours in the rolling hybridization tube incubator. The probes were labeled with α-^{32}P dCTP (NEG) using Prim-It Random Primer Labeling Kit (Stratagene) according to the manufacturer's instructions. The labeled probes were purified with MicroSpin S-300HR columns (GE Healthcare). 1µl labeled probe was used to measure the radioactivity with scintilla counter (Beckman counter LS6000SC). The rest of probes were denaturized at 95°C for 3min, cooled down on ice, then added into the hybridization tube. Final concentration of probe would be 2 million cpm/ml in 10 ml. The membrane was incubated at 65°C o/n. On the next day, the membrane was washed with SET solution, 3 times for 1 hour each. The blot was air dried until slightly damp, wrapped in plastic wrap. Membrane was exposed in Imaging Plate BAS-IP-MS 2300 (Fuji Film) for 4-48 hours at -70°C. The signals were developed by FLA-3000 Scanner (Fuji Film) with the software BASReader 3.14. The images were analyzed with the software AIDA 3.15.

3.1.8 Total RNA isolation and purification

To avoid RNase contamination all experiments involving RNA were conducted with filtertips (Starlab). Tissue were dissected in DEPC treated PBS on ice, quick-frozen, and stored at -80°C.

Table 10: The tissue and corresponding amount used for RNA pool

Adult tissue:	100mg/sample
Embryonic tissue number per pool:	
Heart:	9 for E9.5, 6 for E10.5, 3 for E11.5
Brain:	6 for E9.5, 4 for E10.5, 3 for E11.5
Yolk sac:	3 for each stage
Tail:	6 for E9.5, 3 for E11.5
Liver:	6 for E11.5

To reduce viscosity of lysate and shear genomic DNA, samples were homogenized with an Ultra-Turrax T-8 (IKA®-Werk) in 1 ml TRIzol per 100 mg adult tissue sample or 0.5 ml TRIzol for embryonic tissue. Total RNA was isolated with TRIzol according to the manufacturer's instructions then purified with RNeasy Mini Kit according to manufactur-

er's recommendations. RNA quality was controlled using the Agilent 2100 Bioanalyzer (Agilent Technologies, Inc) and the Agilent RNA 6000 Nano Kit.

3.1.9 Formaldehyde agarose gel electrophoresis

100-500 µg of total RNA was separated on denaturing formaldehyde agarose gels to control quality and possible degradation. RNA was loaded with 5× RNA loading buffer onto a 1.2% (w/v) FA gel prepared with 1/10 volume of 10× FA gel buffer, UltraPure™ agarose, and 0.5 µg/ml ethidiumbromide solution. The separation took place in 1× FA gel running buffer for 40 min at 100 volts in an agarose gel chamber Mupid®-ex (Eurogentec GmbH). Ribosomal RNA was visualized on a UV unit (U-RFL-T; Olympus) at 312 nm. The 28S ribosomal RNA from mouse tissue was present with intensity approximately twice that of the 18S RNA band. Diffuse bands would have indicated degradation during preparation.

3.1.10 Synthesis of cDNA

For quantitative real-time polymerase chain reaction (RT-PCR) it was necessary to generate cDNA. Therefore total RNA was reverse transcribed using the two-step Thermoscript first-strand synthesis system according to the manufacturer's guidelines:

2µl dNTP Mix (10 mM)
1µl Random Primer (50 ng/µl)
1 µg RNA Template
- µl to a final of 12µl with RNase free dH_2O

RNA and primer were denatured by incubating at 65°C for 5 min. A mastermix was prepared and added to the denatured primer/RNA mix:

4µl cDNA Synthesis Buffer (5×)
1µl DTT (0.1 M)
1µl RNase OUT (40 U/µl)
1µl DEPC-treated water
1µl Thermoscript RT (15 U/µl)

The cDNA synthesis was performed in the PCR-Thermocycler PTC-200 (MJ Research) at 65°C for 60 min and terminated by incubation at 85°C for 5 min.

3.1.11 Real-time PCR

Quantitative RT-PCR was carried out using the TaqMan® probe-based chemistry (Applied Biosystems) on an ABI 7900HT Fast Real-Time PCR System. Primer and probes were designed using Primer Express 1.5 (Applied Biosystems) and ordered from BioTez GmbH or ordered as TaqMan® Gene Expression Assays from Applied Biosystems. Real-time PCR amplification reactions were performed using the qPCR MasterMix Plus (Eurogentec GmbH) according to manufacturer's specifications with 2× TaqMan universal PCR master mix, 900 nM primer, and 250 nM probe. Thermal cycling conditions were as follows:

Program:

step	temperature	time	
1. Annealing	50°C	2 min	
2. Denaturing	95°C	10 min	
3. Denaturing	95°C	15 sec	
4. Extension	60°C	1 min	Setp 2-4, 50×
5. Storage	4°C	∞	

Data were collected and analyzed with the Sequence Detection System 1.2 or 2.2 software (Applied Biosystems). The Comparative CT Method (Δ CT Method) was used as described in the User Bulletin 2: ABI PRISM 7700 Sequence Detection System.

3.1.12 Microarray analysis

DNA microarray analysis was run for CAR wildtype, heterozygous and knockout hearts from E9.5 embryonic heart pools. Hearts were collected as pools according to genotype; each pool contained 9 embryonic hearts. DNA microarray methods were applied as standard protocol described in the manufacturer's instructions (Affymetrix). Briefly, total RNA was extracted from hearts using the RNeasy total RNA isolation kit (Qiagen). The preparation quality was assessed by agarose-formaldehyde gel electrophoresis. Labeled and defragmented cRNA was hybridized to GeneChip® Mouse Genome 430 2.0 Array (Affymetrix) which carry probes representing 45,101 probe sets. Following hybridization,

arrays were washed and stained with streptavidin-phycoerythrin in the Affymetrix Fluidics Station 450 and further scanned using the Affymetrix GeneChip Scanner 3000 7G. The image data were analyzed with GCOS 1.4 using Affymetrix default analysis settings. Raw data from microarray scans were normalized and analyzed by Dr. Herbert Schulz from Max-Delbrück-Center. Transcripts absent from all samples were excluded from analysis. After normalization, the data was filtered according to the following criteria were considered as a valid signal: (a) either WT or KO expression signal value ≥100; (b) the "probesets p value" of considered signal <0.05; (c) fold change difference between genotypes ≥1.2. Transcripts were defined as differentially expressed only if they passed filtering criteria listed above.

3.2 Cell biology methods

Primary cell culture was prepared from E9.5, E10.5 and E11.5 knockout, heterozygous, and wildtype embryonic tissue or adult knockout and wildtype hearts.

3.2.1 Isolation of primary mouse embryonic cardiomyocytes

The pregnant mouse was sacrificed according to the day of the vaginal plug (E9.5 to E11.5) by cervical dislocation. The mouse was laid on its back and swabbed with 70% ethanol. A cut across the belly was made and the skin was cut away to expose the gut. With sterile forceps and scissors, the uterus was dissected out and placed into a petri dish with ice-cold sterile PBS. The embryos were isolated from the uterus, and released from yolk sacs, then transferred to a second petri dish with ice-cold sterile PBS. The heart was scooped out with a pair of forceps (#5 Dumont) or spring scissors and transferred into a sterile 1.5ml tube with a sufficient volume of 0.05% Trypsin/EDTA to cover the heart. All hearts were incubated at 4°C for 5 to 10 hours or o/n, and then incubated at 37°C for 15 min. Tubes were centrifuged at 800g for 3 min and the trypsin/EDTA could be removed (this step could be skipped if trypsin volume is less than 50µl). 5× volumes of DMEM

with 10% FBS were added and the heart tissue was dissociated by pipetting through a pipette several times. Hearts were plated out 1 heart/well (e.g. E11.5, 24-well plate) and incubated at 37°C with 5% CO2 in an incubator (Binder) with water vapor saturated. Most of fibroblasts were removed by differential adherence at 37°C for 30min-1h, (this step can be skipped for E9.5-E10.0 heart). Cardiomyocytes should attach in 1-3 hours. Medium was changed after 16-24 hours for the first time and then every 48 hours.

3.2.2 Isolation of embryonic fibroblasts

Pregnant mice were sacrificed by cervical dislocation at the appropriate day after the vaginal plug. The uterus was removed and transferred into a petri dish with ice-cold PBS. The embryos were dissected of the uterus tissue and head and if possible internal organs were removed. Embryos were kept in 100µl trypsin-EDTA solution o/n at 4°C to allow trypsin to penetrate the tissue. Using scissors finely mince the tissue. Embryos were digested at 37°C for 10 min after removing excessive trypsin solution. Digestion was stopped by adding 5 volumes of feeder medium. Cells were separated by pipetting up and down and plated on cell culture dishes and incubated at 37°C. PMEFs should attach and begin to divide in 1-3 days. The medium was changed after 2 days. When the cells were confluent, usually after 3-4 days, the cultures were ready for freezing. Cells were frozen in 10% DMSO at 2×10^6 cells/vial (labeled P0). Cells were monitored every day and pictures were taken with the camera system from Visitron System GmbH (Model: 2.2.1). Media were changed every other day.

3.2.3 Isolation of epithelial cells from yolk sac

3.2.3.1 Coating procedures

Cell culture dishes were coated with rat tail collagen, type 1 (BD Biosciences) at 5µg/cm^2 diluted in 0.02N acetic acid and incubated at RT for one hour. The remaining solution was carefully aspirated and the dishes were rinsed well to remove acid, using PBS or serum

free medium. Plates may be used immediately or may be air dried and stored at 2-8°C for up to one week under sterile conditions.

3.2.3.2 Primary yolk sac epithelial cells preparation

The yolk sac was taken into DMEM solution and finely minced into small pieces before it was moved into enzyme digestion. The tissue and collagenase (500U/ml) mixture were incubated in a 37°C shaker for 40min-1hour until the epithelium cells could be observed separating from the matrix. The digestion step was stopped and the cells were centrifuged down. The pellet was resuspended in DMEM or PBS. Then glass pipe was used to divide the cells from the matrix, air bubbles should be avoided. The cell solution was removed to a small culture dish at incubated 37°C for 2 hours or longer. The supernatant was carefully collected and moved into a new collagen coated culture dish and incubated at 37°C. Culture medium was changed daily.

3.2.4 Isolation of adult cardiomyocytes

The mouse was intraperitoneal injected with 0.5cc heparin diluted in PBS to 100IU/ml and scarified by cervical dislocation. After sterilization with 70% ethanol, the peritoneal cavity and chest were opened. The heart was gently lifted and the pulmonary vessels were cut. A cut was made at about 2mm from the aorta entry into the heart. The heart was then immediately placed in a 60mm dish containing 10ml perfusion buffer at RT. The heart was cannulated, and the aorta was tied to the cannula with a 6-0 silk thread. The perfusion was started immediately (3ml/min) with perfusion buffer for 4 min and then switched to the MC digestion buffer for 8-10 min at 3ml/min. The ventricle was cut from the cannula, gently teased into several small pieces with fine forceps in 2.5 ml MC digestion buffer and dissociated through pipette for several times. The cell suspension was transferred to a 15ml polypropylene conical tube. The plate was rinsed with 2.5 ml of myocyte stopping buffer 1, and MC stop 1 was combined with the cell suspension for a final volume of 5ml.

The dissociation was continued until all the large pieces of heart tissue were dispersed in the cell suspension. Rod-shaped and round Myocytes were counted using a hemacytometer. After gravity sedimentation for 8-10 min in the 15ml tube, the supernatant was transferred to a new 15ml tube and centrifuged for 1 min at 180×g. The new pellet was resuspended in 5ml myocyte sopping buffer 2, combined with the original sedimented myocytes, and adjusted to a total volume of 10 ml with MC stop 2. The combined pellets were transferred to a 60 mm nonstick valmark dish and calcium reintroduction was performed (4 min in each step): 50µl 10mM $CaCl_2$, 50µl 10mM $CaCl_2$, 100µl 10mM $CaCl_2$, 30µl 100mM $CaCl_2$, 50µl 100mM $CaCl_2$. The Myocytes were transferred to a new 15ml tube for gravity sedimentation for 8-10 min. The supernatant was transferred to another new 15ml tube and centrifuged for 1 min at 180×g. Both pellets were resuspended and combined in 5 ml of MC plating medium (1.2mM Ca^{2+}) at 37°C. Rod-shaped and round Myocytes were counted again. After calculation, the rod-shaped myocytes were plated with a concentration of 25,000 myocytes/ml in a laminin-coated dish. Myocytes were incubated for 1 hr for attachment, then the plating medium was removed and unattached myocytes were washed away. The myocytes were incubated in MC culture medium at 37°C, 5% CO_2 until use.

3.2.5 Preparation of cardiac muscle slices and dye coupling studies

3.2.5.1 Preparation of adult mouse cardiac muscle slices

Mice hearts at the indicated times were quickly removed after cervical dislocation under deep ether anesthesia and transferred to ice-cold oxygenated standard salt solution (SSS) containing (mM): 125 NaCl, 4 KCl, 10 glucose, 1.25 NaH_2PO_4, 25 $NaHCO_3$, 2 $CaCl_2$, and 1 $MgCl_2$. Ventricles were longitudinal cut and embedded in 2.5 % low melting temperature agarose (Biozym Scientific, Oldendorf, Germany) at 30°C. The blocks were glued to the stage of a vibrating blade microtome (Leica Microsystems, Nussloch, Germany) and 250 µm-slices were prepared.

The cardiomyocytes were selected according to the following criteria: The dye diffused into the initial cell within the first minute. The rectangular shape could be recognized. The cell should be localized within a fiber. The fiber displayed apparently regular contraction.

3.2.5.2 Dye coupling studies on adult mouse cardiac muscle slices

To examine gap junctional coupling slices were transferred into a submerged recording chamber. Glass capillaries prepared by a puller (P-97, Sutter Instrument Inc.) were filled with 2% (w/v) 6-carboxyfluorescein (Sigma). The pipette resistance was 30-40 MOhm. Pipette solution contained 120mM KCl, 4mM NaCl, 5mM glucose, 5mM EGTA, 10mM HEPES, 0.5mM $CaCl_2$ and 4mM $MgCl_2$ (pH 7.3). Individual cardiomyocytes were injected with the dye by iontophoretic injection for 4 min taking negative voltage pulses of 0.8 V (duration 500 ms, 1 Hz) using EPC-9 (HEKA Elektronik). Intracellular communication was monitored by fluorescence microscopy and optical images were recorded by a CCD camera. For fluorescence images filter set 46 was used (Zeiss; Exc. 500/20 nm, FT 515 nm, Em. 535/30 nm). The area of dye spread was quantified by software BioVision (Vision). The investigator was blinded to the genotype.

3.3 Biochemical methods

3.3.1 Preparation of total protein extract and quantification

3.3.1.1 Total protein extract from adherent cells

Cell culture medium was removed from culture dishes containing about 1×10^7 to 2×10^7 cells. The cells were rinsed twice with ice-cold PBS to remove medium. 200µl ice-cold lysis buffer was added to 150 mm culture dish (or 100µl lysis buffer to 100 mm culture dish). The cells were scraped in lysis buffer, and the cell suspension was collected and transferred into a 1.5ml microcentrifuge tube. The cell lysates were sonicated with a sonicator SH70G (Bandelin electronic GmbH) at 70% intensity four times for 10 seconds

each time with 10-15 second intervals on ice to rupture the cells and to shear nuclear DNA. The homogenate was centrifuged at 90,000 × g or more for 30 min at 4°C in a Beckman Table Top TL-100 ultracentrifuge. The resulting supernatant fraction was transferred to a 1.5ml microcentrifuge tube for protein concentration determination before use.

3.3.1.2 Total protein extract from tissues

Tissues from adult and embryonic mice were harvested in PBS on ice and snap frozen in liquid nitrogen. For total protein extraction, embryonic tissue samples were homogenized using a micro mortar and adult tissue samples were homogenized with an Ultra-Turrax T-8 (IKA®-Werk) in 1ml of lysis buffer per 250 mg wet weight. All samples were treated with a sonopuls sonicator SH70G (Bandelin electronic GmbH) at 70% intensity on ice until the lysis was completed. Cell debris and nuclei were separated by centrifugation at 90,000× g for 30 min at 4°C in a Beckman Table Top TL-100 ultracentrifuge. An aliquot of the solubilised protein solution was removed for protein quantification and the remaining solution was quick-frozen in liquid nitrogen and stored in aliquots at -80°C.

3.3.1.3 Protein quantification

For protein quantification, different methods were utilized. Either a commercial Bradford assay (Bio-Rad) or BCA assay (PIERCE) were performed using the protocols from manufactures. The protein concentration was determined before the addition of SDS-PAGE sample buffer. Bovine serum albumin (BSA) should be used as the protein standard. Protein concentration was quantified using plastic cuvettes in a spectrophotometer (GE Healthcare) at a wavelength of 595 nm in Bradford assay or SynergyHT multi-detection microplate reader (BioTek) at a wavelength of 562 nm in BCA assay. To improve accuracy each sample was measured in triplicates. The respective lysis buffer was used as the blank value.

3.3.2 SDS-polyacrylamide electrophoresis (SDS-PAGE)

The separation of proteins by molecular mass was carried out according to Laemmli's method (Laemmli, 1970). The protein solution was denatured by application of 2× Laemmli-buffer, 0.2% (v/v) ß-mercaptoethanol at 95°C for 5 min. Depending on the molecular mass of the protein, electrophoresis was performed with 6-12% acrylamide gels at 60-120 volts in a mini gel chamber SE 250 (Hoefer™) in 1× electrophoresis buffer. A prestained protein ladder was applied to estimate the size of the proteins.

3.3.3 Western blotting

The SDS protein gel was transferred to a hybond-C extra nitrocellulose-membrane (GE Healthcare). Membrane, Whatman 3MM filter paper and fiber pads were equilibrated in transfer buffer. The transfer was performed in a Trans-Blot Cell (Bio-Rad) at 70 V for 1 h and 40 V for 2 hours while cooling or o/n at 20 V and 4°C. The membrane was stained with Ponceau S to confirm the transfer. For immunodetection the membrane was incubated in blocking solution for 60 min and with the specific first antibody diluted in PBS with 5% skim milk for 2 h at RT or o/n at 4°C. The membrane was washed 1× with PBST, and 2× with PBS for 15 min each. Horseradish peroxidase-conjugated goat anti-rabbit IgG (GE Healthcare), goat anti-mouse IgG (Calbiochem), and donkey anti-goat IgG (Santa Cruz Biotechnology, Inc.) were used as the secondary antibodies diluted 1:2000 in PBS with 5% skim milk and incubated with the membrane for 60 min at RT. The membrane was washed as described above and developed by chemiluminescence staining using ECL (SuperSignal West Pico Chemiluminescent Substrate or SuperSignal West Femto Maximum Sensitivity Substrate, Pierce) according to manufacturer's instructions. The chemiluminescence was detected in an Intelligent Dark Box with a LAS-1000 CCD camera (both FUJIFILM). To re-probe the membrane with a different antibody, it was washed with PBST, incubated for 30 min at 50°C with stripping solution, washed again with PBST, and developed by chemiluminescence staining using ECL to confirm complete

absence of the signal. The membrane was blocked again for 60 min before incubating with the first antibody.

3.4 Animal procedures

3.4.1 Setting up timed matings and dissection

Timed matings were set up in the afternoon and the morning of detecting a vaginal plug was regarded as day 0.5 post conception (E0.5 or 0.5 d.p.c). Pregnant mice were sacrificed following institutional guidelines and the German animal protection law. Embryos were harvested at different stages of development. The exact developmental stage of embryos was determined by the number of somites. Whole mount embryos for immunohistology were fixed o/n in freshly prepared 4% PFA in PBS, pH 7.4 at 4°C. In order to prepare protein lysates for expression analysis hearts were dissected in PBS, quick-frozen, and stored at -80°C. For RNA studies, hearts were dissected in RNase free PBS and treated as described in section 3.1.8.

3.4.2 Preparation of paraffin sections

Whole mount embryos were processed through a series of increasing graded alcohol concentrations. The embryos were transferred sequentially to 70%, 80%, 90%, 96%, and 100% ethanol for two hours each. They were then placed in a second 100% ethanol solution to ensure that all water was removed. Xylol was used as clearing agent 2× for 20 min. Embryos were embedded either sagittally or transversally and 5µm sections were cut on the microtome HM355S (MICROM). Up to 6 sections were placed on 3-aminopropyltriethoxysilane (APTEX) coated slides and stored at RT.

3.4.3 Immunoperoxidase staining

PFA fixed and paraffin embedded tissue sections were baked at 60°C for 1h, then deparaffinized in xylenes/graded ethanol and rinsed in PBS twice. Antigens were unmasked by heat treatment with 10 mM sodium citrate buffer, pH 6.0 at 95°C for 5 min. Slides were

cooled down in the buffer for approximately 20 min and washed in ddH_2O 3× for 2 min each. Excess liquid was aspirated from slides. Specimens were incubated for 1 hour in goat blocking serum in PBS and then incubated with primary antibodies for 30 min at RT or o/n at 4°C. Optimal antibody concentration was determined by titration and listed in table 4. Unbound antibodies were removed by washing three changes of PBS for 5 min each. After incubation with biotin-conjugated secondary antibody diluted in PBS with 1.5% normal blocking serum for 30 min, excess secondary antibody was washed away with PBS. Then ABC Elite reagent (Vector Laboratories, Burlingame, CA) were used, sections were developed with DAB kit (Dako, Glostrop, Denmark) and counterstained with hematoxylin (Sigma-Aldrich, Germany) according to manufacturer's instructions. Specimens were dehydrated through alcohols and xylenes, mounted with permanent mounting medium and covered with a glass coverslip. Pictures were taken by a light microscope (Leica DMI 6000B).

3.4.4 H&E staining

Before staining of the sections, all traces of wax had to be removed with two incubation steps in xylol for 5 min. The sections were rehydrated sequentially in 100%, 96%, 90%, 80%, 70% ethanol, and H_2O for 5 min. The staining of the nuclei was performed with 20% Mayer's haemalaun solution (Merck) for 1 min then developed under the running tap water for 5 min. The cytoplasm and connective tissue were counterstained pink with 1% eosin solution for 2 min. Stained sections were dehydrated through a series of increasing graded alcohol concentrations (70%, 80%, 90%, 96%, and 100%) and cleared 2× with xylol for 5 sec before mounting with canada balsam (Merck) and cover slips. Multiple serial sections were analyzed for each developmental stage and genotype on the CK30 microscope with bright field (Olympus).

3.4.5 PAS staining

Sections were brought to water via xylene and ethanol. Sections were placed into 1% periodic acid for 10-30 min. After rinsing 3× with distilled water, the sections were well washed under running tap water and transferred into Schiff's reagent for 10-30 min. Then Schiff's reagent was washed off with distilled water and the sections were washed with tap water for about 10 min. Slides were counterstained with Mayer's hemalum for 2 min then developed with tap water until hemalum was blued. Dehydration and mounting steps were same as previously described in section 3.4.3

3.4.6 Trichrome staining

Paraffin embedded tissue slides were deparaffinized and rehydrated as described before. Tissues were fixed with Bouins solution o/n. Slides were rinsed under running tap water for 60 min, and then briefly washed with ddH_2O. Nuclei were stained in Weigerts haematoxylin working solution for 7 min, then developed under running tap water for 7 min. Sections were stained with Biebrich-Scarlet-Acid fuchsin solution for cytoplasma. After rinsing with ddH_2O, slides were put in phosphotungstic/phosphomolybdic acid working solution for 4 min, and then transferred directly into aniline blue for 5 min in which collagen will be stained. Sections were fixated and differentiated in 1% acetic acid, then rinsed with ddH_2O, dehydrated very quickly through 95% ethanol and 100% ethanol, clarified in xylene and mounted with mounting medium.

3.4.7 Immunoperoxidase staining

PFA fixed and paraffin embedded tissue sections were baked at 60°C for 1h, then deparaffinized in xylenes/graded ethanol and rinsed in PBS twice. Antigens were unmasked by heat treatment with 10 mM sodium citrate buffer, pH 6.0 at 95°C for 5 min. Slides were cooled down in the buffer for approximately 20 min and washed in ddH_2O 3× for 2 min each. Excess liquid was aspirated from slides. Specimens were incubated for 1 hour in

goat blocking serum in PBS and then incubated with primary antibodies for 30 min at RT or o/n at 4°C. Optimal antibody concentration was determined by titration and listed in table 4. Unbound antibodies were removed by washing three changes of PBS for 5 min each. After incubation with biotin-conjugated secondary antibody diluted in PBS with 1.5% normal blocking serum for 30 min, excess secondary antibody was washed away with PBS. Then ABC Elite reagent (Vector Laboratories, Burlingame, CA) were used, sections were developed with DAB kit (Dako, Glostrop, Denmark) and counterstained with hematoxylin (Sigma-Aldrich, Germany) according to manufacturer's instructions. Specimens were dehydrated through alcohols and xylenes, mounted with permanent mounting medium and covered with a glass coverslip. Pictures were taken by a light microscope (Leica DMI 6000B).

3.4.8 Preparation of cryosections

Dissected and fixed embryos were equilibrated with 30% sucrose in PBS for 6 h at RT. For cryosections, embryos were embedded sagittally in Tissue Tek® (OCT Compound, Vogel) and 5µm sections were cut using the cryostat (Cryocut 3000, Leica) at -20°C to -25°C and placed on 3-aminopropyl-triethoxysilane (APTEX) coated slides. Slides were immediately used for immunofluorescence staining or stored at -20°C.

3.4.9 Immunofluorescence staining

3.4.9.1 Immunofluorescence staining of cells

Cells were washed in PBS and fixed with ice-cold methanol for 15 min at -20°C. After washing and permeabilization, cells were blocked with 2% BSA and 1% normal goat serum in PBS for 30min, incubated with primary antibody (diluted in PBS) for at least 1h in wet chamber at RT (100µl for each coverslip) and then washed with PBS. Secondary antibody (diluted in PBS) was applied for 30 min at RT in wet chamber. Nuclei were stained for 30 min with DAPI diluted 1:2000 in PBS together with secondary antibodies. Immu-

nofluorescence stained cells were washed with PBS, rinsed with water, mounted with fluorescence protecting medium Fluorescent Mounting Medium (DakoCytomation) and dried o/n.

3.4.9.2 Immunofluorescence staining of cryosections

Prior to staining, sections from PFA perfused animals or embryos were air dried, re-fixed with 4% PFA for 15 min, rinsed with PBS, blocked and permeabilized (with 10% goat serum, 0.3% Triton X-100, 0.2% BSA in PBS) for 1 hour. Cryosections were incubated for 2 hours at RT or o/n at 4°C with primary antibodies in a wet chamber, followed by rinsing with PBS. The fluorescent-conjugated secondary antibodies were applied 1:1000 in PBS. DAPI was used to stain nuclei. Sections were incubated for 2 hours at RT, and followed by washing and mounting procedures.

3.4.10 Tamoxifen injection

Tamoxifen stock solution was prepared in peanut oil with the concentration of 10mg/ml and stored at -20°C in aliquots (Kuhbandner et al., 2000). For the tamoxifen treatment of the inducible heart specific CAR KO mice, the dosage of 30mg tamoxifen/kg B.W. was used. For neonatal mice, the mice were properly marked and carefully weighted before the intraperitoneal injection. The injection started from P6 and lasted for 10 days. For adults, only male mice were used for intraperitoneally injection, 5 times per week, for two weeks. The hearts were harvested at 2, 3, 3.5, 4, 8, 12 or 14 weeks after the first injection started.

3.4.11 Virus infection

cDNA-generated CVB3 Nancy (Kandolf and Hofschneider, 1985) was grown and propagated in Vero cells. Stock virus was prepared by 3× freezing and thawing and purified by sucrose gradient centrifugation. The same stock was used to infect mice by intraperitoneal

injection with 5×10^4 plaque-forming units (pfu) of purified CVB3 3 months after induction with tamoxifen. No background specific differences in virus infection between the mixed 129SVJ/C57black6 and either parental strain were detected (data not shown). Animals were sacrificed at 10 or 28 days post injection with virus (p.i.), non-infected knockout and Cre-negative animals were used as controls. Prof. Dr. Karin Klingel and Dr. Martina Sauter performed virus infection and the following *in situ* hybridizations in Tübingen University.

3.4.12 *In situ* hybridization and quantification of CVB3 infection

CVB3 RNA in paraffinated tissue sections was detected by radioactive *in situ* hybridization. At the indicated time points, tissue samples were fixed in 4% paraformaldehyde/ 0.1 M sodium phosphate buffer (pH 7.2) and embedded in paraffin for detection of viral RNA using α-^{35}S-labeled enterovirus-specific RNA probe as previously described (Klingel et al., 1992). Tissue sections were exposed for 3 weeks and counterstained with hematoxylin and eosin. The detection of replication is a robust and sensitive method to document virus infected cells. Lacking sensitive assays for virus entry *in vivo* and since CAR has never been implied in replication of CVB3, *in situ* hybridization was considered the best way to detect replication as a measure for virus entry dependent on CAR. To quantify the area fraction of infection, ImageJ v.14.1k (http://rsb.info.nih.gov/ij) was used as outlined in the user manual.

3.5 Confocal microscopy

Protein localization was documented using Carl Zeiss Laser Scanning Microscope LSM 5 Pascal Version 3.0 SP2 with Carl Zeiss PLAN-NEOFLUAR 40×/100× objective lens (1.3 NA) or beam scanning confocal microscope Leica TCS SP5 equipped with 63× HCX PL APO oil immersion objective lens (1.32 NA). Images were exported from the LSM 5 Image Browser (Zeiss) or LAS AF software (Leica) and processed with and Photoshop CS2.

3.5.1 3D reconstruction

The confocal microscope pictures of one cardiomyocyte were taken by serial scanning from top to bottom. The 3D reconstruction of the dataset was created using the Meta Imaging Series Software (Molecular Devices). Each image section was aligned and stacked one on top of another to create a three-dimensional volume calculated using the 3D reconstruction tool of Metamorph 7.1.7.

3.6 Surgical procedures

3.6.1 Hemodynamic measurements

The hemodynamic measurements were performed by Dr. Dirk Westermann. The animals were anesthetized (thiopental 125 mg/kg i.p.), intubated, and artificially ventilated (n=30). As recently described, a 1.4 F microconductance pressure catheter (ARIA SPR-719; Millar-Instruments, Inc., Texas, USA) was positioned in the left ventricle (LV) for continuous registration of LV pressure–volume (PV) loops in an open-chest as described previously in a closed-chest model (Westermann et al., 2007). Calibration of the volume signal was obtained by hypertonic saline (10%) wash-in technique (Steendijk et al., 2001). Systolic function was quantified by LV end-systolic pressure (LVP, mmHg) and dP/dt_{max} (mmHg/s) as an index of LV contractility. Diastolic function was measured by LV end-diastolic pressure (LVEDP, mmHg) and dP/dt_{min} (mmHg/s). Global cardiac function was quantified by the end systolic and diastolic volume (ESV and EDV, µl), ejection fraction (EF, %-calculated) and heart rate (HR, beat/min).

3.6.2 Surface ECG and *in vivo* electrophysiology studies

Each mouse was lightly anesthetized with isoflorane (1.6 Vol% isoflorane/air) and ECG standard intervals were measured in 6-limb leads as described previously (Royer et al., 2005) (n=6 for neonates, n=16 for adults) by Dr. Robert Fischer. The severity of the AV conduction defect was graded according to standard clinical diagnostic criteria. As AV-

block first degree is not defined for mouse, the classification was based on the distribution of PR intervals in the control group of this study (mean + 2×SD). Thus, in adults, PR intervals > 48 ms were considered as prolonged. Additional intermittent block of a single AV-conduction was classified as AV-block second degree. Third degree (complete) heart block was diagnosed when no atrial impulse propagated to the ventricles.

3.6.3 Arteriovenous (AV) shunt

Mice at 8 weeks of age were anesthetized with 1% isoflorane and placed supine at 37°C on a heating pad. A ventral abdominal laparotomy was performed. The intestines were displaced laterally and wrapped with normal saline-soaked sterilized gauze to retain moisture. The aorta and vena cava between the levels of renal arteries and iliac bifurcation were then exposed by blunt dissection of the overlaying adventitia. Both vessels were temporarily occluded proximal and distal to the intended puncture site. A needle (18 gauge) held on a plastic syringe was inserted into the exposed abdominal aorta and advanced through the medial wall into the vena cava to create the shunt. The needle was inserted and withdrawn across the medial wall several times through the same hole, to ensure the size and presence of the shunt, before it was finally withdrawn from the aorta. The ventral aortic puncture site was immediately sealed with a drop of cyanoacrylate (All Purpose Instant Krazy Glue®, Krazy Glue) after withdraw of the needle. The sham procedure was identical except that the vessels were not perforated.

3.7 Statistics

For statistical analysis, GraphPad Prism 5.0 software was used. Results are expressed as means ± SEM. Statistical significance between groups was determined using the Mann Whitney U test for hemodynamic and electrophysiology data. Expression values were compared using an unpaired two-tailed t test to assess differences between two groups. The significance level was chosen as $P<0.05$.

4 Results

Both complete CAR KO and adult cardiac specific inducible CAR KO models were established. Germline deletion of CAR is embryonic lethal secondary to cardiac malformation and malformed myofilaments. With the conditional heart specific deletion of CAR in the adult mouse, the roles of CAR as a virus receptor were investigated. Loss of CAR can prevent CVB3 induced myocarditis and pathological changes *in vivo*. The cardiac analysis revealed novel physiological functions of CAR that facilitate the evaluation of potential side effects of a CAR directed antiviral therapy.

4.1 Generation of the coxsackievirus and adenovirus receptor (CAR) conventional and tissue specific conditional knockout model

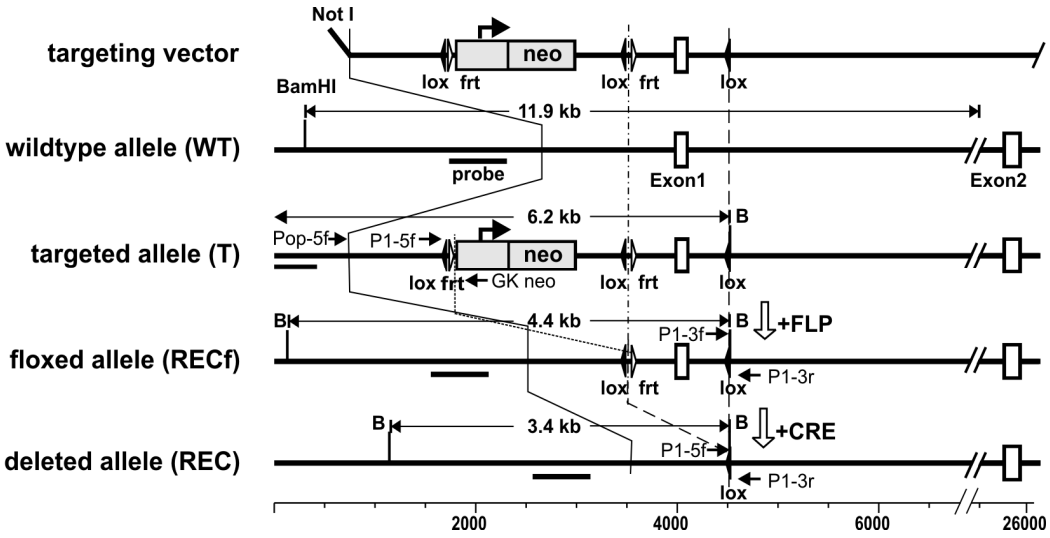

Figure 4: Outline of the targeting strategy. Exon 1, which contains the translation start, was replaced with the floxed exon 1 and the FRT flanked neo-cassette. The neo-cassette was subsequently removed by germline expression of the FLP recombinase. A conventional CAR KO and an inducible heart specific CAR KO using the MerCreMer fusion protein (MCMcre) were generated. Scale bar: 1000bp. neo: neomycin, lox (locus of x-over) sites, FLP: FLP recombinase, frt: FLP recombination target, Cre: control of recombination recombinase.

The targeting vector for the CAR KO was generated by Dr. Michael Radke in the lab. Cre-mediated recombination was used to generate CAR deficient mice. Exon 1 together with part of 5' UTR was replaced with the floxed exon 1 and the FRT flanked neo-cassette. The neo-cassette was subsequently removed by germline expression of the FLP recombinase, which works on FRT site (Fig. 4).

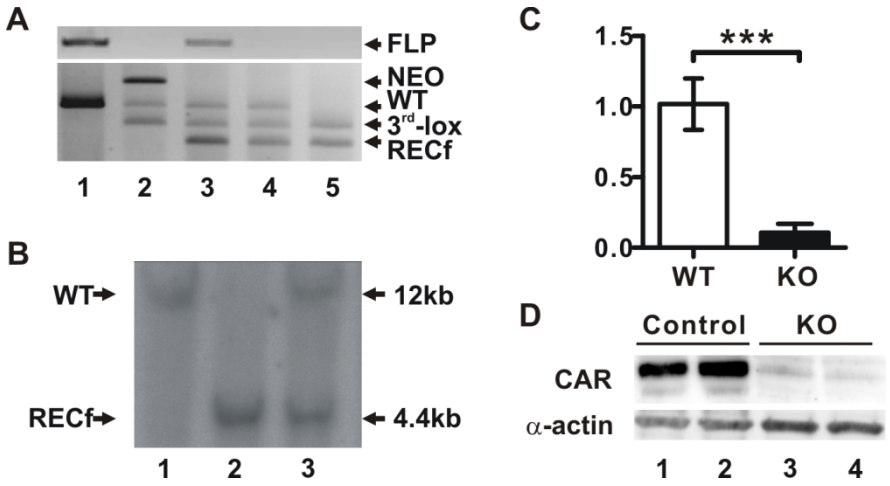

Figure 5: Verification of inducible heart specific CAR KO model. A) PCR based genotyping using the primers indicated in Figure 4 was used to detect the fragments corresponding to wildtype (WT), NEO, 3rd-lox, and RECf allele. The colony was established by mating FLP transgenics (1) to targeted animals (2). The resulting double heterozygous animals (3) were used to obtain floxed heterozygous (4) and homozygous animals (5). B) For Southern blot genomic DNA was digested with BamHI, hybridized with a 600 bp PCR product (probe). The 12 kb WT allele and the 4.4 kb RECf allele were used to distinguish wildtype (1), knockout (2), and heterozygous animals (3). C) After tamoxifen injections CAR mRNA expression dropped to < 10% in KO animals (n=8 for WT, n=15 for KO, *** P≤0.001). D) Protein levels as determined by western blot (CAR compared to α-actin) followed at 2weeks (3) and 14 weeks (4) as compared to two sets of controls – vehicle (Vh) injected MCM+ (1) or tamoxifen treated MCM- (2) animals.

To generate the inducible heart specific CAR knockout mice, floxed animals were bred with transgenic mice that harbored the heart specific mutant estrogen receptor fusion protein (MerCreMer) (Peng et al., 2007). MerCreMer is activated by injection of tamoxifen. After a 2-week injection regimen (30mg tamoxifen/ kg B.W. /d; 5 injections per week), a reduction in CAR mRNA and protein levels was achieved (Fig. 5C, D). After one week of tamoxifen injections CAR mRNA expression dropped to < 10% in KO animals and the

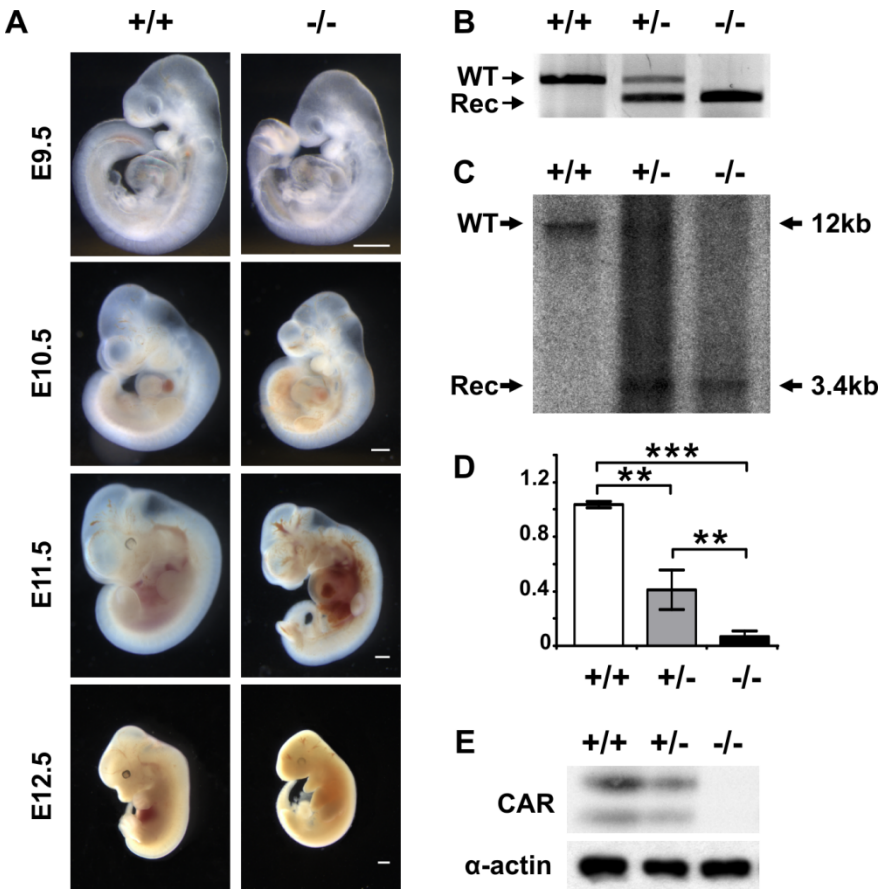

Figure 6: Conventional CAR KO leads to embryonic lethality. A) Time course of WT and conventional KO embryos from E 9.5 to 12.5. Embryos started to exhibit morphological changes from E10.5 and cardiac hemorrhage was often seen in E11.5. After E11.5, embryos went to the progress of resorption. (Size bar: 500μm). B) Both wildtype (WT) and recombinated signal (Rec) signal could be detected in heterozygous animals by PCR genotyping. In KO embryos, only Rec was present. C) Southern blot verificated that in KO embryos, only a 3.4kb Rec signal band was detectable. D) TaqMan assay showed CAR mRNA levels reduced in heterozygous and absent in KO (n=6, ** P≤0.01; *** P≤0.001). E) Western blot showed the CAR protein typically appears as a doublet as 42/46 kDa in WT and heterozygous but not in KO. Blots were reprobed with an anti-α-actin antibody to confirm equal loading (repeated at least 6 times).

low levels were maintained as far as we checked for at least 16 weeks. Protein levels were determined by western blot followed at 2 and 14 weeks as compared to two control animals (vehicle injected MCM+ and tamoxifen injected MCM-). α-actin was used as a loading control to confirm the even loading (Fig. 5D).The primers indicated in Figure 4 was used to detect the fragments corresponding to wildtype (WT, 419 bp), NEO (536 bp), 3rd-lox (349 bp), and RECf (297 bp) allele by PCR genotyping (Fig. 5A). For Southern blot,

the 12 kb WT allele and the 4.4 kb RECf allele were used to distinguish wildtype, knockout, and heterozygous animals (Fig. 5B).

The conditional mouse model was converted into a constitutive mouse model. Therefore, the animals with floxed exon 1 were crossed with transgenic mice expressing Cre under the control of the protamine promoter (The Jackson Laboratory) (Fig. 4). CAR expression is undetectable from day E9.5 in KO embryos. PCR analysis of DNA for wild type, heterozygous and homozygous knockout revealed a 419 bp product for wild type allele (WT) and a 251 bp band for recombinated allele (Rec) (Fig. 6B). For Southern blot genomic DNA was digested with BamHI, hybridized with a 600 bp PCR product (probe). Wildtype mice showed a 12 kb hybridization signal while a 3.4 kb signal for the disrupted knockout allele presented as expected in Southern blot analysis. Both hybridization signals were detected for heterozygous animals (Fig. 6C). TaqMan assay of CAR mRNA expression level and Western blots of total embryonic protein on SDS-PAGE confirmed the result that the mRNA and protein were undetectable in homozygous knockout embryos (Fig. 6D, E).

4.2 CAR is required for the early embryonic development

4.2.1 Deletion of CAR causes embryonic lethality at midgestation

So far, not a single homozygous KO was obtained in more than 800 offspring from breedings ($CAR^{+/-} \times CAR^{+/-}$) that should produce theoretically 25% CAR KO animals, suggesting that $CAR^{-/-}$ animals died during embryonic development or shortly after birth.

To explore when the death occurred, the timed matings were set up between heterozygous animals. More than 1000 embryos were examined between the age of E8.5 and E13.5. $CAR^{+/+}$, $CAR^{+/-}$ and $CAR^{-/-}$ embryos showed a proper Mendelian proportion 1:2:1 until E9.5. $CAR^{-/-}$ live embryos (indicated by beating heart) started to decrease from E10.5 to E11.5. Beyond E11.5, all the $CAR^{-/-}$ embryos were found undergoing resorption or al-

ready resorbed. Genotyping resorption bodies confirmed the homozygous deletion of CAR. These results indicated that germline deletion of the CAR allele resulted in midgestation lethality around embryonic day 10.5 to 11.5 (Table 11) and resorption from E11.5 (Fig. 6A).

Table 11: progeny from heterozygote intercrosses

d.p.c.	+/+	+/-	-/-
E9.5	**77 (21.3%)**	**194 (53.7%)**	**90 (25.8%)**
E10.5	**123 (28.6%)**	**227 (52.8%)**	**80 (18.6%)**
E11.5	**75 (34.9%)**	**106 (49.3%)**	**34 (15.8%)**
E12.5	**13 (26.5%)**	**36 (73.5%)**	**0 (0%)**
E13.5-15.5	**8 (53%)**	**7 (47%)**	**0 (0%)**

Number and percentage of live offspring from $CAR^{+/-} \times CAR^{+/-}$ matings. d.p.c: days post coitum.

4.2.2 CAR deficiency causes heart and vessel malformation

Up to E9.5, there was no obvious difference between WT and KO. Knockout and wild-type embryos showed proper development of a beating heart. The CAR deficient embryos started to show delayed development from E10.5, indicated by the body size of embryos (Fig. 6A). Cardiac morphological changes in conventional KO mice were observed after E10.5. Cardiac hemorrhage was more frequent in KO embryos (Fig. 6A and Fig. 7B). The KO embryonic body was loosely organized and fluffy. Blood leaked out and accumulated in the pericardial and peritoneal cavity. The enlarged space inside the pericardium and the manifested prominence of the ventricle part were present in E10.5 KO embryos, suggestive of a severe cardiac dysfunction (Fig. 7A). On histological examination, the ventricular wall was abnormally thickened (Fig. 7C a-d). Endocardial cushion and atrium chamber were enlarged in KO embryos (Fig. 7C). Aorta and cardinal veins were slightly enlarged and malformed in KO embryos (Fig. 7C g, h). The atrium wall and the atrioventricular canal are essentially normal. From E11.5 knockout embryos failed to thrive. The yolk sac and the yolk sac vessels were unchanged. No obvious changes in collagen and

glycogen storage were observed with trichrome staining (Fig. 7C c, d) or periodic acid Schiff's staining (Fig. 7C e, f).

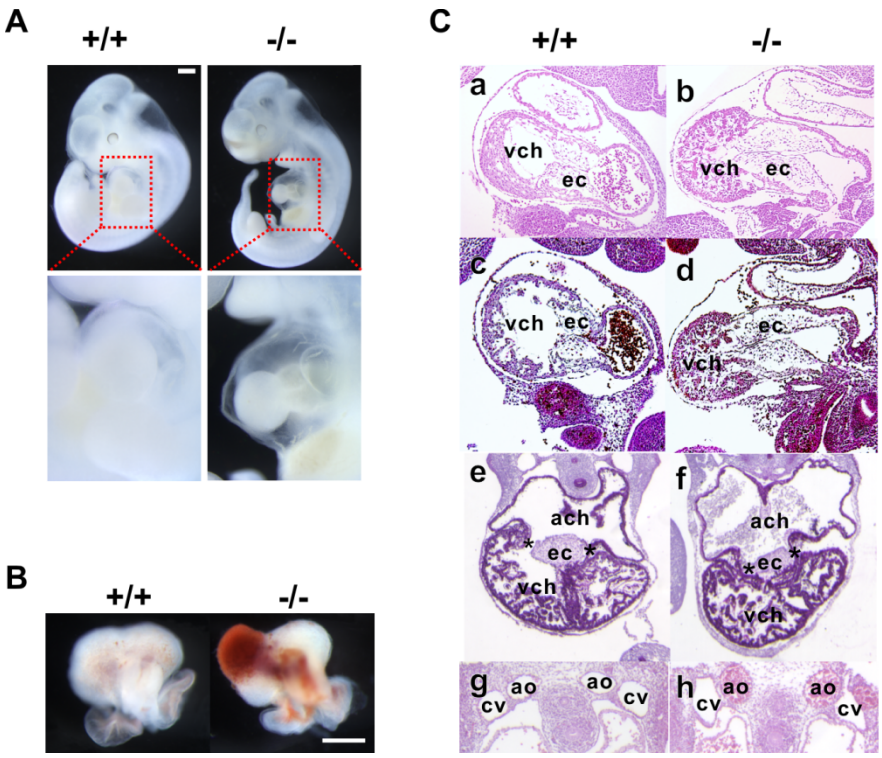

Figure 7: Morphological changes in conventional KO mice. A) Embryonic analysis showed enlarged space inside the pericardium in conventional CAR KO mice at E10.5. Bar, 0.5 mm. B) Cardiac hemorrhage was more frequent in KO embryos. Bar, 0.5 mm. C) Histology at E10.5 (H&E a, b, trichrome staining, c, d) and E11.5 (Shiffer's staining, e, f, H&E, g, h) indicated an increase in ventricular wall thickness (a-d). Endocardial cushion and atrium chamber were enlarged in KO embryos (a-d, e, and f). Aorta and cardinal veins were slightly enlarged in KO embryos (g, h). No obvious collagen and glycogen storage change were observed. Abbreviations: ach, atrium chamber; vch, ventricular chamber; ec, endocardial cushion; ao, aorta; cv, cardinal vein;*, atrioventricular canal.

4.2.3 Myofibril disorganization in knockout embryonic cardiac cells

Since the major abnormalities were observed in embryonic heart in CAR deficient animals, the investigation was focused on the cardiomyocytes. Co-staining CAR with monoclonal antibody α-actinin (a z-disc protein) revealed that myofibril organization disruption in CAR KO embryos (Fig. 8). In both cryosections and primary cultured

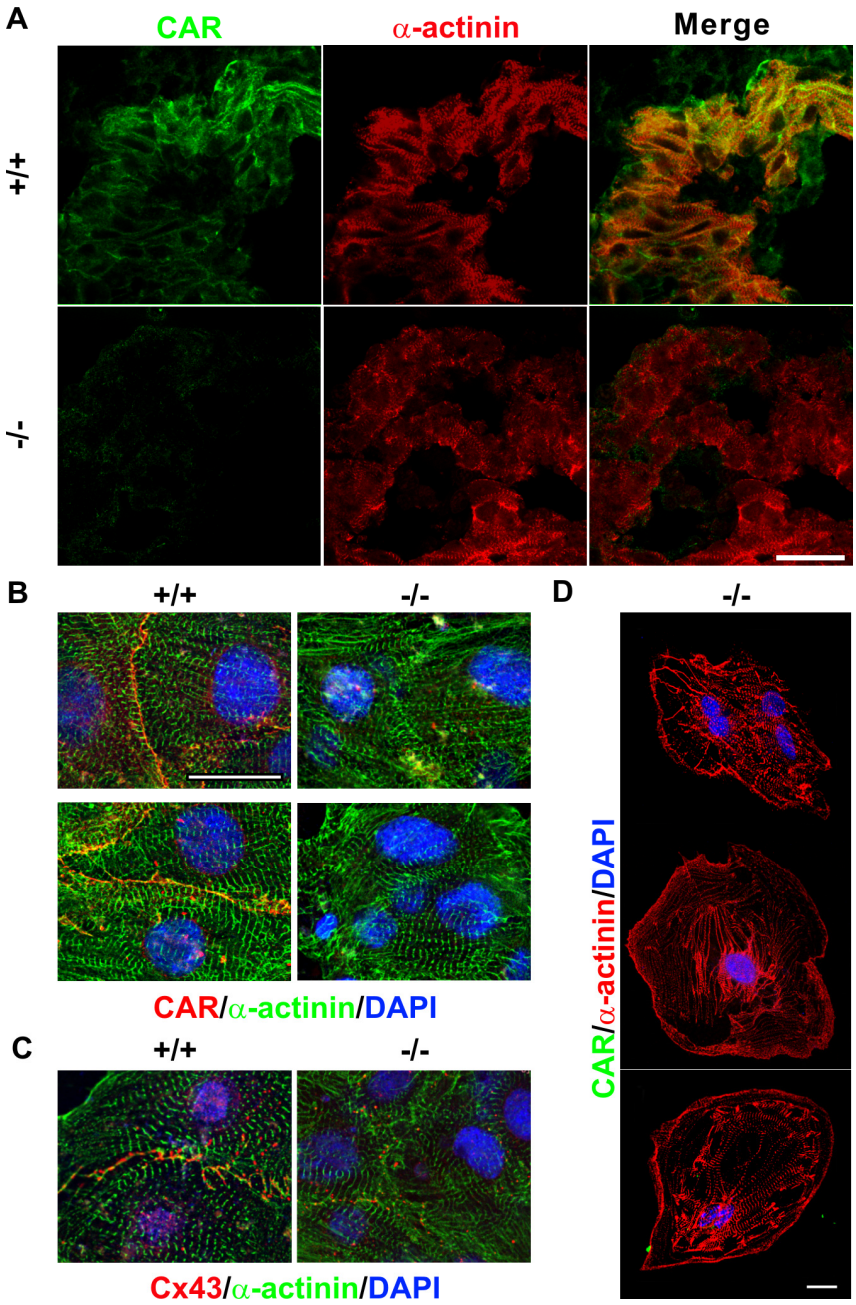

Figure 8: Embryonic cardiomyocytes staining. A) CAR was dominantly expressed at the cell-cell contact between WT cardiomyocytes (green). Myofibers showed normal orientation and striation as stained by anti-Z disc protein α-actinin in red. No CAR expression was detected in KO. The myofibrils were shortened and disorganized in KO heart. B) Co-staining of CAR (red) with α-actinin (green). CAR was expressed along the cell-cell contacts in $CAR^{+/+}$ cells, myofibrils were well organized and the transition between adjacent cells were normal. CAR did not express in $CAR^{-/-}$ cells, and the myofibrils were disorganized and the transition was discontinued between adjacent cardiomyocytes. C) Co-staining of Connexin43 (red) with α-actinin (green) revealed that in $CAR^{-/-}$ cells, Cx43 expression was reduced. D) Three examples of $CAR^{-/-}$ cardiomyocytes with disorganized myofibrils stained with α-actinin (red)**.** Size bar: 25µm.

cardiomyocytes from wildtype E10.5 embryos, the myofibrils were well assembled and continuously transitioned between adjacent cardiomyocytes and showed normal striation. In contrast, myofibrils of CAR deficient myocytes were more diffuse, shortened and disorganized as compared to wildtype (Fig. 8).

In some individual CAR KO cardiomyocytes, as showed in figure 8D, the Z-discs were so narrow that appeared as spotted aggregates instead of striated pattern.

4.2.4 The structure of ependymal cells in the brain was disrupted

The ventricles of the brain and the central canal of the spinal cord are lined with ependymal cells. They form tight junctions and control the exchange of substances between these nervous tissue and cerebrospinal fluid (CSF) as the blood-CSF barrier. High levels of CAR mRNA and protein expression were observed in the embryonic brain. The mRNA level at E11.5 is more than 2-fold higher than that in E9.5 (Fig. 18H). From immunofluorescence staining studies of E11.5 embryos, it was found that in wildtype embryos, CAR was predominately expressed in ependymal cells and the choroid plexus (Fig. 9A, B). While normal ependymal cells formed a simple cuboidal or low columnar epithelium, in CAR deficient embryos, the structure of ependymal cells was disrupted and the formation was not preserved (Fig. 9C).

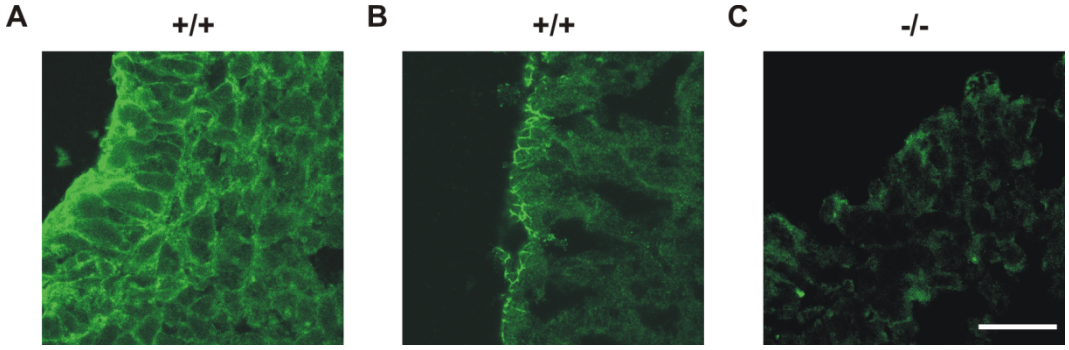

Figure 9: CAR expression in brain. A) CAR expression was detected in epithelial cell-cell contacts within ependymal cell layer lining the ventricles at E11.5. B) The epithelial cells of choroid plexus also expressed CAR at E11.5. C) CAR expression was undetectable in KO brain, and the epithelial structure was disrupted.

4.2.5 Expression levels of connexins and apolipoproteins are altered in the embryonic CAR KO heart

Towards a better understanding of the molecular basis underlying the embryonic lethality in CAR KO mouse, microarray analysis was used to compare expression levels between wildtype, heterozygous and knockout embryonic heart. Since some of E10.5 embryos are already in the progress of resorption, in order to minimize secondary effects, total mRNA pools from nine E9.5 hearts of each genotype was used for the microarray experiment. Due to the limited sample resource, only one pool was analyzed per genotype. There were 296 probe sets which represent around 270 genes was significantly changed between genotypes (≥2 fold, 60 of which ≥3 fold). Those genes were annotated and classified according to the subcellular localization and function respectively. 39% affected genes were localized extracellular and 19% were membrane proteins (Fig. 10A). 20% for the regulated genes were involved in signaling and 17% in metabolism, furthermore, 11% related to lipid metabolism (Fig. 10B). The lists of select affected genes are provided in appendix (Table 12, 13).

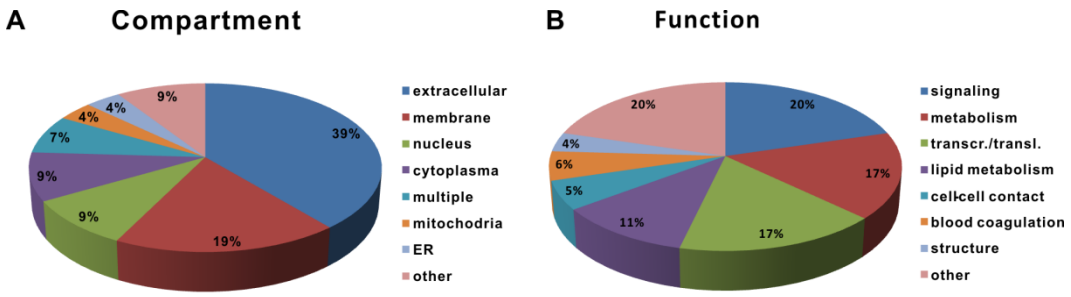

Figure 10: The classification of changed genes according to Affymetrix screen on E9.5 hearts. 296 probe sets which represent around 270 genes was significantly changed between genotypes (≥2 fold, 60 of which ≥3 fold). A) According to the subcellular localization, 39% affected genes were localized extracellular and 19% were membrane proteins. B) As annotated and classified according to the functions, 20% for the regulated genes were involved in signaling and 17% in metabolism, furthermore, 11% related to lipid metabolism.

Microarray results showed dramatic increase of apolipoproteins, such as Apo A-I, Apo B, Apo C2 and Apo M, together with the main HDL receptor cubilin. To verify the microarray results, the expression levels of some altered genes were tested using independent pools from mouse embryonic heart at E9.5 (3 pools) and E11.5 (1 pool) (Fig. 11). The increase of Apo A-I and the corresponding receptor cubilin was confirmed at both stages (Fig. 11A, E). While the rest of tested genes did not show altered expression level at E9.5, the expression pattern of those genes changed mostly in E11.5 embryonic heart. The mRNA levels of the connexins, Cx40, Cx43 and Cx45 were reduced, especially for Cx45 (>50%) (Fig. 11F). ZO-1 and MUPP-1 mRNA levels were decreased >30%, while Asph and N-cadherin levels had relative stable (Fig. 11G). Notably, fos mRNA level had increased more than 100%, and atrial natriuretic factor (ANP) mRNA decreased to 25% compared to wildtype (Fig. 11H).

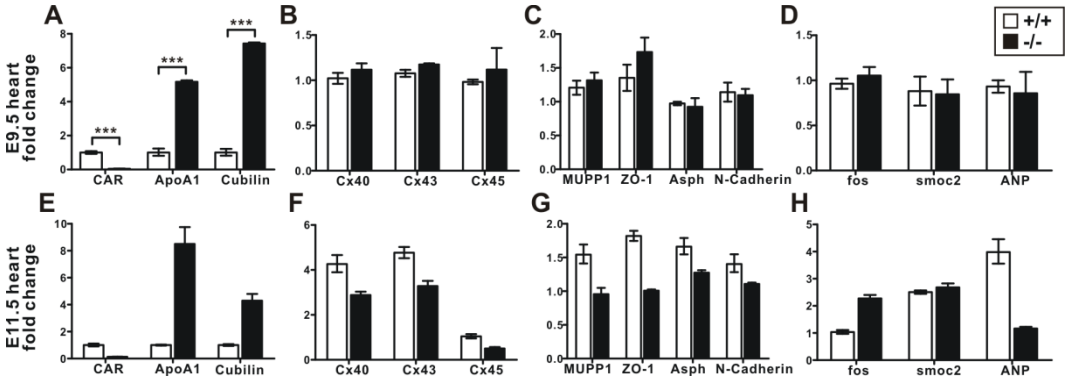

Figure 11: mRNA levels of genes that might be regulated by loss of CAR. A-D) mRNA levels of E9.5 heart was analyzed by 3 different pools for each genotype. CAR expression was absent in KO heart, with increased level of Apo A-I and cubilin (A). The expression levels of other genes were largely unchanged (n=3 per group, *** $p \leq 0.001$, all dada was normalized to the expression level of 18S RNA, and the corresponding WT expression level of each gene was set to 1.) E-H) mRNA expression levels of E11.5 heart. Only one pool for each genotype was analyzed, hence statistical significance was not able to show. Similar trend of Apo A-I and cubilin increase could be observed (A). Connexins, MUPP1, ZO-1, Asph, N-cadherin and ANP showed a trend of decrease and fos showed a trend of increase (F-H). Smoc2 expression levels stayed unchanged in both E9.5 and E11.5 (D, H). (All data was normalized with 18S RNA and WT CAR expression level was set as 1.)

The protein changes of several regulated genes were investigated by western blot using total protein extracts from whole E10.5 and E11.5 embryos (Fig. 12). Coincident with what was observed by qPCR, Cx43 and Cx45 were also reduced at protein level in the whole embryo (Fig. 12A) as well as in cardiomyocytes (for Cx43, Fig. 8C). ZO-1, N-cadherin and Apo A-I did not show any change of total protein expression (Fig. 12A), suggesting the change of those proteins might be tissue or organ specific, or there could be compensatory expression in other tissues or organs. Especially for Apo A-I, expression increased dramatically during the development (Fig. 12B).

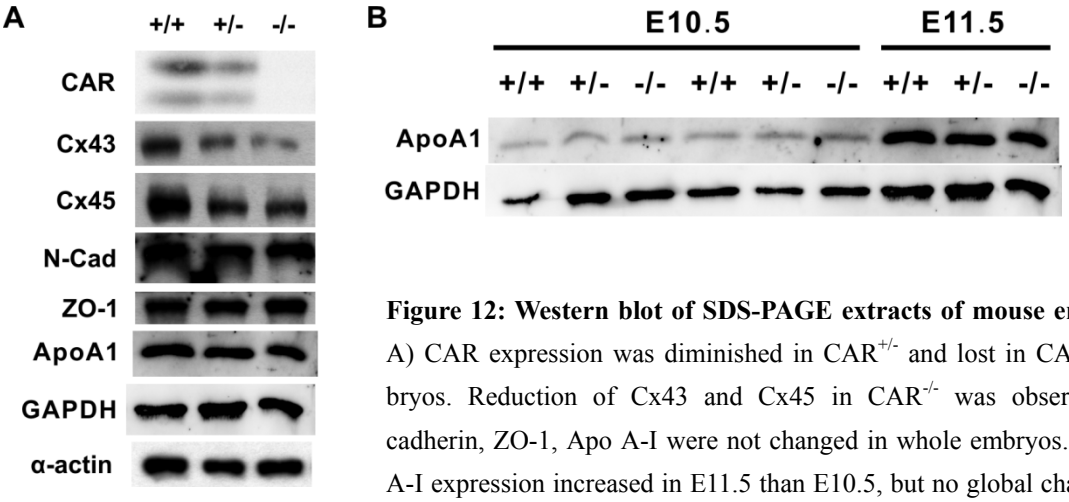

Figure 12: Western blot of SDS-PAGE extracts of mouse embryos. A) CAR expression was diminished in $CAR^{+/-}$ and lost in $CAR^{-/-}$ embryos. Reduction of Cx43 and Cx45 in $CAR^{-/-}$ was observed. N-cadherin, ZO-1, Apo A-I were not changed in whole embryos. B) Apo A-I expression increased in E11.5 than E10.5, but no global change between genotypes. GAPDH and α-actin were used as loading controls.

4.3 Cardiac deletion of the coxsackievirus and adenovirus receptor abolishes CVB3 infection and prevents myocarditis *in vivo*

4.3.1 Tamoxifen predisposes mice to lethal CVB3 induced pancreatitis

Since CAR deficiency results in embryonic lethality (Dorner et al., 2005; Asher et al., 2005b; Chen et al., 2006), the conditional knockout approach was used to evaluate CAR as a therapeutic target in CVB3 induced myocarditis in the adult heart as described before. CVB3 readily infects cardiomyocytes *in vitro* and *in vivo* (Klingel et al., 1992; Kandolf and Hofschneider, 1985). The CVB3 Nancy strain which has been shown to depend

on CAR for infection (Shafren et al., 1997) was used in this study. After 2 weeks of tamoxifen injections, protein levels in the KO were <10% of WT-levels (Fig. 5D). Following this approach, CVB3 infection of 3-month old mice with $2x10^5$ plaque-forming units (pfu) caused lethality in both tamoxifen injected cardiac knockout animals and the tamoxifen injected cre negative littermate controls starting at day 5 after infection (Fig. 13A). The underlying pathology was characterized by total necrosis of exocrine pancreatic acinar cells (Fig. 13B). Together with the increased serum levels of pancreatic enzymes and markers of gastrointestinal disease, this indicated a fulminant form of acute pancreatitis (Fig. 13C). To circumvent the unexpected and severe of the acute pancreatitis, the virus load was changed to 5×10^4 pfu and the time between application of tamoxifen treatment and CVB3 infection was separated by 10 weeks. This approach restored survival to 100% and enabled us to investigate the effect of CAR on CVB3 induced myocarditis.

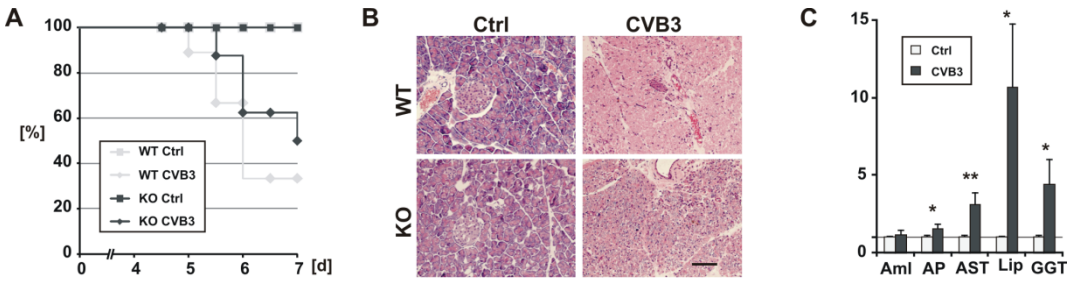

Figure 13: Tamoxifen predisposes mice to lethal CVB3 induced pancreatitis. A) CVB3 infection led to premature death of tamoxifen pretreated animals. Lethality from day 5 after infection at a dose of $2x10^5$ pfu was independent of the genotype (WT vs. KO) and presented only in the CVB3 infected mice (diamonds) , (n=23, $P\leq0.05$). B) Hematoxylin/Eosin staining of the control and CVB3 infected pancreas. The CVB3 infected pancreas of either genotype showed severe acute necrosis of the acinar cells (day 5 p.i.). C) Blood chemistry after day 5 revealed signs of acute pancreatitis with increased serum levels of Amylase (Aml), Alkaline Phosphatase (AP), Aspartate Aminotransferase (AST), Lipase (Lip), and Gamma-Glutamyl Transferase (GGT) in the CVB3 infected animals (normalized to uninfected control levels as 1). (n=18, * $P\leq0.05$; ** $P\leq0.01$).

4.3.2 Cardiac CVB3 infection can be abolished by eliminating CAR

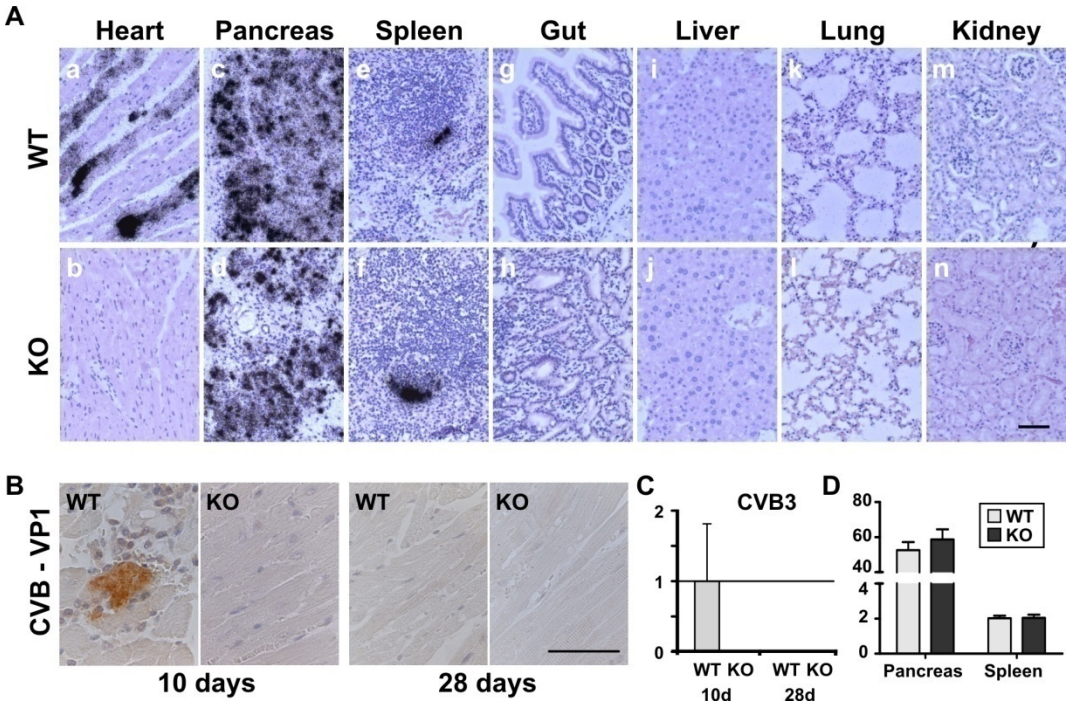

Figure 14: A) The distribution of replicating virus was visualized by *in situ* hybridization using a probe specific to CVB3. In the wildtype heart about 30% of cardiomyocytes were infected at day 10 p.i. as indicated by the silver grain precipitates (dark signal) reflecting virus RNA (a), while not a single virus positive cell could be detected in knockout hearts (b). The extent of infection of other susceptible organs was similar in wildtype and knockout mice (c, e vs. d, f). Gut, liver, lung, and kidney were not infected in either KO or WT animals (g-n). (Size bar: 50µm). B) Coxsackievirus protein was detected using an antibody directed against VP1 with focal expression in myocytes at 10 days after infection only in the WT heart. (Size bar: 50µm). C) Virus RNA was only present in the wildtype heart at day 10 as determined by TaqMan analysis. D) Quantification of CVB3 infection in pancreas and spleen (n=3 per group). At day 10 p.i., the area fraction of infection in pancreas was 52.6% in WT and 58.7% in KO (P=0.36) and in spleen 2% independent of the genotype (P=0.87).

To document that whether elimination of CAR can efficiently block virus uptake into cardiomyocytes, *in situ* hybridization was applied to detect virus RNA and immunohistochemistry to visualize CVB3-VP1 protein in single infected cardiac cells. As shown in Figure 14, virus replication was detected in the heart, pancreas, and spleen, while small intestine, liver, lung, and kidney did not show signs of infection 10 days post intraperitoneal infection with CVB3. Unexpectedly, not a single infected cardiomyocyte within 60

tissue sections derived from 20 knockout hearts was detected. In contrast, virus entry and replication did not differ between genotypes in spleen or pancreas at day 10 p.i. (Fig. 14D) and was identical to the published data (Klingel et al., 1996). Hence, in the inducible CAR deficient mice only the heart was protected from virus entry and subsequent replication.

4.3.3 Loss of CAR prevents viral myocarditis

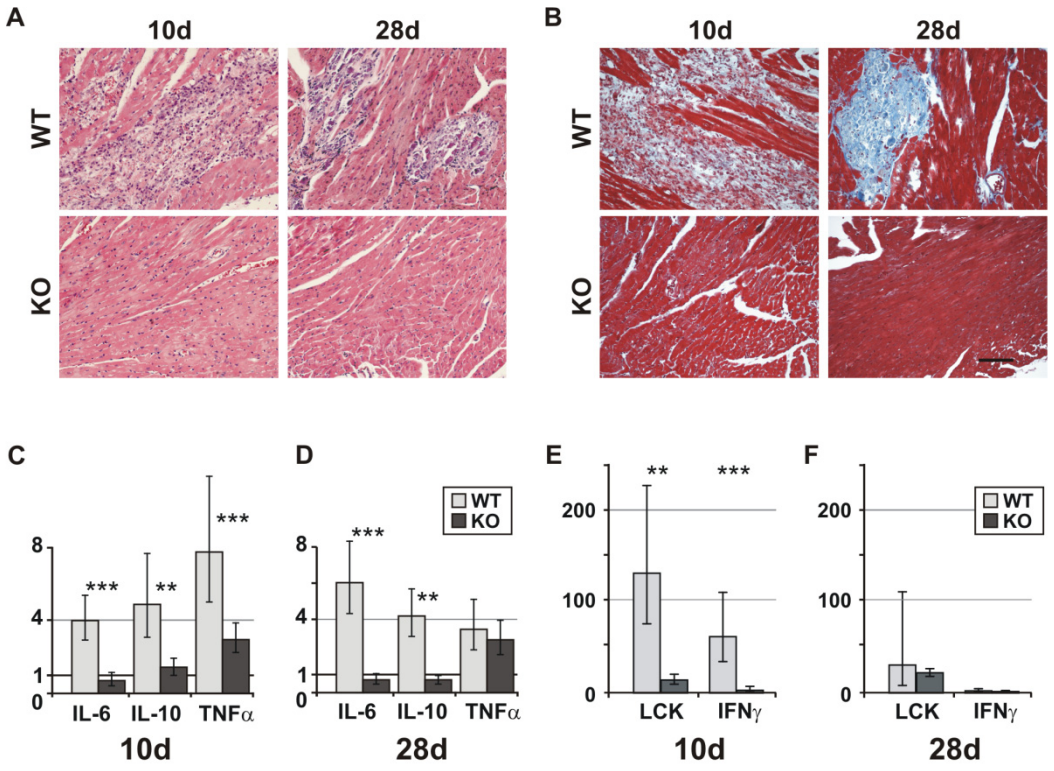

Figure 15: A) After infection with CVB3, wildtype animals showed myocyte necrosis and inflammation with infiltration of mononuclear cells, which was not detectable in the CAR knockout animals. B) Trichrome staining revealed increased collagen deposition in areas of the cardiac lesion in wildtype animals, but not in CAR knockout mice. The fibrotic lesions solidified at day 28 p.i. in the heart of wildtype mice. Size bar: 50µm. C, D) After 10 days or 28 days p.i. markers for inflammation such as IL-6, IL-10, and TNFα were elevated in either genotype, with high levels in the wildtype animals. E, F) Cardiac mRNA levels of inflammation markers LCK and IFNγ were >10× different between LCK and IFNγ, (n=36, ** P≤0.01; *** P≤0.001).

In CVB3 infected WT mice, myocyte necrosis and signs of inflammation were manifest, as shown by infiltration of mononuclear inflammatory cells at day 10 after infection and subsequent fibrosis at day 28 (Fig. 15A, B). In contrast, the CAR deficient knockout hearts did not show any significant morphological changes. The protection of CAR deficient hearts from myocarditis was also reflected by the cardiac mRNA levels of the cytokines IL-6, IL-10, TNFα, IFNγ and the T-cell protein LCK with only minor elevations in the KO as compared to the marked increased in WT mice (Fig. 15C-F).

4.3.4 Cardiac function is preserved in CAR deficient mice after CVB3 infection

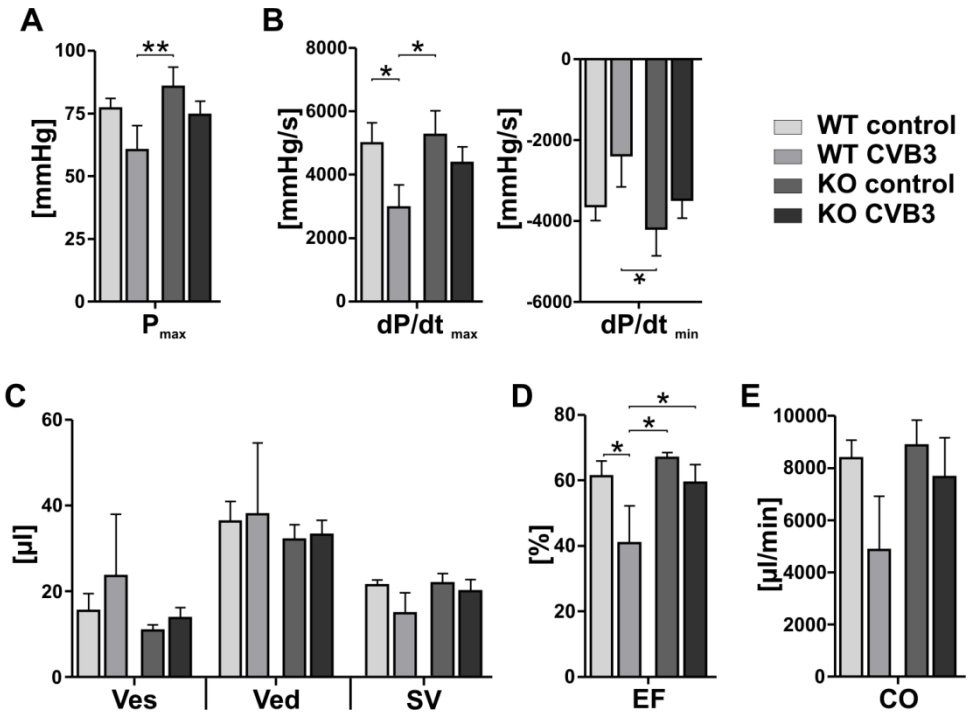

Figure 16: Effect of CAR deletion and CVB3 infection on cardiac function. Unlike CAR knockout animals, contractile function of CVB3 infected WT hearts was reduced as compared to non-infected WT control animals. Statistical significance was obtained for contractility (dP/dt_{max}, B) and ejection fraction (D). In contrast, cardiac function was preserved in infected versus control knockout animals (dark bars in A through E). Animals were investigated 10 days after CVB3 infection. (n= 30, * P≤0.05; ** P≤0.01). Ves: end-systolic volume, Ved: end-diastolic volume, CO: cardiac output, SV: stroke volume.

The functional consequences of CAR deficiency were evaluated by conductance catheter. Results showed that contractile function was maintained after CVB3 infection of CAR KO animals (Fig. 16). While contractile function was impaired in control animals 10 days after infection (reduced contractility and ejection fraction and a trend to reduced developed pressure, cardiac output, and relaxation), CAR KO animals were unaffected. The maintenance of systolic (EF, P_{max}, dP/dt_{max}) and diastolic properties (dP/dt_{min} as a measure for active relaxation) in CVB3 infected knockout hearts demonstrated that the elimination of CAR did not only prevent structural changes, but also preserved cardiac function after infection with CVB3.

4.3.5 The expression level of CAR's co-receptor DAF is not changed in KO heart

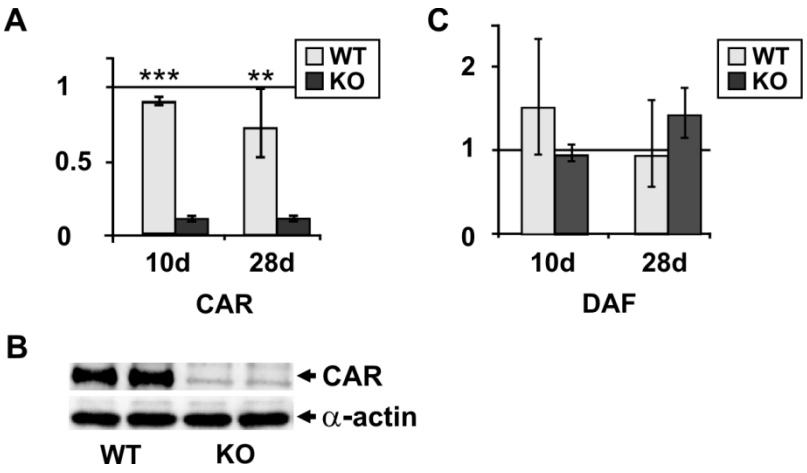

Figure 17: The expression level of DAF was not changed in CAR KO. CAR RNA (A) and protein levels (B) were altered with a strong effect in MCM animals 3 months after the tamoxifen treatment), while the expression of the co-receptor DAF was not significantly changed (C). (n=3 per group, ** P≤0.01; *** P≤0.001).

Some coxsackievirus strains, such as CVB3 Nancy applied in this study, bind to an additional receptor, the complement regulatory protein decay acceleration factor (DAF/CD55), (Shafren et al., 1995). To investigate if DAF is regulated as loss of CAR, the mRNA expression of DAF was measured. Although DAF is likely to be accessible to pathogens in the airway or intestinal lumen and may enable viruses to cross the epithe-

lium despite the inaccessibility of CAR, the DAF expression level in myocardium was neither significantly changed, nor able to make CVB3 accessible to myocardium alone without CAR (Fig. 17).

4.3.6 Factors other than CAR expression levels influence CVB3 distribution in target organs

CAR has been identified important for CVB3 tropism; knowledge of the subcellular localization, expression pattern and levels of CAR is relevant for virus entry. A survey of CAR protein and mRNA expression in various cell types and tissues was carried out. CAR is expressed in various cell types. In polarized epithelial cells, CAR was shown localized in tight junctions of the apical side (Fig. 18A). A similar expression pattern can be found in primary cultured yolk sac cells (Fig. 18B, C). On the cell boundary, CAR is partially co-localized with E-cadherin and ZO-1, and cytoskeletal proteins such as α-tubulin formed a connected network independent on CAR localization. In primary cultured neurons, CAR is highly expressed (Fig. 18D). In adult liver, CAR expression is different from other cell types or typical epithelial tissue. CAR was detected in bile canaliculi and it localized more basolateral side of hepatocytes, without showing co-localization with ZO-1 (Fig. 18F). In the hepatic artery, CAR was not detected. In adult cardiomyocytes, CAR expression was restricted to intercalated discs where it co-localized with Cx43 as shown in 3D reconstruction (Fig. 18G). In normal embryos, CAR is dominantly expressed in cardiac cells (Fig. 8), brain ependymal cells (Fig. 9A, B) and epithelium layer of embryos (Fig. 18E). CAR mRNA levels in brain were markedly upregulated during development, while downregulated in heart (Fig. 18H). The mRNA was also detectable in liver, yolk sac and tail (Fig. 18H).

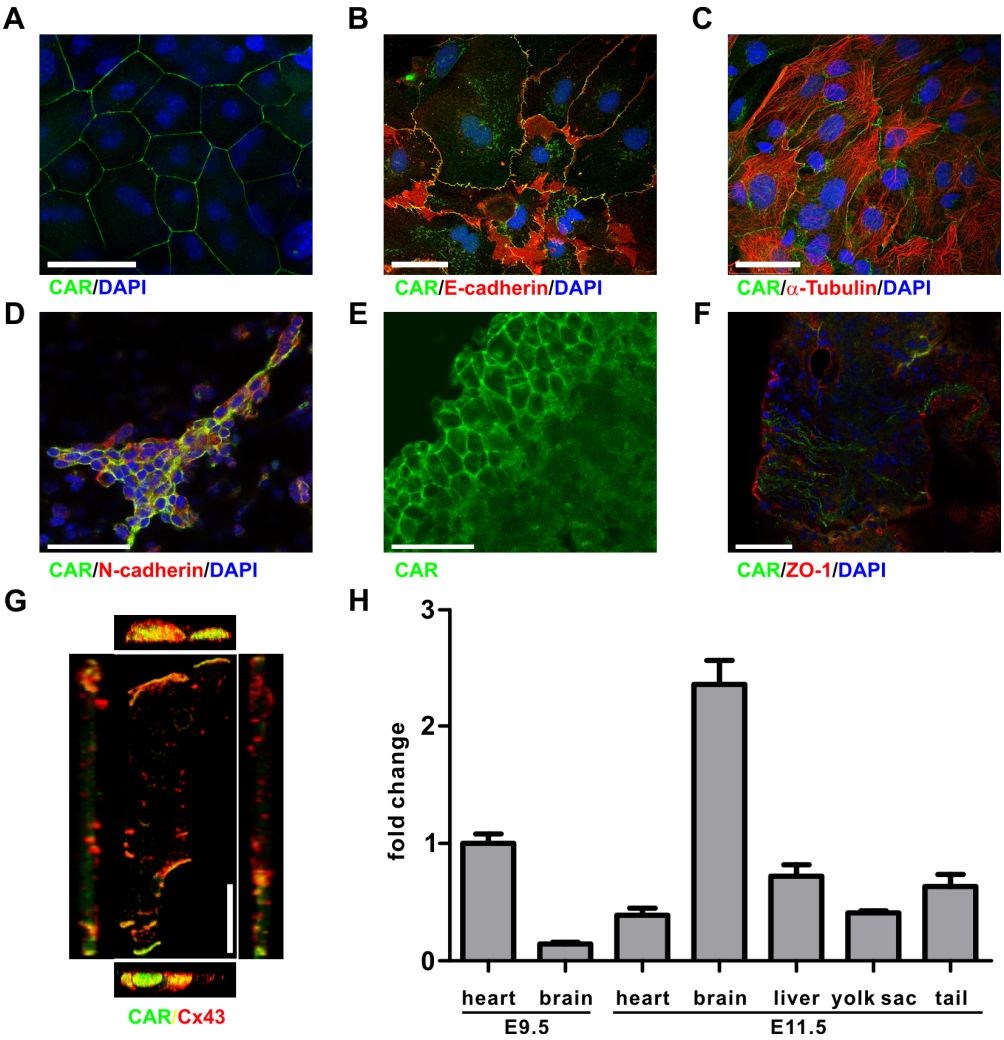

Figure 18: CAR localization in different cell types. A) Localization of CAR in epithelial cells. B) Co-localization of CAR and E-cadherin in primary cultured yolk sac epithelial cells. C) In primary cultured yolk sac epithelial cells, α-tubulin formed a network independent on CAR localization. D) Co-localization of CAR and N-cadherin in primary cultured neuron cells. E) CAR typically expressed at the epithelial layer of the embryonic body trunk. F) CAR (green) localized at epithelial cells in adult liver, but not co-localized with ZO-1 (red). G) 3D reconstruction of the adult primary cultured cardiomyocyte showed that CAR and connexins 43 co-localized at intercalated disc. CAR was stained in green and cell nuclei in blue. Size bar, A-F: 50µm, G: 20µm. H) CAR expression distribution in different tissue at E9.5 and E11.5. At E11.5, CAR was highly expressed in the brain.

To relate the distribution of virus infection RNA to CAR expression, CAR mRNA and protein levels for all tissues tested were determined (Fig. 19A, B). Not only did CAR expression levels differ by up to 25-fold between organs susceptible for virus infection

(spleen vs. pancreas), but conversely tissues that were not susceptible such as gut, liver, and lung expressed CAR at levels that were 3- to 10-fold higher than cardiac expression.

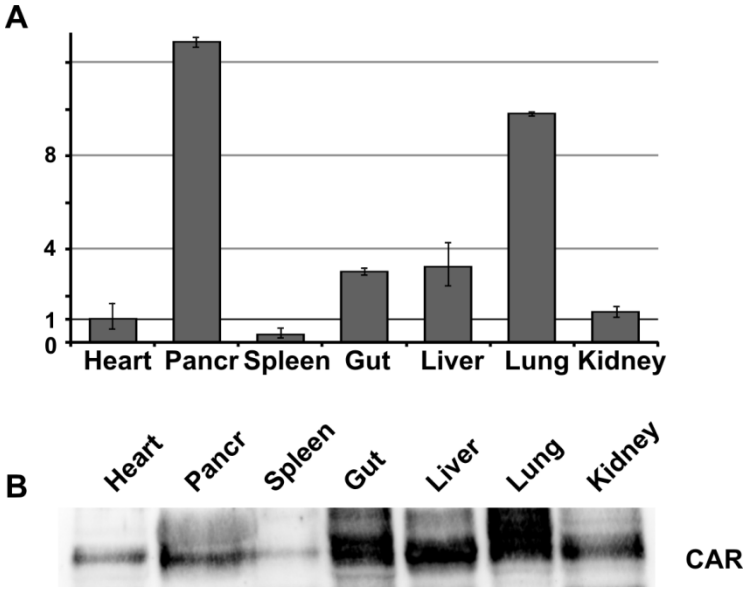

Figure 19: Expression of CAR in the adult mouse heart, pancreas (pancr), spleen, gut, liver, lung, and kidney (wildtype males at 6 months of age). CAR mRNA (A) and protein levels (B) differed between tissues but did not correlate with infectivity of the tissue. Low levels of CAR expression were documented for adult heart, spleen, and kidney. CAR mRNA levels differed >10× in pancreas and lung. RNA levels were normalized to heart, (n=3). Increased protein expression was confirmed for pancreas, gut, liver, and lung.

4.4 CAR regulates cardiac conduction and cell-cell communication in neonates and adults

In addition to providing direct genetic evidence that CAR is CVB3 receptor and cardiac deletion of CAR can abolish CVB3 infection and prevent viral myocarditis, the potential unwanted effects that might be associated with the loss of CAR in the postnatal heart should also be also addressed. Despite efficient postnatal depletion of CAR, the cardiac inducible KO animals did not show an obvious adult phenotype. This includes the initial cardiac assessment by echocardiography that did not show signs of reduced contractile function or dilation in the first month after induction with tamoxifen. The routine monitoring of cardiac activity during anesthesia using the electrocardiogram (ECG) uncovered

that loss of CAR leads to impaired electrical conductance from atrium to ventricle (Lisewski et al., 2008). While depolarization and repolarization of the KO-ventricle was normal (QRS complex and QT interval), the conduction of the electrical activity from atrium to ventricle was disturbed. This is reflected in the prolonged PR interval after induction of the KO and corresponded to a problem at the level of the AV-node. The PR conduction time increased with progressive deletion of CAR from as early as 1.5 weeks after tamoxifen induction (at a time where CAR protein levels started to decline). The prolongation of the PR interval is the hallmark of first degree AV conduction block (AVB I°), which could be documented in all KO animals from week 2 after induction. Blocks of a higher degree were present from 4 weeks after induction of the CAR KO, including partial failure of AV conduction (AVB II°, 25%) or total dissociation of atrial and ventricular rhythms (AVB III°, 37.5%).

4.4.1 Impaired early development in neonatal CAR KO mice

CAR showed a high expression level in embryonic stage, and decreased in adult phase. A relative higher expression level of CAR is maintained in neonates compared to adults. The neonatal mice were investigated to find out if they have similar disturbance of AV conduction as adults after tamoxifen treatment. Tamoxifen treatment can cause abortion of pregnant female mice, the attempt to induce Cre recombination and produce cardiac specific CAR KO embryos during embryonic development was failed (data now show).

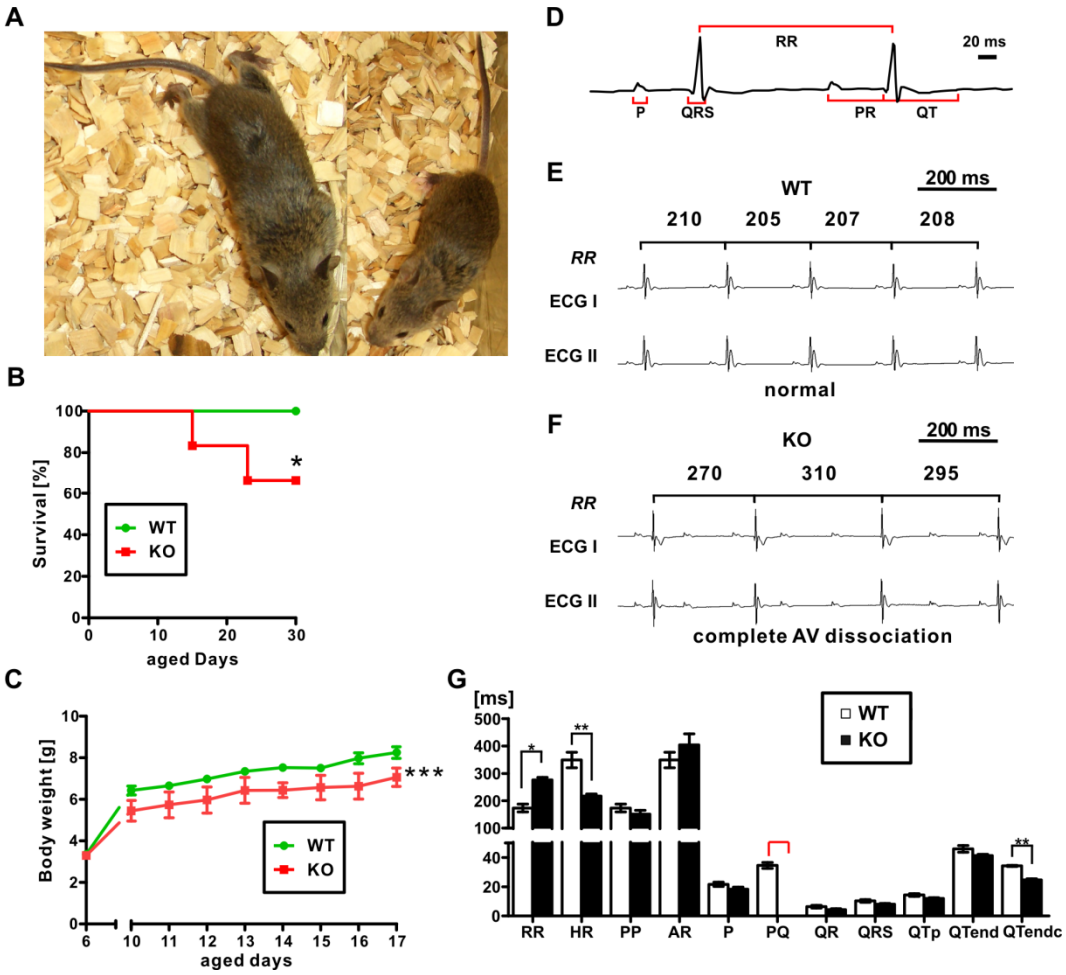

Figure 20: Heart specific deletion of CAR resulted in lethality and AV block in neonatal mice. A) Littermates comparison of a WT mouse (left) and cardiac specific CAR deficient mouse (right) after tamoxifen injection at P15. B) CAR deficiency resulted in premature death of tamoxifen pretreated animals. Lethality occurred from day 8 after injection (n=13, * P≤0.05). C) Cardiac deletion of CAR slowed down the body weight increase of neonatal mice (n=13, *** P≤0.0001). D) Annotated ECG curve: the PR-interval corresponds to the time between atrial and ventricular depolarization; RR interval corresponds to the heart rate. E-F) Simultaneous recordings from surface ECG (ECG I/ECG II) were displayed. The KO showed complete AV dissociation with prolonged RR interval, which represents slower heart beating rate. G) Quantification of the ECG changes in KO and control animals after the 10-day treatment with tamoxifen. Increased RR interval and decreased HR and QTendc corresponded to lower heart rate, the immesurable PQ interval in KO reflected complete AV dissociation (AVB III°) (n=3 per group, * P≤0.05, ** P≤0.01).

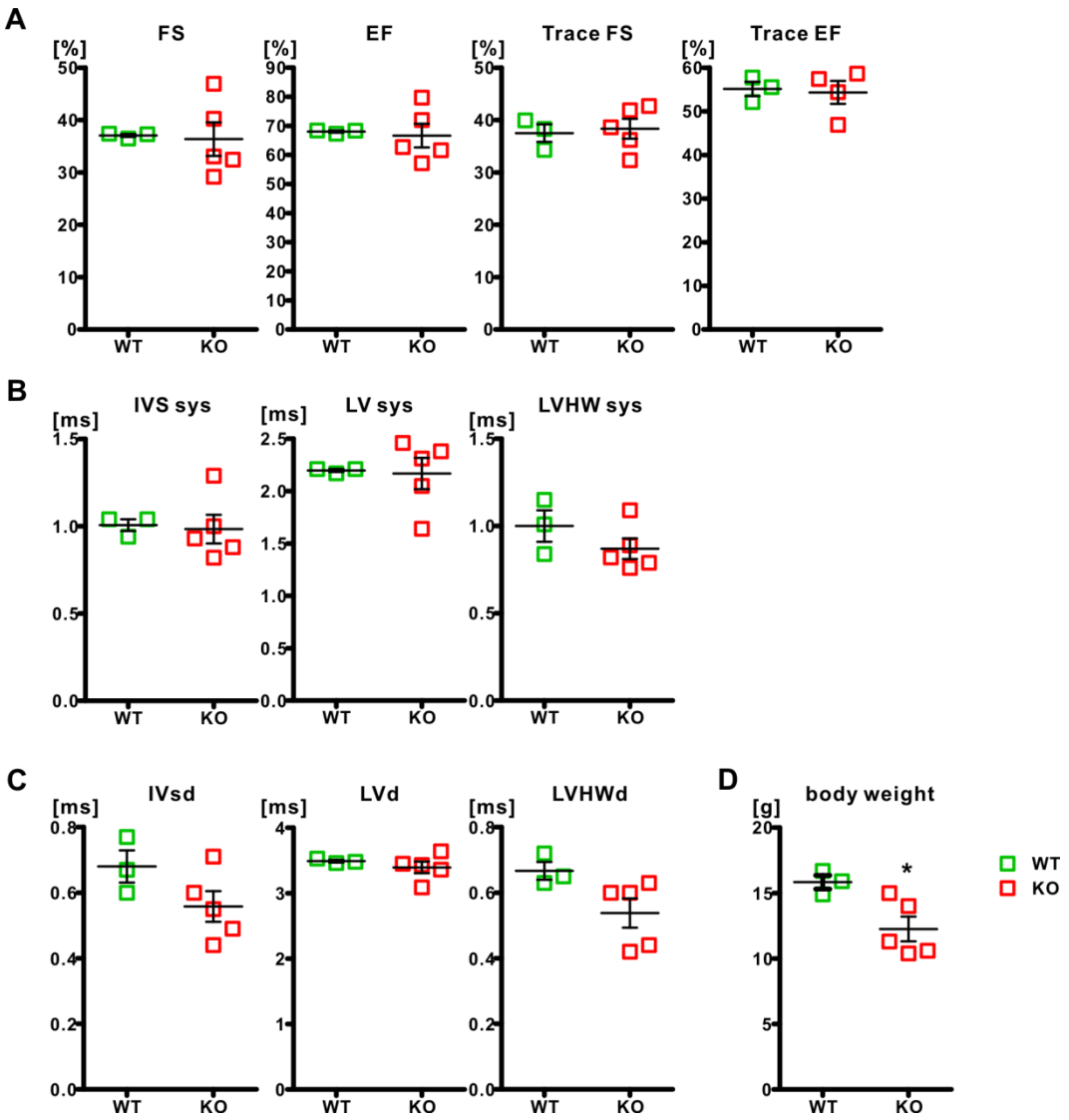

Figure 21: Echocardiography evaluation of cardiac specific CAR KO vs. WT after tamoxifen induction. Statistical significance was only obtained for body weight (n=3 for WT, n=5 for KO, * P≤0.05). The contractile functions were preserved both in systolic and diastolic properties. Although increased variance was increased in KO mice, there was no statistical significance.

Nevertheless, CAR could be efficiently eliminated from the neonatal mouse heart via injection of tamoxifen to P6 neonates both on mRNA and protein level. Neonatal littermates received tamoxifen injections for 10 days individually, and the body weight was recorded every day before injection. 8 days after the first tamoxifen injection, nearly 40% of neonates that carried MerCreMer allele started to die and the mortality kept growing after the injection was terminated (Fig. 20B). PCR genotyping was used to check the recombina-

tion in the heart, all of those died mice showed a very strong recombination band. The KO mice were manifest smaller and had significant reduction of body weight (Fig. 20A, C). The surviving KO animals were sent for ECG analysis that documented severe AV-nodal IIIº block with immesurable PQ and PR interval, which indicated complete AV dissociation (Fig. 20F, G). The KO animals had a slower heart rate, indicated by prolonged RR interval and QTendc (Fig. 20G).

Similar to the adult KO mice, the echocardiography of neonatal KO mice did not show signs of reduced contractile function or dilation, although the variance was increased in KO mice (Fig. 21).

4.4.2 Cell-cell communication is increased in the adult CAR KO heart

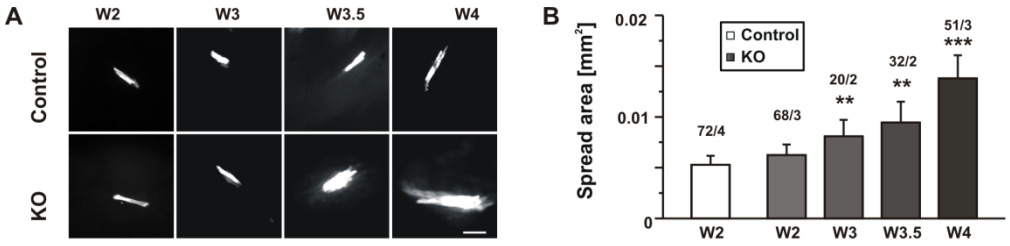

Figure 22: Altered cell-cell communication in the CAR KO heart. A) After injection of fluorescein, the dye was passed to neighboring cells. Representative cells from KO and control cardiac slices from week 2 through 4 after induction of the KO were shown. The increased longitudinal and lateral coupling was most prominent in cardiac slices at the 4-week-time point. B) Quantification of >200 injections representing 14 independent hearts documented the significantly increased coupling from week 3 after induction of the KO. The area at the end of the 4 min injection period was used to compare cell-cell communication at the indicated times. For each time point, the number of injections and number of animals is provided (injections/animals). ** P≤0.01; *** P≤0.001, Mann-Whitney test, Scale bar: 100 µm.

In the absence of a major anatomical or structural defect in adult KO mice, a functional approach was used to explore the mechanism underlying the conduction block. To analyze the activity of gap junctions, which have previously been implied in isolated AV conduction disease (Simon et al., 1998; Nikolski et al., 2003) a dye coupling assay was adapted to be used on cardiac slices using carboxyfluorescein, which facilitated the detec-

tion of coupling in myometrial cells as compared to lucifer yellow (Ciray et al., 1995). This assay enabled us to investigate cell-cell communication between cardiomyocytes *in situ*. In parallel with the reduction of CAR protein levels, cellular exchange of the fluorescein dye increased from week 2 to 4 (Fig. 22A, B). The area covered by dye-filled cells after 4 min was used to quantify coupling efficiency. While coupling was not significantly different between wildtype (WT) and CAR KO cardiomyocytes at week two after initiating tamoxifen injection, dye spread increased significantly from week 3 (Fig. 22B).

4.4.3 Altered expression of the cell-cell contact proteins in CAR KO hearts

Since the dye coupling experiments indicated a problem in cell-cell communication, the structure and protein composition of the intercalated discs and the expression and localization of gap junction proteins was followed. Intercalated discs of CAR KO cardiomyocytes had a normal ultrastructure that did not show widened gaps between cells or increased folding (Lisewski et al., 2008).

To determine which genes contribute to the development of the AV-block phenotype, preliminary expression profiling data from mouse atria was obtained, that showed the expected downregulation of CAR (>10fold down in the KO) and suggest a specific role of connexin 43 and connexin 45. The expression of other proteins related to arrhythmia such as channels, other connexins, and transcription factors was largely unchanged (data not shown). The expression analysis was extended to cardiac ventricle (where differences in coupling were documented) and revealed that RNA levels of both cell-cell contact and adaptor proteins were altered secondary to the loss of CAR (Fig. 23). This includes reduced expression of ZO-1, an adaptor protein that binds both CAR and connexins (Cohen et al., 2001b; Toyofuku et al., 1998) (Fig. 23A). Expression of connexins was differentially affected in the CAR KO heart. On the mRNA level, Cx45 expression was reduced only late in the development of the phenotype, while Cx37 and 40 changed only transiently

(Fig. 23B, C). The altered protein levels of Cx45 and Cx43 (both >40% reduction) in KO hearts as compared to Cx40, which was unchanged on mRNA level (Fig. 23D), indicated a selective effect of CAR on a subset of connexins. Other proteins involved in cell-cell junctions, such as β-integrin, vinculin, N-cadherin and E-cadherin, were largely unchanged (Fig. 23D).

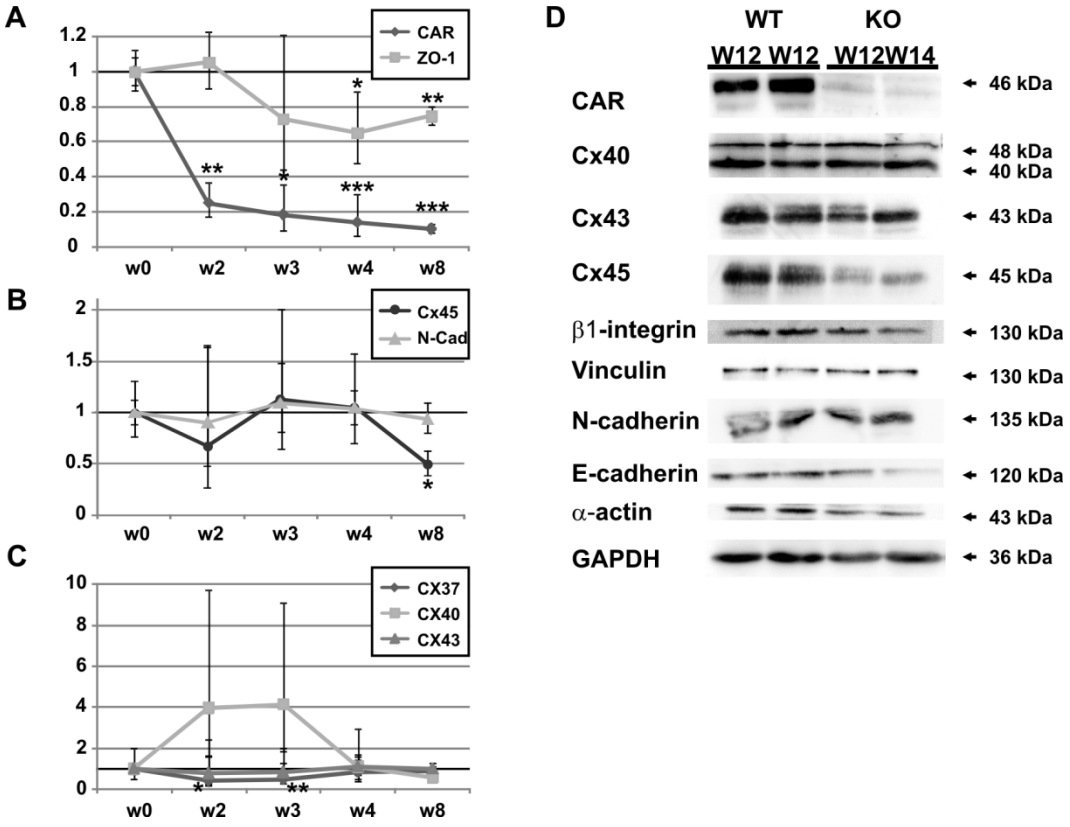

Figure 23: A) After induction of the KO, expression of CAR and its adaptor protein ZO-1 was reduced significantly from week 2 and 4, respectively. B) The composition of the gap junction was altered because of differential expression of Cx37 (transiently reduced) and Cx40 (transiently increased, albeit not significantly). Expression of Cx43 was unchanged. C) Cx45 was the only connexin with RNA levels significantly altered late in the progression of the phenotype (reduced from >8w). The adherens junction protein N-cadherin was unchanged. All expression data were normalized to GAPDH and levels at week 0 (before induction) were set to 1. (n=3 per group. * P≤0.05, ** P≤0.01). D) Cardiac expression of Cx40 and Cx45 was confirmed on the protein level with down-regulation of Cx45 but not Cx40 in animals at >8w after induction of the phenotype. GAPDH was used as a loading control. After normalization to GAPDH, Cx45 levels were reduced by 45% (p=0.012), Cx43 levels by 43% (p=0.015), and Cx40 levels were not changed significantly (n=4).

4.4.4 Localization of connexin 43 is dependent on CAR

Protein composition of the intercalated disc was analyzed in isolated cardiomyocytes at 8 weeks after induction of the phenotype. Co-staining with α-actinin antibodies confirmed the proper orientation of the myofilament and connection to the intercalated disc (Fig. 24A). Although the structure of the intercalated discs was maintained, protein composition changed in response to the loss of CAR. Protein composition of the intercalated disc was analyzed in isolated cardiomyocytes at 8 weeks after induction of the phenotype. While expression and localization of the adherens-junction protein N-cadherin was unaffected (Fig. 24B), the localization of the gap junction protein Connexin 43 (Cx43) was altered in KO cardiomyocytes 8 weeks after induction (Fig. 24C). Reduced amounts of proteins were accumulated in subdomains within the intercalated disc of the KO. Strikingly, the tight junction protein ZO-1 expression and localization at the intercalated disc was not markedly altered, although it was reduced on mRNA level (Fig. 24D). Those observations indicate a functional link between tight and gap junctions, but not between tight and adherens junctions that involves CAR.

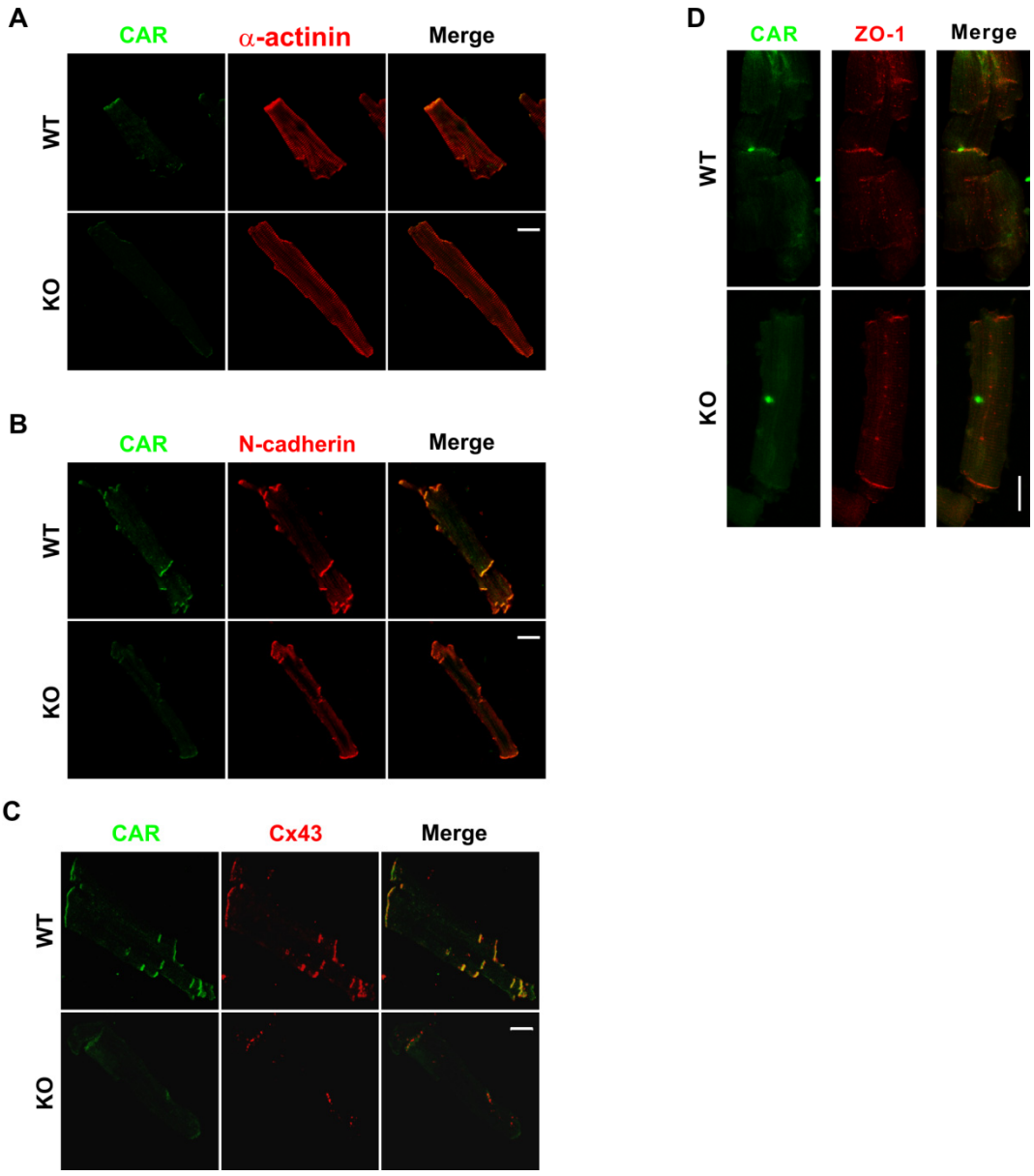

Figure 24: Localization of connexin 43 is dependent on CAR. In the absence of CAR, intercalated discs were maintained with proper localization of N-cadherin but changes in expression and localization of Cx43. A) Staining with anti-CAR and anti-α-actinin antibodies showed the proper localization of CAR in wildtype cardiomyocytes and correct orientation of the myofilaments. In knockout cells specific CAR staining was reduced to <10% compared to WT cardiomyocytes. B) Staining with anti-CAR and anti-N-cadherin antibodies documented the proper expression and localization of N-cadherin upon deletion of CAR. C) Staining with anti-CAR and anti-Connexin43 (Cx43) antibodies revealed that Cx43 expression was reduced in KO cardiomyocytes 8 weeks after induction. Residual Cx43 protein was localized in subdomains within the intercalated disc. D) Staining with anti-CAR and anti-ZO-1 antibodies showed that CAR was partially co-localized with ZO-1, while no significant reduction of ZO-1 in KO cells. Comparable results were obtained in 3 independent experiments. Scale bar: 20µm.

4.5 Heterozygous CAR KO animals appear phenotypically normal but responded differentially to volume overload

In some animal models, haploinsufficiency can also cause changes in phenotype. As investigated in CAR heterozygous knockout animals, no obvious morphological or physiological changes were observed between wildtype and heterozygous animals in more than 1000 offspring, and the survival rate was unaffected. A volume overload challenge was applied on $CAR^{+/+}$ and $CAR^{+/-}$ animals to provoke a phenotype. Arteriovenous shunt (AV-shunt) and sham surgeries were performed on both $CAR^{+/-}$ mice at the age of 8 weeks. 2 weeks after surgery, the shunt site could still be observed under the ultrasound (yellow arrow in Fig. 25A), and the blood flow from artery to the vein at the shunt site could be detected by Doppler. The HW/BW ratio in the WT AV-shunt group was significantly increased comparing to sham $CAR^{+/+}$ (n=4, $p<0.01$) and sham $CAR^{+/-}$ (n=4, $p<0.01$) group. $CAR^{+/-}$ AV-shunt group showed a trend to increased HW/BW ratio, statistical significance was not obtained between genotypes (Fig. 25C).

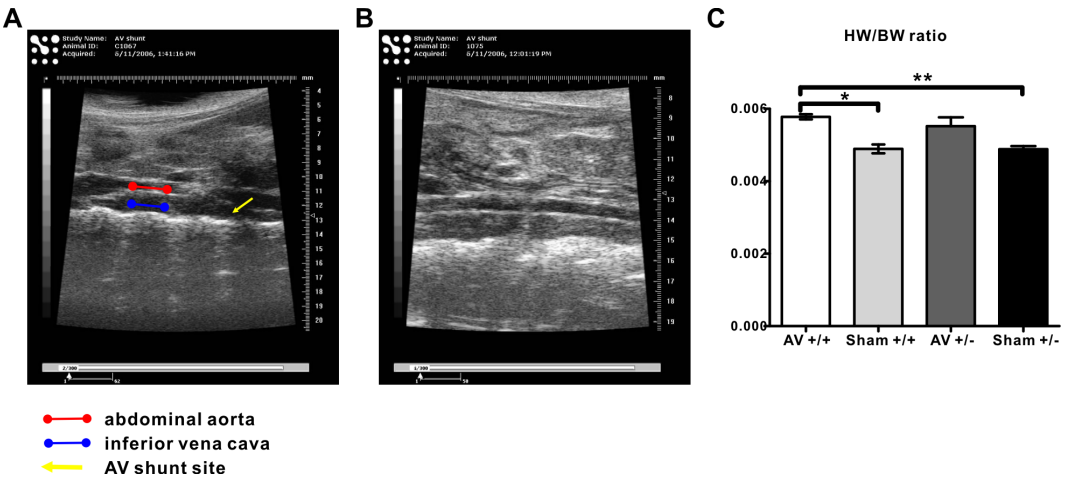

Figure 25: AV shunt surgery causes an increased HW/BW ratio that does not differ between genotypes. A) Ultrasound showed at AV shunt site, a blood flow from artery (along the red line) to the vein (along the blue line) was indicated by the yellow arrow. B) Sham operated animal does not have AV shunt with regular blood flow. C) The HW/BW ratio was significantly increased in $CAR^{+/+}$ AV shunt mice compared with sham operated mice but not in $CAR^{+/-}$ AV shunt mice (n=4 per group, *$p \leq 0.05$, ** $p \leq 0.01$)

5 Discussion

Since the first identification of the coxsackievirus and adenovirus receptor (CAR) in 1997, CAR has been widely studied as a virus receptor and as a cell-cell contact protein in embryonic development and disease. A CAR loss of function mutant was generated to study the role of CAR during embryonic development. With the cardiac-specific inducible CAR knockout model, the potential of CAR as a therapeutic target in cardiac disease was evaluated.

The objective of this work is to understand the importance of CAR as a virus receptor *in vivo* and if elimination of CAR is necessary and sufficient to block virus entry and CVB3 induced diseases such as myocarditis and cardiomyopathy.

5.1 Characterization of the embryonic lethality

5.1.1 Differences and similarities of various CAR knockout models

Knockout technology is widely used to investigate a particular gene of interest and to define its function in the live organism. The considerable interest in CAR's physiological function can be appreciated from the fact that in the past three years, five labs have independently published four constitutive and five conditional CAR-knockouts that affect CAR exon 1 or 2 (Dorner et al., 2005; Asher et al., 2005b; Chen et al., 2006; Lim et al., 2008; Lisewski et al., 2008).

All CAR splice variants (including the soluble isoforms) described so far, contain both exon 1 and 2 (Dorner et al., 2004; Thoelen et al., 2001b). Thus, loss of the transcription start site and translation start codon in the KO of exon 1 (Dorner et al., 2005) versus the possible frameshift resulting from the deletion of exon 2 (Asher et al., 2005b; Chen et al., 2006) should both cause similar phenotypes. Excision of exon 1, which contains the transcription and translation start site, affects the expression of all CAR isoforms. Like all

other CAR KO strategies, the approach in this study developed a beating heart but died with 100% penetrance. The failure of getting live offspring from the intercrosses of CAR heterozygous mice indicated that CAR is essential for embryonic development. The embryonic lethality of these animals occurred relative earlier (from E10.5) and started the process of resorption from E11.5 (Fig. 6A , Table 11), while the targeting exon 2 knockouts appeared grossly normal at the stage E10.5 and the resorption process started at E12 (Asher et al., 2005b; Chen et al., 2006). Differences of genetic background, or alternative splicing that might result in a partial rescue of the exon 2 KO could explain those discrepancies.

5.1.2 The cardiac pathology of the conventional CAR KO

The cardiac pathology caused by CAR deficiency included thoracic hemorrhage and enlargement of the pericardial space. Only one paper so far showed the signs of regional apoptosis in exon 2 KO (Asher et al., 2005b). Apoptosis signals were neither changed in Affymetrix results comparing KO and WT nor were any apoptosis proteins such as caspase 3, 8 and 9 detectable with western blot in E11.5 embryos, which coincided with the majority of published data. The apoptosis Asher et al observed can be induced by myocardium hypoxia when the embryos are close to death (Sugishita et al., 2004). Another possibility is that the embryos they examed might have slight difference between the age, since cardiomyocyte apoptosis is prevalent during the remodeling of the embryonic cardiac development but the intensity of caspase expression is differed from the stages (Abdelwahid et al., 1999; Knaapen et al., 2001).

The heart specific knockout of exon 2 under the control of cardiac troponin T promoter resulted in death by E12.5, with hyperplasia of the left ventricular myocardium, distention of the cardinal veins and underdeveloped sinuatrial valves (Chen et al., 2006). Similarly, our CAR KO animals showed ventricular thickening, malformation of cardinal veins and

enlarged endocardial cushions. Endocardial cushions are a pair of thickened tissue sections in the embryonic atrial canal. During embryonic development, they meet and fuse to form a septum dividing the canal into two channels, which eventually become the atrioventricular orifices. Increased cell proliferation and reduced apoptosis within the cushion mesenchyme and endothelium could cause endocardial cushion enlargement as secondary effect of CAR deficiency, since CAR is absent in endocardial cushions but proliferation was observed in the heart (Chen et al., 2006). Similarly, the major heart phenotypes of Noggin mutant embryos are thicker myocardium and larger endocardial cushions. Both defects result from increased cell number and can be rescued by halving the gene dosage of Bmp4 (Choi et al., 2007). The endocardial cushion enlargement was also reported in many other mutants. Protein tyrosine phosphatase (Shp2) mutation Q79R-Shp2 results in embryonic lethality by embryonic day 14.5, and mutant mouse embryos have significantly enlarged endocardial cushions in the atrioventricular canal and in the outflow tract accompanying with increased ERK activation (Krenz et al., 2008). Overexpression of Wnt-9a in avian heart results in enlarged endocardial cushions and AV inlet obstruction. Wnt-9a-mediated cell proliferation in cardiac cushions can be inhibited by the secreted Wnt antagonist Frzb (Person et al., 2005).

Asph (aspartate beta-hydroxylase) also known as Junctin (JCN), is a transmembrane protein located at the cardiac junctional sarcoplasmic reticulum (SR) and forms a quaternary protein complex with the ryanodine receptor, calsequestrin, and triadin in the SR lumen of cardiac muscle (Fan et al., 2007; Fan et al., 2008). An increased expression of junctin is associated with an impaired Ca^{2+} homeostasis, and downregulation of junctin is a compensatory mechanism in human heart failure (Gergs et al., 2007). CAR KO showed cardiac defects such as ventricle hypertrophy and atrium dilation at E11.5 (Fig. 7C) which will finally develop to heart failure. The RNA levels of junctin were downregulated at

E11.5, suggesting that the reduction of junctin might also be a compensatory effect of a failing embryonic heart.

In the CAR KO heart at E11.5, expression of the atrial and trabecular marker atrial natriuretic factor (ANP) was attenuated, indicating a faiure of normal atrial or trabeculae formation (Cayli et al., 2002; Toshimori et al., 1987). Various *in vitro* models were used to gain insight into pathways involved in the hypertrophy response. Both homozygous and heterozygous ANP deficient animal models exhibited ventricular hypertrophy (Klinger et al., 1999; Sun et al., 2000). Thus, it is reasonable to suspect that the mechanisms of ventricular hypertrophy in CAR KO heart caused by the decreased level of ANP.

5.1.3 CAR in myofibril organization

In isolated embryonic CAR KO cardiomyocytes, the disorganization of myofibrils was often observed. Co-staining of CAR and α-actinin or α-tubulin did not show a direct link between CAR and myofibrils or cytoskeleton proteins. The Z-discs in CAR KO cardiomyocytes appeared as spotted aggregates and myofibrils were more diffuse, shortened and disorganized (Fig. 8). Such observation is consistent with the previous findings (Dorner et al., 2005; Chen et al., 2006) that myofilament bundles in CAR-null mice were thinner than those in wildtype embryos (very few >1 μm in width). This disorganization did not occur in isolated adult CAR KO cardiomyocytes (Fig. 24), indicating that CAR is needed for myofilament organization in embryos but not essential for its maintenance in adult cardiomyocytes. The attainment of mature sarcomeres is partially regulated by cell adhesion (Shiraishi et al., 1997), myofibrils can be seen to branch and individual myofibrils are aligned laterally in register by the intermediate-filament protein desmin (Li et al., 1997), forming a three-dimensional network that is linked between cells through intercalated discs. Adherens junctions serve as anchor site for developing myofibrils, however, the adherens junction protein N-cadherin and the focal adhesion protein vinculin did not

show any change in either embryos or adults (Fig. 12A, 23D), suggesting that CAR might mediate myofilament organization by interacting with other adaptor proteins.

In the CAR deficient heart, mRNA expression of various apolipoproteins such as Apo A-I and its receptor cubilin were increased. Elevated plasma concentrations of apolipoproteins are a risk factor for a variety of atherosclerotic disorders including coronary heart disease (Marcovina and Koschinsky, 2002; Marcovina et al., 1999; Scanu, 2003). It is reported that Apo A elicits a dramatic rearrangement of the actin cytoskeleton characterized by increased central stress fiber formation and redistribution of focal adhesion (Pellegrino et al., 2004). In addition to actin cytoskeleton remodeling, Apo A activates a Rho/Rho kinase-dependent intracellular signaling cascade that results in increased myosin light chain phosphorylation with attendant rearrangements of the actin cytoskeleton (Pellegrino et al., 2004). The elevation of Apo A-I in CAR KO cardiomyocytes could be one of the reasons for the disorganization of myofilaments. Cubilin is an endocytic receptor in epithelial Apo A-I/HDL metabolism (Kozyraki et al., 1999). It is required for embryonic development and is essential for the formation of somites, definitive endoderm and visceral endoderm (VE) and for the absorptive function of VE including the process of maternal-embryo transport of HDL (Smith et al., 2006). Although there is no direct evidence of cubilin expression in the normal heart, the sudden increased cubilin and apolipoprotein mRNA level in CAR deficient heart suggested an aberrance of lipid uptake and cell membrane permeability caused by the elevation of cubilin and Apo A-I. This is possibly a secondary effect of CAR deficiency, and might be restricted to the heart region, because total Apo A-I protein levels did not differ between genotypes. The Apo A-I and cubilin expression levels are much lower than the other tissues, such as yolk sac (data now shown). The differential expression levels in the heart might be concealed by other tissues, where Apo A-I and cubilin are highly expressed since the total protein lysate used for Western blot was from the whole embryo.

ZO-1 directly interacts with actin filaments, it links tight junction proteins to actin cytoskeleton(Dejana et al., 2000; Fanning et al., 2002). We suspect that CAR is required for myofibril organization by forming a CAR-ZO-1-actin complex. Determining whether CAR keeps a force balance against myofibrils and maintains the stability of the complex through interactions with ZO-1 could help us have a better understanding of the underlying mechanism.

5.1.4 CAR is related to gap junctions

Gap junctions between cardiomyocytes permit the conduction of electrical impulses pass through and excitations will spread from an excited cell to cells connected to it. Disruptions of the gap junction molecule connexins often resulted in impaired communication and electrical conductance between cells. Both Cx43 and Cx45 protein was decreased by >50% in KO heart at E11.5. Cx43 showed diminished and sporadic distribution at cell-cell contacts in cultured cardiomyocytes (Fig. 8C). The mRNA levels of most connexins did not change at E9.5. At E11.5, the protein reduction of Cx43 and Cx45 in KO heart was more obvious comparing to the change on mRNA levels. The reduced Cx43 and Cx45 in KO heart suggested an abnormal cell-cell communication secondary to the loss of CAR. The differential expression of connexins at mRNA and protein level might indicate that CAR might help stabilize connexins in cardiomyocytes.

The PDZ-domain proteins, such as MUPP1 (Coyne et al., 2004) and ZO-1(Lim et al., 2008), their mRNA levels were also decreased at E11.5. Both MUPP1 and ZO-1 interact with CAR tail via the PDZ-domain (Coyne et al., 2004). In cultured Caco-2 cells, siRNA silenced CAR expression leads to the destabilization of the junction and relocalization of MUPP1, but does not affect MUPP1 protein expression (Coyne et al., 2004). In CAR KO heart, the decreased mRNA levels of MUPP1 might be a secondary response to the destabilization of MUPP1 protein. Unlike MUPP1, cell culture model showed that ZO-1 loca-

lization and expression are independent of CAR, but correlated with Cx43 in cardiomyocyte (Toyofuku et al., 1998). ZO-1 reduction could be observed both in embryonic and adult KO on mRNA levels, but not on protein levels, suggesting that CAR and ZO-1 expression regulation is not directly correlated. Absence of CAR indirectly cause decreased ZO-1 mRNA levels possibly via impaired Cx43 expression. Those observations indicate a functional link between CAR and gap junctions.

5.1.5 CAR in epithelial permeability

According to its localization, CAR has been suggested to have a role in cell permeability (Raschperger et al., 2006). The lack of tight junctions between ependymal cells and choroid plexus allows a free exchange between CSF and nervous tissue (Gotow and Hashimoto, 1982) In wildtype embryos, CAR was expressed in ependymal cells, predominately at the apical side of the epithelium (Fig. 9). While normal ependymal cells formed a simple cuboidal or low columnar epithelium, the structure of ependymal cells was disrupted and the formation was not preserved in CAR deficient embryos (Fig. 9C), implicating lost of tight junctions in ependymal cells and an impaired control of substance exchange between the epithelium layer. For comparison, CAR mRNA levels of E9.5 and E11.5 embryonic brains were analyzed. While CAR mRNA levels in heart were decreased, significant higher levels of E11.5 brain were detected. The results indicated that CAR as a tight junction protein, it might play a role in the regulation of epithelial permeability and tissue homeostasis in embryonic development.

5.2 Evaluation of CAR as a therapeutic target in CVB3 induced cardiac disease

In addition to providing a genetic tool to generate loss of function mutants, the mouse is also a suitable animal model to study the role of CAR in CVB3 induced pancreatitis and myocarditis, since pathomechanisms and disease progression are similar in human patients and mice (Coyne and Bergelson, 2006; Tracy et al., 2000).

Viral myocarditis is one of the main causes of acute and chronic heart failure and coxsackievirus is one of the important causative agents, which especially in children accounts for a significant fraction of cases of terminal heart failure (Feldman and McNamara, 2000). The disease process is mimicked in CVB3 infected mice with acute myocarditis that proceeds to a chronic phase which can ultimately lead to chronic cardiomyopathy (Fairweather and Rose, 2007). To efficiently produce surviving heart-specific CAR KO animals and generate an adult KO model without a potentially complicating developmental phenotype, the inducible heart specific KO was established. The tight control of recombination by tamoxifen eliminates developmental effects that might arise from the embryonic loss of CAR expression. To establish the animal model the heart specific tamoxifen inducible knockout was infected with the cardiotropic CVB3 Nancy strain that has been described to produce severe myocarditis in mice (Klingel et al., 1996). Here, this study explores the acute response to CVB3 in heart specific CAR KO.

5.2.1 Tamoxifen treatment aggravates acute pancreatic induced by CVB3 infection

The efficient control of the MerCreMer transgene with tamoxifen enabled us to reduce CAR protein levels to <10%. While the genetics are predictable and produce the desired elimination of CAR exon 1 only after tamoxifen induction in the adult, the virus load resulted in an unexpected lethality of >50% of animals starting at day 5 after infection with a severe form of acute pancreatitis in both tamoxifen injected knockout and wildtype control animals. An even stronger lethality has been described for a different strain of CVB3, where 4 x10^3 pfu per mouse resulted in a 50% mortality by day 5 after infection that left no survivors by day 7 (Asher et al., 2005a). Acute pancreatitis is not only caused by CVB3, but has also been described in the breast cancer patients treated with tamoxifen (Kanel et al., 1997). Therefore, we aimed to restore survival by the combination of decreased virus load and increased time between application of virus and tamoxifen to avoid

overlapping effects. Indeed, a reduced virus load of 5x 10^4 pfu and separation of tamoxifen injections and virus treatment by >2 months completely restored survival.

5.2.2 CAR is necessary but not sufficient for virus entry in the mouse model of CVB3 infection

With CAR deficient animals surviving the applied virus load, we were able to investigate the role of CAR in viral myocarditis. CAR has not only been implied in the progression of viral myocarditis based on its function as a virus receptor, but various approaches to study CAR *in vivo* have indicated that reduced CAR expression or interference with CAR function could affect the disease process. CAR has been implied in the early phases of myocarditis with reduced expression of CAR in MyD-88 deficient mice that are partially protected from CVB3 induced pathology (Fuse et al., 2005). Although virus load was reduced in the MyD-88 knockout cardiomyocytes as compared to the experiments described here, it is unclear if this effect can be attributed to the reduced expression of CAR or to the concomitantly increased IFN-α. Soluble recombinant CAR has been used as an efficient tool to abolish CVB3- mediated myocarditis in mice indicating the importance of the CAR-CVB3 interaction in the disease process (Yanagawa et al., 2004). While this approach is closer to the application as a therapeutic strategy, its effects can result from interaction of soluble CAR with the virus particle, endogenous CAR, or additional extracellular proteins.

Here, a loss of function approach was used to exclusively investigate CAR in the acute phase of CVB3 induced myocarditis. With CAR expression reduced to 10% of WT levels, the cardiac tissue was able to completely abolish cardiac pathology in CVB3 infected KO mice (Fig. 13). Structural changes were absent as determined by histology and not a single infected cardiomyocyte could be detected by *in situ* hybridization within a total of 20 investigated KO hearts (Fig. 14).

As the MerCreMer transgene directs expression of the recombinase exclusively to the heart, virus replication is retained in both pancreas and spleen of KO mice. This might help explain the increase in TNFα expression that − albeit reduced in comparison of the CVB3 infected CAR knockout − the CVB3 infected control heart was 3-fold increased as compared to non-infected animals based on cardiac RNA levels. Although CAR expression has been detected in multiple tissues including heart, brain, pancreas, liver, lung, and gut (Fechner et al., 1999; Bergelson et al., 1998; Tomko et al., 2000), the majority of those organs from wildtype mice did not show signs of virus infection (gut, liver, lung, and kidney). As confirmed on RNA and protein level, these organs do express CAR, at levels that exceed cardiac expression in gut, liver, and lung that were nevertheless not infected. Failure of virus to enter these cells could derive from the spatial separation of the virus and its receptor or the insufficient expression of co-receptors, or intracellular adaptor proteins, such as ZO1 and MUPP1 (Shafren et al., 1997; Cohen et al., 2001b; Cohen et al., 2001a; Coyne et al., 2004). The cytoplasmic protein expressed in those cells can block the virus entry might also lead to the complete immunity to CVB3 infection in the heart. The cryoEM reconstruction of full-length CAR-CVB3 complexes shows that adjacent CAR molecules, bind to the CVB3 canyon at the same density (He et al., 2001). Lacking of sufficient CAR molecules to form this bivalent association of the adjacent receptors might cause the failure of CVB3-CAR complex formation offered another possible reason that a very low-level expression of CAR can prevent cells from virus entry and subsequent pathological changes.

Conversely, low levels of CAR expression as detected in the spleen do not preclude CVB3 infection. Unlike the heart, where most cells are CAR-deficient, permissive cells in the spleen apparently do express CAR at sufficient levels to become infected. Overall, the tissue distribution and expression analysis indicate that CAR is necessary but not sufficient for virus entry in the mouse model of CVB3 infection. Its co-receptor DAF can by

itself not mediate virus uptake (Milstone et al., 2005). There are DAF binding and non-binding strains of CVB3, but even the DAF binding variant cannot mediate lytic infection without CAR (Shafren et al., 1997). Thus, CAR exerts a dominant effect on virus entry that in the KO could not be overcome by DAF. In the CAR KO heart, DAF expression was not significantly changed (Fig. 17C) indicating that it does not contribute to the phenotype.

5.2.3 Cardiac function after CVB3 infection

To verify that CAR deficiency did not only prevent morphological changes associated with myocarditis but also retained normal cardiac function, the contractile and elastic properties of CVB3 infected and untreated KO and WT animals were analyzed *in vivo* using the conductance catheter. In the acute phase CAR deficient hearts were unaffected, while CVB3 infected control hearts showed an impaired contractile function with a significant reduction in parameters of systolic function.

5.2.4 Direct virus-mediated pathology versus a secondary autoimmune component in myocarditis

In addition to documenting the crucial role of CAR for virus entry into the heart *in vivo*, the established animal model provides novel insights into the pathogenesis of CVB induced myocarditis. It has been argued that CVB myocarditis (at least, the chronic phase of disease) is autoimmune in nature. As the MerCreMer transgene is not expressed in T-cells, there is no reason to expect that putative autoreactive T-cells would not be induced in the conditional CAR KO. Here it is shown that virus infection of cardiomyocytes is a prerequisite for myocarditis and that even as late at 28 days post-infection, the KO-heart looks normal. All other susceptible organs can become infected and show the expected pathology in the CAR KO. This suggests a critical role for the productive infection of

cardiomyocytes in the disease and argues against a primary autoimmune component in pathogenesis.

So far, various therapeutic approaches to combat CVB3 infection have been proposed using CAR-transgenic erythrocytes to redirect and capture virus particles (Asher et al., 2005a) or soluble CAR to compete with the cell surface receptor (Dorner et al., 2006; Yanagawa et al., 2004; Lim et al., 2006). While the former has led to reduced lethality, the latter has worked in tissue culture (Goodfellow et al., 2005) but produced inconsistent results *in vivo* either ameliorating or aggravating the disease process in mice (Yanagawa et al., 2004; Lim et al., 2006). Based on the findings in this study one could speculate that CAR indeed provides a suitable target in the prevention and possible treatment of viral myocarditis.

5.3 CAR and cell-cell communication

Any strategy that changes its behavior will have to keep in mind the protein's roles in the healthy heart. CAR is not only relevant for virus uptake and cardiac remodeling, but also has a previously unknown function in the propagation of excitation from the atrium to the ventricle that could explain the association of arrhythmia and coxsackievirus infection of the heart. That might be the side effects of loss-of CAR.

5.3.1 CAR is important in postnatal remodeling

The switch from myocyte hyperplasia to hypertrophy occurs during the early postnatal period (Li et al., 1996). The neonatal phase is a critical period for the transition from embryonic stage to adulthood. During murine neonatal cardiac development and remodeling, a marked increase in numbers of cardiac fibroblasts and a resultant decrease in percentages of myocytes in late neonatal development (day 15) is reported (Banerjee et al., 2007). Cardiac myocytes display a significant increase from days 1 to 5 and then decreased from

day 5 to adult. CAR expression levels did not change till the first week after birth, and then gradually decreased after P7 to adult (Kashimura et al., 2004). The relatively high level of CAR expression in heart indicated a role of CAR during the transition of myocardial remodeling. Cardiac specific deletion of CAR in the neonatal phase resulted in a postnatal lethality with nearly 40% penetrance and significant body weight decrease, suggesting that CAR still keeps similar functions neonatally as in the embryonic stage. The decreased body weight might reflect the delayed development caused by the loss of CAR. However, due to the differences of individual development and progressive loss of CAR, disruption of cardiac expression cannot lead to 100% mortality of CAR KO mice. Those surviving mice developed a severe AVB IIIº: a hallmark of complete heart block with no apparent relationship between P waves and QRS complexes. It indicated that the impulse generated in the atria (typically the SA node on top of the right atrium) does not propagate to the ventricles. Furthermore, those mice had a slower heart rate, which displayed as prolonged RR interval on ECG recording.

Recent studies also showed that CAR deficiency causes prolongation of AV conduction (Lim et al., 2008; Lisewski et al., 2008), but the deletion did not cause lethality, slowed heart rate and body weight reduction as observed in neonatal mice. While increases in atrial size could be characterized as secondary to left ventricular dysfunction, accompanying alterations in heart rate or rhythm have been described in other genetic modified mouse models. For example, cardiac specific transgenic mouse line expressing activated RhoA resulted in atrial enlargement, bradycardia and sinus and AV conduction dysfunction (Sah et al., 1999).

Those results indicated that CAR is essential for cardiac conduction system and individual development during the neonatal remodeling phase. A summary of the respective phenotypes and the mechanistic implications is provided in appendix (table 14).

5.3.2 Cell-cell contacts at intercalated discs are linked to cardiac arrhythmia

The contractile tissue of the heart is composed of individual cells with highly specialized cell-cell contacts that ensure mechanical and electrochemical coupling in the beating heart. Communication along the cardiac myofiber is facilitated through the intercalated discs, where various types of these contacts interact in a structured network that when disturbed can lead to heart disease (Perriard et al., 2003). So far, three types of cell-cell contacts have been linked to cardiac arrhythmia in human and animal models related to proper function of the intercalated disc: adherens junctions, desmosomes, and gap junctions. Proteins of the adherens junction and the desmosome affect conduction in part indirectly through gap junctions, whose role in the cardiac conduction system is well established. Adherens junctions contain transmembrane proteins of the cadherin family and interact with the catenins at the cytoplasmic side to provide coupling to the contracting sarcomeres (Li et al., 2006). Together with desmosomes, which connect intermediate filaments (mainly desmin) to the cell surface, they mediate force transmission between neighboring cardiomyocytes (Li et al., 2006). Gap junctions are clusters of transmembrane channels which link the cytoplasmic compartments of adjacent cells and control electrical coupling between cardiac myocytes (Peters, 2006). The channels are formed from connexins, which are differentially expressed between the specialized cells of the electrical conduction system - including sinuatrial and atrioventricular node (largely Cx45), atrial cardiomyocytes (Cx40), and the working myocardium (Cx43) (Carson, 2001). Their differential gating properties facilitate the sequential depolarization of atria and ventricle and changes in the protein composition of the gap junction were associated with increased propensity to ventricular arrhythmias (Wilhelm et al., 2006; Betsuyaku et al., 2006). Cell uncoupling due to the loss of connexins from intercalated discs occurs very rapidly in myocardial infarction and could contribute to the increased risk of arrhythmia in the failing heart (Beardslee et al., 2000).

In addition to primary defects of connexins, secondary changes that disturb gap junction function and assembly can also result in arrhythmia. Thus, altered expression of or mutations in adherens junction proteins, desmosomes, and associated proteins (N-cadherin, β-catenin, g-catenin, plakophilin-2, desmoplakin) can lead to altered expression of connexins and impaired impulse propagation (Li et al., 2005; Oxford et al., 2007; Gard et al., 2005; Saffitz, 2005). The results from this thesis indicated that tight junction proteins are linked to cardiac function and disease. As a virus receptor CAR was linked to cardiac disease through coxsackievirus B3 (CVB3) that can induce myocarditis and ultimately dilated cardiomyopathy (Tomko et al., 1997; Bergelson et al., 1997). In addition to virus particles, CAR interacts with proteins related to cell-cell contact formation, endocytosis, and signal transduction (Fig. 26). In the heart, unlike in epithelial cells, CAR does not contribute to the formation of a classical tight junction – in fact the cardiac tight junction protein Claudin-5 localizes to the lateral cell border and is (unlike CAR) downregulated in heart failure (Mays et al., 2008; Sanford et al., 2005). These findings suggest differential roles of these tight junction proteins in the heart.

Thus, proper interplay of all known cell-cell contacts (including the tight junction) determines the electrical properties of the adult heart. Loss of the tight junction protein CAR leads to severe AV block, but leaves the electrical properties of the atrial and ventricular myocardium remarkably unaffected. Detailed characterization of the electrical activity of KO hearts revealed no difference in atrial depolarization, so that slowed atrial conduction as a reason for the delayed AV conduction (increased PR interval) can be excluded. Physiologically, the PR interval is mainly determined by the conduction through the AV node followed by the His-Purkinje bundles. As the His-Ventricle (HV) interval was equal in CAR KO and control mice, one can conclude that CAR regulates AV conduction directly within the AV node.

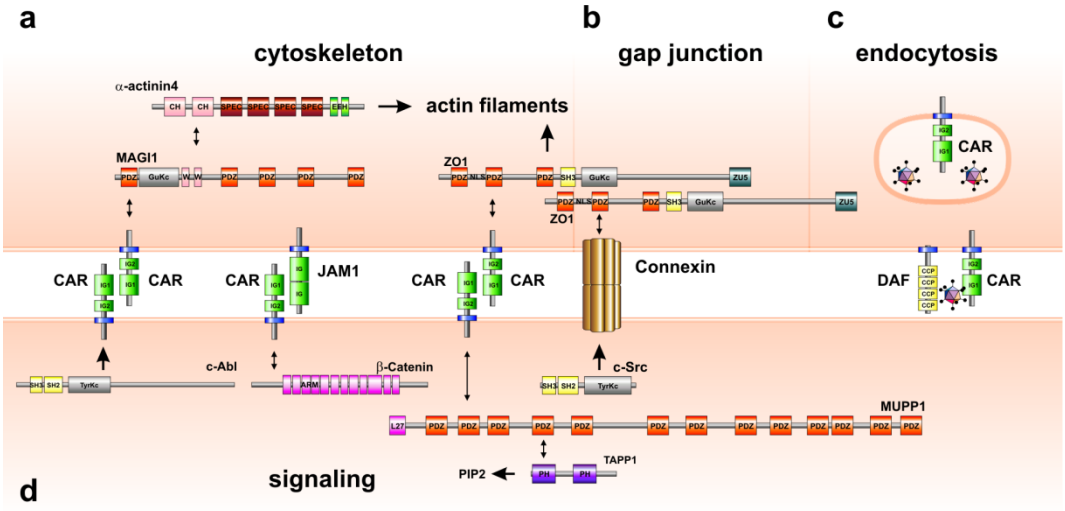

Figure 26: CAR is a multifunctional receptor that interacts with proteins related to cell-cell contact formation, endocytosis, and signal transduction. a) CAR can hetero- or homodimerize via the extracellular Ig-domains. The cytoplasmic tail interacts with various PDZ domain proteins, among them ZO-1 (zona occludens 1) and MAGI1 (membrane associated guanylate kinase, WW and PDZ domain containing 1) that link to actin filament assembly. b) The common binding protein ZO-1 mediates interaction between the cytoplasmic tails of CAR and connexins to modulate the gap junction activity. c) Together with its co-receptor decay accelerating factor (DAF/CD55), CAR mediates virus binding and uptake. d) Links to signal transduction include the interaction of CAR with β-catenin and MUPP1 (multi-PDZ domain protein 1). Both CAR and connexins are substrates of tyrosine kinase.

5.3.3 Cross-talk of tight junction and gap junction

Towards understanding the molecular mechanism underlying the AV-block phenotype, the KO model generated in this study was compared to published animal models with arrhythmia that involves prolonged PR-intervals (Lisewski et al., 2008). With the severe AV-block in the absence of atrial or ventricular arrhythmia mimicked in the Cx45 KO and reduced Cx43 and Cx45 expression in embryonic CAR KO heart, one can hypothesize that CAR affects electrical conduction indirectly through gap junctions. Since the size of the murine AV-node prevents functional studies of the AV-nodal cells, gap junction activity in cardiomyocytes was investigated as a proof of concept. While dye coupling is widely used to study gap junctions in cultivated cardiomyocytes (Oxford et al., 2007), the method has been adapted to be used in cardiac slices, which largely preserves the structures

required for intercellular communication. The increased dye coupling from week 3 after induction of the KO was shown in Figure 22 indicating crosstalk of the tight and gap junction. Thus, CAR might affect conduction through altered compartmentalization of connexins. A similar dependence has been shown for N-cadherin and connexins with decreased expression of Cx40 and 43 in the N-cadherin KO heart (Li et al., 2005). On a molecular level the functional interaction of gap and tight junction is supported by coprecipitation and co-localization of Cx40 and Cx43 with tight-junction molecules occludin, claudin-5, and ZO-1 in endothelial cells (Nagasawa et al., 2006).

The increased dye coupling does not lead to altered electrical properties of the atrium or ventricle in CAR KO. This indicates that CAR KO cardiomyocytes, unlike AV-nodal cells, are not limited by gap junction activity, a feature that could derive both from altered expression of connexins and differential localization of CAR between the cell-types. Atrioventricular conduction is altered in various connexin KO animals such as the cardiac KO of Cx45 (Nishii et al., 2003) or the KO of Cx40, which displays a combination of intra-atrial block, ectopic rhythms, and altered atrial propagation in the right atrium (Bagwe et al., 2005). None of the ectopic rhythms described in the Cx40 KO or of the spontaneous or the inducible ventricular tachyarrhythmias of the Cx43 KO (Danik et al., 2007) could be detected in the CAR KO heart. These results indicate a residual function of Cx40 and Cx43 in the CAR KO and further underscore the specific role of CAR in AV conduction. In part, this is reflected in the differential expression of connexins in the KO heart: Cx40 protein levels are maintained at physiological levels, while Cx45 expression is reduced in the KO heart. Together with the functional analysis indicating that Cx40 or Cx45 are affected in CAR KO (both share the AV block phenotype with the CAR KO) the expression analysis suggests that the effect of CAR is mediated by Cx45.

The documented crosstalk of CAR and connexins in ventricle is comparable to the mechanism of action of N-cadherin in cardiac conduction defects. The documented changes

in conduction could explain both the AV-block and. It is important to note that different connexins are expressed in the conduction system and the myocardium. Furthermore, the preliminary expression profiling analysis indicated that the regulation of connexin expression in response to the loss of CAR differs between atrium and ventricle. Thus, altered communication of connexins can differentially affect the conduction system (AV-block and sick sinus syndrome) and the ventricle where the defect is compensated with no indication for electrical abnormalities but increased coupling.

Towards understanding the molecular basis of the isolated AV-block, one would envision a mechanism where loss of CAR results in an altered protein composition of the tight junction, as documented by expression and immunofluorescence analysis (Fig. 11B and 20). While the tight junction as a whole is not affected with normal ultrastructure and proper sublocalization of N-cadherin, connexins specifically respond to the loss of CAR with redistribution away from the intercalated disc and reduced protein levels can be observed. This redistribution and reduction of connexins can potentially be due to a combination of reduced expression and degradation of mislocalized protein. The presence of CAR protein might have the function of stabilizing connexins at the intercalated discs. The AV-node shows less compartmentalization and a more homogenous distribution of CAR along the plasma membrane (Lisewski et al., 2008). This would explain the isolated effect on the AV-node where no predetermined structure such as the intercalated disc would facilitate proper electrical conduction.

Multiple diseases have been associated with the tight junction, ranging from deafness and cancer to allergies and infections (Cereijido et al., 2007). This study describes a novel role for the tight junction in arrhythmia. Not only does this have implications for CAR as a potential diagnostic marker for familial cases of AV block, but it might also help explain how virus proteins or autoantibodies that interact with tight junction proteins such as CAR can cause arrhythmia (Sato et al., 1989). Shedding of virus proteins from infected

cells is an important mechanism to disrupt CAR-CAR interaction at the tight junction and facilitate virus passing epithelial barriers (Walters et al., 2002). In the heart, this virus induced disruption of CAR-dimers would be expected to produce the same effect as the loss of CAR and thus ultimately lead to uncoupling and electrical conduction defects, which can accompany viral myocarditis (Kishimoto et al., 1984). Autoantibodies in rheumatic women have been shown to cause AV block by dysregulating Ca^{2+} homeostasis in cardiomyocytes (Salomonsson et al., 2005). A similar mechanism could result from autoantibodies that interfere with tight junction proteins.

5.4 CAR expression levels determine the severity of the phenotype

Germline deletion of CAR caused embryonic lethality with cardiac defect, but haploinsufficiency did now show any abnormalities. One can conclude that CAR is critical to the early stage of development when CAR appeared highly expressed, but a certain amount of CAR expression is sufficient to maintain normal physiological function during embryonic development.

The animals are less susceptible to loss of CAR after birth and in adulthood, cardiac specific deletion in adulthood did not affect the survival rate. Those animals developed a strong phenotype of AV-nodal block. The degree of AV-nodal block is dependent on the progression of induction, indicating that the atrial-ventricular conduction is regulated by the expression level of CAR. When CVB3 infected CAR deficient animals, cardiomyocytes showed 100% resistance to the virus infection, while there was still <10% CAR expression. More CAR expression preserved, more side effects due to loss of CAR will be prevented. To minimize the side effects, it is necessary to investigate that to what extent, CVB3 entry can efficiently be blocked.

Moreover, not only loss of CAR can protect hearts from virus entry and subsequent pathological change, but it has also been shown that CAR haploinsufficiency can prevent

cardiac hypertrophy from volume overload stimulation. The result indicated that with less CAR expression, the heart could be protected from hypertrophy or at least, the progress of hypertrophy is delayed. CAR heterozygous animals have less receptor available, they have a potential to uptake less virus and alleviate the severity of the pathological changes after virus application.

5.5 Conclusions

Constitutive deletion of coxsackievirus and adenovirus receptor (CAR) is embryonic lethal at midgestation (E11.5) with impaired cardiac development and myofibril disorganization. Apolipoproteins were accumulated in the knockout heart, indicating CAR is involved in lipid uptake. Connexin expression was decreased in the knockout, suggesting an abnormal cell-cell communication secondary to the loss of CAR. Those results indicated that CAR is a multi-functional protein that is essential for embryonic development.

So far, various therapeutic approaches to combat CVB3 infection have been proposed. CAR-transgenic erythrocytes were used to redirect and capture virus particles (Asher et al., 2005a) or soluble CAR has been applied to compete with the cell surface receptor (Yanagawa et al., 2004; Lim et al., 2006; Dorner et al., 2006). While the former has led to reduced lethality, the latter has worked sufficiently in tissue culture (Goodfellow et al., 2005) but produced inconsistent results *in vivo* either ameliorating or aggravating the disease process in mice (Dorner et al., 2006; Yanagawa et al., 2004; Lim et al., 2006). Based on the findings in this study one could speculate that CAR indeed provides a suitable target for the prevention and possible treatment of viral myocarditis.

The potential unwanted effects that might result from the loss of CAR in the adult heart were addressed in the inducible CAR KO animals, which developed AV nodal block. The underlying mechanism involves the crosstalk of tight and gap junctions with altered ex-

pression and localization of connexins that affect the communication between CAR knockout cardiomyocytes at the intercalated disc.

6 Outlook

Analyzing CAR deficient embryos helps to understand its role in embryonic development and physiological functions. So far, published data suggested that CAR is important for embryonic development and tissue homeostasis (Dorner et al., 2005; Asher et al., 2005b; Chen et al., 2006; Raschperger et al., 2006; Lim et al., 2008; Lisewski et al., 2008). This work provided the molecular basis underlying the embryonic lethality. However, data obtained in this study did not explain sufficiently if the phenotype is mediated by loss of the homophilic interaction of CAR between cells or via its role in endocytosis and signal transduction. Thus, it is necessary to distinguish the various cell type specific functions of CAR and the signaling pathways involved in embryonic development. To investigate the role of CAR in myofilament assembly, we have generated a GFP-tagged titin to label the sarcomere. This strain can be used to follow differentiation and fusion of cardiomyocytes and the transition of the myofilament between cells comparing CAR deficient and control animals.

While the homozygous knockout displays a strong embryonic and distinct adult phenotype, we have so far not investigated a potential phenotype in heterozygous deficient animals in detail. One possibility would be the use of challenging conditions such as pressure and volume overload or adrenergic stimulation. CAR haploinsufficient animals appeared phenotypically normal. After volume-overload, the animals only showed a slight tendency of reduced hypertrophy that could be increased with a stronger stimulus – possibly the combination of pressure overload and adrenergic stimulation. The heterozygous animals could also be used to investigate a potentially beneficial effect with less receptor available for virus uptake that could reduce the severity of myocarditis in infected animals.

We showed that CAR is necessary but not sufficient for CVB3 entry, and that loss of CAR can protect the heart from viral myocarditis with the potential for side effects that include AV-nodal block. Additional studies are needed to establish a save level for CAR to prevent pathology and reduce unwanted side effects.

Since tamoxifen aggravates CVB3 induced myocarditis, it would be desirable to obtain a cardiac inducible Cre that uses a different agent to activate recombination, possibly using tetracycline-inducible expression of the recombinase. This model would facilitate the investigation of CAR's therapeutic potential in the infected heart compared to the prevention weeks before exposure to the virus.

At this time, there is no genetic defect of CAR associated with human disease, but the findings here would suggest tight junction proteins as potential disease genes in genetic forms of isolated AV block. It might be possible to identify patients with reduced CAR levels (heterozygotes) in a cohort with inherited AV-block of unknown cause or patients with reduced susceptibility to viral myocarditis.

Finally, the role of CAR in arrhythmogenesis has implications for CVB3 infection and patients with heart disease resulting from antibodies against proteins of the tight junction, which may lead to better screening methods to identify persons at risk of potentially fatal arrhythmia and possibly to novel therapies.

References

Abdelwahid, E.; Pelliniemi, L. J.; Niinikoski, H.; Simell, O.; Tuominen, J.; Rahkonen, O. and Jokinen, E. (1999): Apoptosis in the pattern formation of the ventricular wall during mouse heart organogenesis, *Anat.Rec.* 256, (2): 208-217.

Abdolazimi, Y.; Mojarrad, M.; Pedram, M. and Modarressi, M. H. (2007): Analysis of the expression of coxsackievirus and adenovirus receptor in five colon cancer cell lines, *World J.Gastroenterol.* 13, (47): 6365-6369.

Anders, M.; Christian, C.; McMahon, M.; McCormick, F. and Korn, W. M. (2003): Inhibition of the Raf/MEK/ERK pathway up-regulates expression of the coxsackievirus and adenovirus receptor in cancer cells, *Cancer Res.* 63, (9): 2088-2095.

Anderson, D. R.; Wilson, J. E.; Carthy, C. M.; Yang, D.; Kandolf, R. and McManus, B. M. (1996): Direct interactions of coxsackievirus B3 with immune cells in the splenic compartment of mice susceptible or resistant to myocarditis, *J.Virol.* 70, (7): 4632-4645.

Asher, D. R.; Cerny, A. M. and Finberg, R. W. (2005a): The erythrocyte viral trap: transgenic expression of viral receptor on erythrocytes attenuates coxsackievirus B infection, *Proc.Natl.Acad.Sci.U.S.A.* 102, (36): 12897-12902.

Asher, D. R.; Cerny, A. M.; Weiler, S. R.; Horner, J. W.; Keeler, M. L.; Neptune, M. A.; Jones, S. N.; Bronson, R. T.; Depinho, R. A. and Finberg, R. W. (2005b): Coxsackievirus and adenovirus receptor is essential for cardiomyocyte development, *Genesis* 42, (2): 77-85.

Atkins, A. R.; Osborne, M. J.; Lashuel, H. A.; Edelman, G. M.; Wright, P. E.; Cunningham, B. A. and Dyson, H. J. (1999): Association between the first two immunoglobulin-like domains of the neural cell adhesion molecule N-CAM, *FEBS Lett.* 451, (2): 162-168.

Aurrand-Lions, M.; Duncan, L.; Ballestrem, C. and Imhof, B. A. (2001): JAM-2, a novel immunoglobulin superfamily molecule, expressed by endothelial and lymphatic cells, *J.Biol.Chem.* 276, (4): 2733-2741.

Bagwe, S.; Berenfeld, O.; Vaidya, D.; Morley, G. E. and Jalife, J. (2005): Altered right atrial excitation and propagation in connexin40 knockout mice, *Circulation* 112, (15): 2245-2253.

Banerjee, I.; Fuseler, J. W.; Price, R. L.; Borg, T. K. and Baudino, T. A. (2007): Determination of cell types and numbers during cardiac development in the neonatal and adult rat and mouse, *Am.J.Physiol Heart Circ.Physiol* 293, (3): H1883-H1891.

Bao, Y.; Peng, W.; Verbitsky, A.; Chen, J.; Wu, L.; Rauen, K. A. and Sawicki, J. A. (2005): Human coxsackie adenovirus receptor (CAR) expression in transgenic mouse prostate tumors enhances adenoviral delivery of genes, *Prostate* 64, (4): 401-407.

Barton, E. S.; Forrest, J. C.; Connolly, J. L.; Chappell, J. D.; Liu, Y.; Schnell, F. J.; Nusrat, A.; Parkos, C. A. and Dermody, T. S. (2001): Junction adhesion molecule is a receptor for reovirus, *Cell* 104, (3): 441-451.

Bazzoni, G.; Martinez-Estrada, O. M.; Orsenigo, F.; Cordenonsi, M.; Citi, S. and Dejana, E. (2000): Interaction of junctional adhesion molecule with the tight junction components ZO-1, cingulin, and occludin, *J.Biol.Chem.* 275, (27): 20520-20526.

Beardslee, M. A.; Lerner, D. L.; Tadros, P. N.; Laing, J. G.; Beyer, E. C.; Yamada, K. A.; Kleber, A. G.; Schuessler, R. B. and Saffitz, J. E. (2000): Dephosphorylation and intracellular redistribution of ventricular connexin43 during electrical uncoupling induced by ischemia, *Circ.Res.* 87, (8): 656-662.

Bergelson, J. M.; Cunningham, J. A.; Droguett, G.; Kurt-Jones, E. A.; Krithivas, A.; Hong, J. S.; Horwitz, M. S.; Crowell, R. L. and Finberg, R. W. (1997): Isolation of a common receptor for Coxsackie B viruses and adenoviruses 2 and 5, *Science* 275, (5304): 1320-1323.

Bergelson, J. M.; Krithivas, A.; Celi, L.; Droguett, G.; Horwitz, M. S.; Wickham, T.; Crowell, R. L. and Finberg, R. W. (1998): The murine CAR homolog is a receptor for coxsackie B viruses and adenoviruses, *J.Virol.* 72, (1): 415-419.

Bernal, R. M.; Sharma, S.; Gardner, B. K.; Douglas, J. T.; Bergelson, J. M.; Dubinett, S. M. and Batra, R. K. (2002): Soluble coxsackievirus adenovirus receptor is a putative inhibitor of adenoviral gene transfer in the tumor milieu, *Clin.Cancer Res.* 8, (6): 1915-1923.

Betsuyaku, T.; Nnebe, N. S.; Sundset, R.; Patibandla, S.; Krueger, C. M. and Yamada, K. A. (2006): Overexpression of cardiac connexin45 increases susceptibility to ventricular tachyarrhythmias in vivo, *Am.J.Physiol Heart Circ.Physiol* 290, (1): H163-H171.

Bewley, M. C.; Springer, K.; Zhang, Y. B.; Freimuth, P. and Flanagan, J. M. (1999): Structural analysis of the mechanism of adenovirus binding to its human cellular receptor, CAR, *Science* 286, (5444): 1579-1583.

Bowles, K. R.; Gibson, J.; Wu, J.; Shaffer, L. G.; Towbin, J. A. and Bowles, N. E. (1999): Genomic organization and chromosomal localization of the human Coxsackievirus B-adenovirus receptor gene, *Hum.Genet.* 105, (4): 354-359.

Bowles, N. E.; Javier Fuentes-Garcia, F.; Makar, K. A.; Li, H.; Gibson, J.; Soto, F.; Schwimmbeck, P. L.; Schultheiss, H. P. and Pauschinger, M. (2002): Analysis of the coxsackievirus B-adenovirus receptor gene in patients with myocarditis or dilated cardiomyopathy, *Mol.Genet.Metab* 77, (3): 257-259.

Bowles, N. E.; Ni, J.; Kearney, D. L.; Pauschinger, M.; Schultheiss, H. P.; McCarthy, R.; Hare, J.; Bricker, J. T.; Bowles, K. R. and Towbin, J. A. (2003): Detection of viruses in myocardial tissues by polymerase chain reaction. evidence of adenovirus as a common cause of myocarditis in children and adults, *J.Am.Coll.Cardiol.* 42, (3): 466-472.

Bruning, A.; Stickeler, E.; Diederich, D.; Walz, L.; Rohleder, H.; Friese, K. and Runnebaum, I. B. (2005): Coxsackie and adenovirus receptor promotes adenocarcinoma cell survival and is expressionally activated after transition from preneoplastic precursor lesions to invasive adenocarcinomas, *Clin.Cancer Res.* 11, (12): 4316-4320.

Carson, S. D. (2001): Receptor for the group B coxsackieviruses and adenoviruses: CAR, *Rev.Med.Virol.* 11, (4): 219-226.

Carson, S. D. (2004): Coxsackievirus and adenovirus receptor (CAR) is modified and shed in membrane vesicles, *Biochemistry* 43, (25): 8136-8142.

Carson, S. D.; Chapman, N. N. and Tracy, S. M. (1997): Purification of the putative coxsackievirus B receptor from HeLa cells, *Biochem.Biophys.Res.Commun.* 233, (2): 325-328.

Carson, S. D.; Hobbs, J. T.; Tracy, S. M. and Chapman, N. M. (1999): Expression of the coxsackievirus and adenovirus receptor in cultured human umbilical vein endothelial cells: regulation in response to cell density, *J.Virol.* 73, (8): 7077-7079.

Cayli, S.; Ustunel, I.; Celik-Ozenci, C.; Korgun, E. T. and Demir, R. (2002): Distribution patterns of PCNA and ANP in perinatal stages of the developing rat heart, *Acta Histochem.* 104, (3): 271-277.

Cereijido, M.; Contreras, R. G.; Flores-Benitez, D.; Flores-Maldonado, C.; Larre, I.; Ruiz, A. and Shoshani, L. (2007): New diseases derived or associated with the tight junction, *Arch.Med.Res.* 38, (5): 465-478.

Chappell, J. D.; Prota, A. E.; Dermody, T. S. and Stehle, T. (2002): Crystal structure of reovirus attachment protein sigma1 reveals evolutionary relationship to adenovirus fiber, *EMBO J.* 21, (1-2): 1-11.

Chen, J. W.; Ghosh, R.; Finberg, R. W. and Bergelson, J. M. (2003): Structure and chromosomal localization of the murine coxsackievirus and adenovirus receptor gene, *DNA Cell Biol* 22, (4): 253-259.

Chen, J. W.; Zhou, B.; Yu, Q. C.; Shin, S. J.; Jiao, K.; Schneider, M. D.; Baldwin, H. S. and Bergelson, J. M. (2006): Cardiomyocyte-specific deletion of the coxsackievirus and adenovirus receptor results in hyperplasia of the embryonic left ventricle and abnormalities of sinuatrial valves, *Circ.Res.* 98, (7): 923-930.

Cheung, P. K.; Yuan, J.; Zhang, H. M.; Chau, D.; Yanagawa, B.; Suarez, A.; McManus, B. and Yang, D. (2005): Specific interactions of mouse organ proteins with the 5'untranslated region of coxsackievirus B3: potential determinants of viral tissue tropism, *J.Med.Virol.* 77, (3): 414-424.

Choi, M.; Stottmann, R. W.; Yang, Y. P.; Meyers, E. N. and Klingensmith, J. (2007): The bone morphogenetic protein antagonist noggin regulates mammalian cardiac morphogenesis, *Circ.Res.* 100, (2): 220-228.

Chretien, I.; Marcuz, A.; Courtet, M.; Katevuo, K.; Vainio, O.; Heath, J. K.; White, S. J. and Du, Pasquier L. (1998): CTX, a Xenopus thymocyte receptor, defines a molecular family conserved throughout vertebrates, *Eur.J.Immunol.* 28, (12): 4094-4104.

Chretien, I.; Robert, J.; Marcuz, A.; Garcia-Sanz, J. A.; Courtet, M. and Du, Pasquier L. (1996): CTX, a novel molecule specifically expressed on the surface of cortical thymocytes in Xenopus, *Eur.J.Immunol.* 26, (4): 780-791.

Chung, S. K.; Kim, J. Y.; Kim, I. B.; Park, S. I.; Paek, K. H. and Nam, J. H. (2005): Internalization and trafficking mechanisms of coxsackievirus B3 in HeLa cells, *Virology* 333, (1): 31-40.

Ciray, H. N.; Persson, B. E.; Roomans, G. M. and Ulmsten, U. (1995): Dye-coupling between term pregnant human myometrial cells before labor: carboxyfluorescein versus lucifer yellow, *Cell Biol.Int.* 19, (7): 609-617.

Clark, M. A. and Jepson, M. A. (2003): Intestinal M cells and their role in bacterial infection, *Int.J.Med.Microbiol.* 293, (1): 17-39.

Cohen, C. J.; Gaetz, J.; Ohman, T. and Bergelson, J. M. (2001a): Multiple regions within the coxsackievirus and adenovirus receptor cytoplasmic domain are required for basolateral sorting, *J.Biol.Chem.* 276, (27): 25392-25398.

Cohen, C. J.; Shieh, J. T.; Pickles, R. J.; Okegawa, T.; Hsieh, J. T. and Bergelson, J. M. (2001b): The coxsackievirus and adenovirus receptor is a transmembrane component of the tight junction, *Proc.Natl.Acad.Sci.U.S.A.* 98, (26): 15191-15196.

Coyne, C. B. and Bergelson, J. M. (2005): CAR: a virus receptor within the tight junction, *Adv.Drug Deliv.Rev.* 57, (6): 869-882.

Coyne, C. B. and Bergelson, J. M. (2006): Virus-induced Abl and Fyn kinase signals permit coxsackievirus entry through epithelial tight junctions, *Cell* 124, (1): 119-131.

Coyne, C. B.; Vanhook, M. K.; Gambling, T. M.; Carson, J. L.; Boucher, R. C. and Johnson, L. G. (2002): Regulation of airway tight junctions by proinflammatory cytokines, *Mol.Biol.Cell* 13, (9): 3218-3234.

Coyne, C. B.; Voelker, T.; Pichla, S. L. and Bergelson, J. M. (2004): The coxsackievirus and adenovirus receptor interacts with the multi-PDZ domain protein-1 (MUPP-1) within the tight junction, *J.Biol.Chem.* 279, (46): 48079-48084.

Cunningham, S. A.; Arrate, M. P.; Rodriguez, J. M.; Bjercke, R. J.; Vanderslice, P.; Morris, A. P. and Brock, T. A. (2000): A novel protein with homology to the junctional adhesion molecule. Characterization of leukocyte interactions, *J.Biol.Chem.* 275, (44): 34750-34756.

Danik, S. B.; Rosner, G.; Lader, J.; Gutstein, D. E.; Fishman, G. I. and Morley, G. E. (2007): Electrical remodeling contributes to complex tachyarrhythmias in connexin43-deficient mouse hearts, *FASEB J.*

Davis, B.; Nguyen, J.; Stoltz, D.; Depping, D.; Excoffon, K. J. and Zabner, J. (2004): Adenovirus-mediated erythropoietin production by airway epithelia is enhanced by apical localization of the coxsackie-adenovirus receptor in vivo, *Mol.Ther.* 10, (3): 500-506.

Dejana, E.; Lampugnani, M. G.; Martinez-Estrada, O. and Bazzoni, G. (2000): The molecular organization of endothelial junctions and their functional role in vascular morphogenesis and permeability, *Int.J.Dev.Biol.* 44, (6): 743-748.

Dho, S. E.; Jacob, S.; Wolting, C. D.; French, M. B.; Rohrschneider, L. R. and McGlade, C. J. (1998): The mammalian numb phosphotyrosine-binding domain. Characterization of binding specificity and identification of a novel PDZ domain-containing numb binding protein, LNX, *J.Biol.Chem.* 273, (15): 9179-9187.

Dobrosotskaya, I. Y. and James, G. L. (2000): MAGI-1 interacts with beta-catenin and is associated with cell-cell adhesion structures, *Biochem.Biophys.Res.Commun.* 270, (3): 903-909.

Dorner, A.; Grunert, H. P.; Lindig, V.; Chandrasekharan, K.; Fechner, H.; Knowlton, K. U.; Isik, A.; Pauschinger, M.; Zeichhardt, H. and Schultheiss, H. P. (2006): Treatment of coxsackievirus-B3-infected BALB/c mice with the soluble coxsackie adenovirus receptor CAR4/7 aggravates cardiac injury, *J.Mol.Med.* 84, (10): 842-851.

Dorner, A.; Xiong, D.; Couch, K.; Yajima, T. and Knowlton, K. U. (2004): Alternatively spliced soluble coxsackie-adenovirus receptors inhibit coxsackievirus infection, *J.Biol.Chem.* 279, (18): 18497-18503.

Dorner, A. A.; Wegmann, F.; Butz, S.; Wolburg-Buchholz, K.; Wolburg, H.; Mack, A.; Nasdala, I.; August, B.; Westermann, J.; Rathjen, F. G. and Vestweber, D. (2005): Coxsackievirus-adenovirus receptor (CAR) is essential for early embryonic cardiac development, *J.Cell Sci.* 118, (Pt 15): 3509-3521.

Ebnet, K.; Schulz, C. U.; Meyer Zu Brickwedde, M. K.; Pendl, G. G. and Vestweber, D. (2000): Junctional adhesion molecule interacts with the PDZ domain-containing proteins AF-6 and ZO-1, *J.Biol.Chem.* 275, (36): 27979-27988.

Estevez, M. A.; Henderson, J. A.; Ahn, D.; Zhu, X. R.; Poschmann, G.; Lubbert, H.; Marx, R. and Baraban, J. M. (2008): The neuronal RhoA GEF, Tech, interacts with the synaptic multi-PDZ-domain-containing protein, MUPP1, *J.Neurochem.*

Excoffon, K. J.; Gansemer, N.; Traver, G. and Zabner, J. (2007): Functional effects of coxsackievirus and adenovirus receptor glycosylation on homophilic adhesion and adenoviral infection, *J.Virol.* 81, (11): 5573-5578.

Excoffon, K. J.; Hruska-Hageman, A.; Klotz, M.; Traver, G. L. and Zabner, J. (2004): A role for the PDZ-binding domain of the coxsackie B virus and adenovirus receptor (CAR) in cell adhesion and growth, *J.Cell Sci.* 117, (Pt 19): 4401-4409.

Fairweather, D. and Rose, N. R. (2007): Coxsackievirus-induced myocarditis in mice: a model of autoimmune disease for studying immunotoxicity, *Methods* 41, (1): 118-122.

Fan, G. C.; Yuan, Q. and Kranias, E. G. (2008): Regulatory roles of junctin in sarcoplasmic reticulum calcium cycling and myocardial function, *Trends Cardiovasc.Med.* 18, (1): 1-5.

Fan, G. C.; Yuan, Q.; Zhao, W.; Chu, G. and Kranias, E. G. (2007): Junctin is a prominent regulator of contractility in cardiomyocytes, *Biochem.Biophys.Res.Commun.* 352, (3): 617-622.

Fanning, A. S.; Jameson, B. J.; Jesaitis, L. A. and Anderson, J. M. (1998): The tight junction protein ZO-1 establishes a link between the transmembrane protein occludin and the actin cytoskeleton, *J.Biol.Chem.* 273, (45): 29745-29753.

Fanning, A. S.; Ma, T. Y. and Anderson, J. M. (2002): Isolation and functional characterization of the actin binding region in the tight junction protein ZO-1, *FASEB J.* 16, (13): 1835-1837.

Fechner, H.; Haack, A.; Wang, H.; Wang, X.; Eizema, K.; Pauschinger, M.; Schoemaker, R.; Veghel, R.; Houtsmuller, A.; Schultheiss, H. P.; Lamers, J. and Poller, W. (1999): Expression of coxsackie adenovirus receptor and alphav-integrin does not correlate with adenovector targeting in vivo indicating anatomical vector barriers, *Gene Ther.* 6, (9): 1520-1535.

Fechner, H.; Noutsias, M.; Tschoepe, C.; Hinze, K.; Wang, X.; Escher, F.; Pauschinger, M.; Dekkers, D.; Vetter, R.; Paul, M.; Lamers, J.; Schultheiss, H. P. and Poller, W. (2003): Induction of coxsackievirus-adenovirus-receptor expression during myocardial tissue formation and remodeling: identification of a cell-to-cell contact-dependent regulatory mechanism, *Circulation* 107, (6): 876-882.

Feldman, A. M. and McNamara, D. (2000): Myocarditis, *N.Engl.J.Med.* 343, (19): 1388-1398.

Feuer, R.; Mena, I.; Pagarigan, R. R.; Harkins, S.; Hassett, D. E. and Whitton, J. L. (2003): Coxsackievirus B3 and the neonatal CNS: the roles of stem cells, developing neurons, and apoptosis in infection, viral dissemination, and disease, *Am.J.Pathol.* 163, (4): 1379-1393.

Fujimoto, K. (1995): Freeze-fracture replica electron microscopy combined with SDS digestion for cytochemical labeling of integral membrane proteins. Application to the immunogold labeling of intercellular junctional complexes, *J.Cell Sci.* 108 (Pt 11): 3443-3449.

Fuse, K.; Chan, G.; Liu, Y.; Gudgeon, P.; Husain, M.; Chen, M.; Yeh, W. C.; Akira, S. and Liu, P. P. (2005): Myeloid differentiation factor-88 plays a crucial role in the pathogenesis of Coxsackievirus B3-induced myocarditis and influences type I interferon production, *Circulation* 112, (15): 2276-2285.

Fuxe, J.; Liu, L.; Malin, S.; Philipson, L.; Collins, V. P. and Pettersson, R. F. (2003): Expression of the coxsackie and adenovirus receptor in human astrocytic tumors and xenografts, *Int.J.Cancer* 103, (6): 723-729.

Gard, J. J.; Yamada, K.; Green, K. G.; Eloff, B. C.; Rosenbaum, D. S.; Wang, X.; Robbins, J.; Schuessler, R. B.; Yamada, K. A. and Saffitz, J. E. (2005): Remodeling of gap junctions and slow conduction in a mouse model of desmin-related cardiomyopathy, *Cardiovasc.Res.* 67, (3): 539-547.

Gergs, U.; Berndt, T.; Buskase, J.; Jones, L. R.; Kirchhefer, U.; Muller, F. U.; Schluter, K. D.; Schmitz, W. and Neumann, J. (2007): On the role of junctin in cardiac Ca2+ handling, contractility, and heart failure, *Am.J.Physiol Heart Circ.Physiol* 293, (1): H728-H734.

Goldsmith, M. E.; Kitazono, M.; Fok, P.; Aikou, T.; Bates, S. and Fojo, T. (2003): The histone deacetylase inhibitor FK228 preferentially enhances adenovirus transgene expression in malignant cells, *Clin.Cancer Res.* 9, (14): 5394-5401.

Gonzalez-Mariscal, L.; Betanzos, A. and vila-Flores, A. (2000): MAGUK proteins: structure and role in the tight junction, *Semin.Cell Dev.Biol.* 11, (4): 315-324.

Goodfellow, I. G.; Evans, D. J.; Blom, A. M.; Kerrigan, D.; Miners, J. S.; Morgan, B. P. and Spiller, O. B. (2005): Inhibition of coxsackie B virus infection by soluble forms of its receptors: binding affinities, altered particle formation, and competition with cellular receptors, *J.Virol.* 79, (18): 12016-12024.

Gotow, T. and Hashimoto, P. H. (1982): Intercellular junctions between specialized ependymal cells in the subcommissural organ of the rat, *J.Neurocytol.* 11, (3): 363-379.

Gotthardt, M.; Hammer, R. E.; Hubner, N.; Monti, J.; Witt, C. C.; McNabb, M.; Richardson, J. A.; Granzier, H.; Labeit, S. and Herz, J. (2003): Conditional expression of mutant M-line titins results in cardiomyopathy with altered sarcomere structure, *J.Biol.Chem.* 278, (8): 6059-6065.

Gu, W.; Ogose, A.; Kawashima, H.; Ito, M.; Ito, T.; Matsuba, A.; Kitahara, H.; Hotta, T.; Tokunaga, K.; Hatano, H.; Morita, T.; Urakawa, S.; Yoshizawa, T.; Kawashima, H.; Kuwano, R. and Endo, N. (2004): High-level expression of the coxsackievirus and adenovirus receptor messenger RNA in osteosarcoma, Ewing's sarcoma, and benign neurogenic tumors among musculoskeletal tumors, *Clin.Cancer Res.* 10, (11): 3831-3838.

Hamazaki, Y.; Itoh, M.; Sasaki, H.; Furuse, M. and Tsukita, S. (2002): Multi-PDZ domain protein 1 (MUPP1) is concentrated at tight junctions through its possible interaction with claudin-1 and junctional adhesion molecule, *J.Biol.Chem.* 277, (1): 455-461.

He, Y.; Chipman, P. R.; Howitt, J.; Bator, C. M.; Whitt, M. A.; Baker, T. S.; Kuhn, R. J.; Anderson, C. W.; Freimuth, P. and Rossmann, M. G. (2001): Interaction of coxsackievirus B3 with the full length coxsackievirus-adenovirus receptor, *Nat.Struct.Biol.* 8, (10): 874-878.

Hemmi, S.; Geertsen, R.; Mezzacasa, A.; Peter, I. and Dummer, R. (1998): The presence of human coxsackievirus and adenovirus receptor is associated with efficient adenovirus-mediated transgene expression in human melanoma cell cultures, *Hum.Gene Ther.* 9, (16): 2363-2373.

Hemminki, A.; Kanerva, A.; Liu, B.; Wang, M.; Alvarez, R. D.; Siegal, G. P. and Curiel, D. T. (2003): Modulation of coxsackie-adenovirus receptor expression for increased adenoviral transgene expression, *Cancer Res.* 63, (4): 847-853.

Hirabayashi, S.; Tajima, M.; Yao, I.; Nishimura, W.; Mori, H. and Hata, Y. (2003): JAM4, a junctional cell adhesion molecule interacting with a tight junction protein, MAGI-1, *Mol.Cell Biol.* 23, (12): 4267-4282.

Hirata, Ki; Ishida, T.; Penta, K.; Rezaee, M.; Yang, E.; Wohlgemuth, J. and Quertermous, T. (2001): Cloning of an immunoglobulin family adhesion molecule selectively expressed by endothelial cells, *J.Biol.Chem.* 276, (19): 16223-16231.

Honda, T.; Saitoh, H.; Masuko, M.; Katagiri-Abe, T.; Tominaga, K.; Kozakai, I.; Kobayashi, K.; Kumanishi, T.; Watanabe, Y. G.; Odani, S. and Kuwano, R. (2000): The coxsackievirus-adenovirus receptor protein as a cell adhesion molecule in the developing mouse brain, *Brain Res.Mol.Brain Res.* 77, (1): 19-28.

Hotta, Y.; Honda, T.; Naito, M. and Kuwano, R. (2003): Developmental distribution of coxsackie virus and adenovirus receptor localized in the nervous system, *Brain Res.Dev.Brain Res.* 143, (1): 1-13.

Hurez, V.; Dzialo-Hatton, R.; Oliver, J.; Matthews, R. J. and Weaver, C. T. (2002): Efficient adenovirus-mediated gene transfer into primary T cells and thymocytes in a new coxsackie/adenovirus receptor transgenic model, *BMC.Immunol.* 3: 4

Ide, N.; Hata, Y.; Nishioka, H.; Hirao, K.; Yao, I.; Deguchi, M.; Mizoguchi, A.; Nishimori, H.; Tokino, T.; Nakamura, Y. and Takai, Y. (1999): Localization of membrane-associated guanylate kinase (MAGI)-1/BAI-associated protein (BAP) 1 at tight junctions of epithelial cells, *Oncogene* 18, (54): 7810-7815.

Ishida, T.; Kundu, R. K.; Yang, E.; Hirata, K.; Ho, Y. D. and Quertermous, T. (2003): Targeted disruption of endothelial cell-selective adhesion molecule inhibits angiogenic processes in vitro and in vivo, *J.Biol.Chem.* 278, (36): 34598-34604.

Ito, M.; Kodama, M.; Masuko, M.; Yamaura, M.; Fuse, K.; Uesugi, Y.; Hirono, S.; Okura, Y.; Kato, K.; Hotta, Y.; Honda, T.; Kuwano, R. and Aizawa, Y. (2000): Expression of coxsackievirus and adenovirus receptor in hearts of rats with experimental autoimmune myocarditis, *Circ.Res.* 86, (3): 275-280.

Itoh, M.; Furuse, M.; Morita, K.; Kubota, K.; Saitou, M. and Tsukita, S. (1999): Direct binding of three tight junction-associated MAGUKs, ZO-1, ZO-2, and ZO-3, with the COOH termini of claudins, *J.Cell Biol.* 147, (6): 1351-1363.

Jeansonne, B.; Lu, Q.; Goodenough, D. A. and Chen, Y. H. (2003): Claudin-8 interacts with multi-PDZ domain protein 1 (MUPP1) and reduces paracellular conductance in epithelial cells, *Cell Mol.Biol.(Noisy.-le-grand)* 49, (1): 13-21.

Jiang, S. and Caffrey, M. (2007): Solution structure of the coxsackievirus and adenovirus receptor domain 2, *Protein Sci.* 16, (3): 539-542.

Jiang, S.; Jacobs, A.; Laue, T. M. and Caffrey, M. (2004): Solution structure of the coxsackievirus and adenovirus receptor domain 1, *Biochemistry* 43, (7): 1847-1853.

Kandolf, R. and Hofschneider, P. H. (1985): Molecular cloning of the genome of a cardiotropic Coxsackie B3 virus: full-length reverse-transcribed recombinant cDNA generates infectious virus in mammalian cells, *Proc.Natl.Acad.Sci.U.S.A.* 82, (14): 4818-4822.

Kanel, K. T.; Wolmark, N. and Thompson, P. D. (1997): Delayed severe hypertriglyceridemia from tamoxifen, *N.Engl.J.Med.* 337, (4): 281

Kashimura, T.; Kodama, M.; Hotta, Y.; Hosoya, J.; Yoshida, K.; Ozawa, T.; Watanabe, R.; Okura, Y.; Kato, K.; Hanawa, H.; Kuwano, R. and Aizawa, Y. (2004): Spatiotemporal changes of coxsackievirus and adenovirus receptor in rat hearts during postnatal development and in cultured cardiomyocytes of neonatal rat, *Virchows Arch.* 444, (3): 283-292.

Katoh, M. and Katoh, M. (2003): IGSF11 gene, frequently up-regulated in intestinal-type gastric cancer, encodes adhesion molecule homologous to CXADR, FLJ22415 and ESAM, *Int.J.Oncol.* 23, (2): 525-531.

Kawashima, H.; Ogose, A.; Yoshizawa, T.; Kuwano, R.; Hotta, Y.; Hotta, T.; Hatano, H.; Kawashima, H. and Endo, N. (2003): Expression of the coxsackievirus and adenovirus receptor in musculoskeletal tumors and mesenchymal tissues: efficacy of adenoviral gene therapy for osteosarcoma, *Cancer Sci.* 94, (1): 70-75.

Kim, J. S.; Lee, S. H.; Cho, Y. S.; Choi, J. J.; Kim, Y. H. and Lee, J. H. (2002): Enhancement of the adenoviral sensitivity of human ovarian cancer cells by transient expression of coxsackievirus and adenovirus receptor (CAR), *Gynecol.Oncol.* 85, (2): 260-265.

Kim, M.; Sumerel, L. A.; Belousova, N.; Lyons, G. R.; Carey, D. E.; Krasnykh, V. and Douglas, J. T. (2003): The coxsackievirus and adenovirus receptor acts as a tumour suppressor in malignant glioma cells, *Br.J.Cancer* 88, (9): 1411-1416.

Kimber, W. A.; Trinkle-Mulcahy, L.; Cheung, P. C.; Deak, M.; Marsden, L. J.; Kieloch, A.; Watt, S.; Javier, R. T.; Gray, A.; Downes, C. P.; Lucocq, J. M. and Alessi, D. R. (2002): Evidence that the tandem-pleckstrin-homology-domain-containing protein TAPP1 interacts with Ptd(3,4)P2 and the multi-PDZ-domain-containing protein MUPP1 in vivo, *Biochem.J.* 361, (Pt 3): 525-536.

Kishimoto, C.; Matsumori, A.; Ohmae, M.; Tomioka, N. and Kawai, C. (1984): Electrocardiographic findings in experimental myocarditis in DBA/2 mice: complete atrioventricular block in the acute stage, low voltage of the QRS complex in the subacute stage and arrhythmias in the chronic stage, *J.Am.Coll.Cardiol.* 3, (6): 1461-1468.

Kitazono, M.; Goldsmith, M. E.; Aikou, T.; Bates, S. and Fojo, T. (2001): Enhanced adenovirus transgene expression in malignant cells treated with the histone deacetylase inhibitor FR901228, *Cancer Res.* 61, (17): 6328-6330.

Klingel, K.; Hohenadl, C.; Canu, A.; Albrecht, M.; Seemann, M.; Mall, G. and Kandolf, R. (1992): Ongoing enterovirus-induced myocarditis is associated with persistent heart muscle infection: quantitative analysis of virus replication, tissue damage, and inflammation, *Proc.Natl.Acad.Sci.U.S.A.* 89, (1): 314-318.

Klingel, K.; Stephan, S.; Sauter, M.; Zell, R.; McManus, B. M.; Bultmann, B. and Kandolf, R. (1996): Pathogenesis of murine enterovirus myocarditis: virus dissemination and immune cell targets, *J.Virol.* 70, (12): 8888-8895.

Klinger, J. R.; Warburton, R. R.; Pietras, L. A.; Smithies, O.; Swift, R. and Hill, N. S. (1999): Genetic disruption of atrial natriuretic peptide causes pulmonary hypertension in normoxic and hypoxic mice, *Am.J.Physiol* 276, (5 Pt 1): L868-L874.

Knaapen, M. W.; Davies, M. J.; De, Bie M.; Haven, A. J.; Martinet, W. and Kockx, M. M. (2001): Apoptotic versus autophagic cell death in heart failure, *Cardiovasc.Res.* 51, (2): 304-312.

Korn, W. M.; Macal, M.; Christian, C.; Lacher, M. D.; McMillan, A.; Rauen, K. A.; Warren, R. S. and Ferrell, L. (2006): Expression of the coxsackievirus- and adenovirus receptor in gastrointestinal cancer correlates with tumor differentiation, *Cancer Gene Ther.* 13, (8): 792-797.

Kostrewa, D.; Brockhaus, M.; D'Arcy, A.; Dale, G. E.; Nelboeck, P.; Schmid, G.; Mueller, F.; Bazzoni, G.; Dejana, E.; Bartfai, T.; Winkler, F. K. and Hennig, M. (2001): X-ray structure of

junctional adhesion molecule: structural basis for homophilic adhesion via a novel dimerization motif, *EMBO J.* 20, (16): 4391-4398.

Kozyraki, R.; Fyfe, J.; Kristiansen, M.; Gerdes, C.; Jacobsen, C.; Cui, S.; Christensen, E. I.; Aminoff, M.; de la, Chapelle A.; Krahe, R.; Verroust, P. J. and Moestrup, S. K. (1999): The intrinsic factor-vitamin B12 receptor, cubilin, is a high-affinity apolipoprotein A-I receptor facilitating endocytosis of high-density lipoprotein, *Nat.Med.* 5, (6): 656-661.

Krenz, M.; Gulick, J.; Osinska, H. E.; Colbert, M. C.; Molkentin, J. D. and Robbins, J. (2008): Role of ERK1/2 signaling in congenital valve malformations in Noonan syndrome, *Proc.Natl.Acad.Sci.U.S.A* 105, (48): 18930-18935.

Kuhbandner, S.; Brummer, S.; Metzger, D.; Chambon, P.; Hofmann, F. and Feil, R. (2000): Temporally controlled somatic mutagenesis in smooth muscle, *Genesis.* 28, (1): 15-22.

Li, F.; Wang, X.; Capasso, J. M. and Gerdes, A. M. (1996): Rapid transition of cardiac myocytes from hyperplasia to hypertrophy during postnatal development, *J.Mol.Cell Cardiol.* 28, (8): 1737-1746.

Li, J.; Patel, V. V.; Kostetskii, I.; Xiong, Y.; Chu, A. F.; Jacobson, J. T.; Yu, C.; Morley, G. E.; Molkentin, J. D. and Radice, G. L. (2005): Cardiac-specific loss of N-cadherin leads to alteration in connexins with conduction slowing and arrhythmogenesis, *Circ.Res.* 97, (5): 474-481.

Li, J.; Patel, V. V. and Radice, G. L. (2006): Dysregulation of cell adhesion proteins and cardiac arrhythmogenesis, *Clin.Med.Res.* 4, (1): 42-52.

Li, Z.; Mericskay, M.; Agbulut, O.; Butler-Browne, G.; Carlsson, L.; Thornell, L. E.; Babinet, C. and Paulin, D. (1997): Desmin is essential for the tensile strength and integrity of myofibrils but not for myogenic commitment, differentiation, and fusion of skeletal muscle, *J.Cell Biol.* 139, (1): 129-144.

Lim, B. K.; Choi, J. H.; Nam, J. H.; Gil, C. O.; Shin, J. O.; Yun, S. H.; Kim, D. K. and Jeon, E. S. (2006): Virus receptor trap neutralizes coxsackievirus in experimental murine viral myocarditis, *Cardiovasc.Res.* 71, (3): 517-526.

Lim, B. K.; Xiong, D.; Dorner, A.; Youn, T. J.; Yung, A.; Liu, T. I.; Gu, Y.; Dalton, N. D.; Wright, A. T.; Evans, S. M.; Chen, J.; Peterson, K. L.; McCulloch, A. D.; Yajima, T. and Knowlton, K. U. (2008): Coxsackievirus and adenovirus receptor (CAR) mediates atrioventricular-node function and connexin 45 localization in the murine heart, *J.Clin.Invest.*

Lisewski, U.; Shi, Y.; Wrackmeyer, U.; Fischer, R.; Chen, C.; Schirdewan, A.; Juttner, R.; Rathjen, F.; Poller, W.; Radke, M. H. and Gotthardt, M. (2008): The tight junction protein CAR regulates cardiac conduction and cell-cell communication, *J.Exp.Med.* 205, (10): 2369-2379.

Liu, Y.; Nusrat, A.; Schnell, F. J.; Reaves, T. A.; Walsh, S.; Pochet, M. and Parkos, C. A. (2000): Human junction adhesion molecule regulates tight junction resealing in epithelia, *J.Cell Sci.* 113 (Pt 13): 2363-2374.

MacLellan, W. R. and Schneider, M. D. (2000): Genetic dissection of cardiac growth control pathways, *Annu.Rev.Physiol* 62: 289-319.

Marcovina, S. M.; Hegele, R. A. and Koschinsky, M. L. (1999): Lipoprotein(a) and coronary heart disease risk, *Curr.Cardiol.Rep.* 1, (2): 105-111.

Marcovina, S. M. and Koschinsky, M. L. (2002): A critical evaluation of the role of Lp(a) in cardiovascular disease: can Lp(a) be useful in risk assessment?, *Semin.Vasc.Med.* 2, (3): 335-344.

Mays, T. A.; Binkley, P. F.; Lesinski, A.; Doshi, A. A.; Quaile, M. P.; Margulies, K. B.; Janssen, P. M. and Rafael-Fortney, J. A. (2008): Claudin-5 levels are reduced in human end-stage cardiomyopathy, *J.Mol.Cell Cardiol.* 45, (1): 81-87.

Meier, O.; Gastaldelli, M.; Boucke, K.; Hemmi, S. and Greber, U. F. (2005): Early steps of clathrin-mediated endocytosis involved in phagosomal escape of Fcgamma receptor-targeted adenovirus, *J.Virol.* 79, (4): 2604-2613.

Mena, I.; Perry, C. M.; Harkins, S.; Rodriguez, F.; Gebhard, J. and Whitton, J. L. (1999): The role of B lymphocytes in coxsackievirus B3 infection, *Am.J.Pathol.* 155, (4): 1205-1215.

Miller, C. R.; Buchsbaum, D. J.; Reynolds, P. N.; Douglas, J. T.; Gillespie, G. Y.; Mayo, M. S.; Raben, D. and Curiel, D. T. (1998): Differential susceptibility of primary and established human glioma cells to adenovirus infection: targeting via the epidermal growth factor receptor achieves fiber receptor-independent gene transfer, *Cancer Res.* 58, (24): 5738-5748.

Milstone, A. M.; Petrella, J.; Sanchez, M. D.; Mahmud, M.; Whitbeck, J. C. and Bergelson, J. M. (2005): Interaction with coxsackievirus and adenovirus receptor, but not with decay-accelerating factor (DAF), induces A-particle formation in a DAF-binding coxsackievirus B3 isolate, *J.Virol.* 79, (1): 655-660.

Mino, A.; Ohtsuka, T.; Inoue, E. and Takai, Y. (2000): Membrane-associated guanylate kinase with inverted orientation (MAGI)-1/brain angiogenesis inhibitor 1-associated protein (BAP1) as a

scaffolding molecule for Rap small G protein GDP/GTP exchange protein at tight junctions, *Genes Cells* 5, (12): 1009-1016.

Mizuguchi, H.; Koizumi, N.; Hosono, T.; Ishii-Watabe, A.; Uchida, E.; Utoguchi, N.; Watanabe, Y. and Hayakawa, T. (2002): CAR- or alphav integrin-binding ablated adenovirus vectors, but not fiber-modified vectors containing RGD peptide, do not change the systemic gene transfer properties in mice, *Gene Ther.* 9, (12): 769-776.

Morita, K.; Furuse, M.; Fujimoto, K. and Tsukita, S. (1999): Claudin multigene family encoding four-transmembrane domain protein components of tight junction strands, *Proc.Natl.Acad.Sci.U.S.A* 96, (2): 511-516.

Nagasawa, K.; Chiba, H.; Fujita, H.; Kojima, T.; Saito, T.; Endo, T. and Sawada, N. (2006): Possible involvement of gap junctions in the barrier function of tight junctions of brain and lung endothelial cells, *J.Cell.Physiol.* 208, (1): 123-132.

Nalbantoglu, J.; Larochelle, N.; Wolf, E.; Karpati, G.; Lochmuller, H. and Holland, P. C. (2001): Muscle-specific overexpression of the adenovirus primary receptor CAR overcomes low efficiency of gene transfer to mature skeletal muscle, *J.Virol.* 75, (9): 4276-4282.

Nalbantoglu, J.; Pari, G.; Karpati, G. and Holland, P. C. (1999): Expression of the primary coxsackie and adenovirus receptor is downregulated during skeletal muscle maturation and limits the efficacy of adenovirus-mediated gene delivery to muscle cells, *Hum.Gene Ther.* 10, (6): 1009-1019.

Nikolski, V. P.; Jones, S. A.; Lancaster, M. K.; Boyett, M. R. and Efimov, I. R. (2003): Cx43 and dual-pathway electrophysiology of the atrioventricular node and atrioventricular nodal reentry, *Circ.Res.* 92, (4): 469-475.

Nishii, K.; Kumai, M.; Egashira, K.; Miwa, T.; Hashizume, K.; Miyano, Y. and Shibata, Y. (2003): Mice lacking connexin45 conditionally in cardiac myocytes display embryonic lethality similar to that of germline knockout mice without endocardial cushion defect, *Cell Commun.Adhes.* 10, (4-6): 365-369.

Noutsias, M.; Fechner, H.; de Jonge, H.; Wang, X.; Dekkers, D.; Houtsmuller, A. B.; Pauschinger, M.; Bergelson, J.; Warraich, R.; Yacoub, M.; Hetzer, R.; Lamers, J.; Schultheiss, H. P. and Poller, W. (2001): Human coxsackie-adenovirus receptor is colocalized with integrins alpha(v)beta(3) and alpha(v)beta(5) on the cardiomyocyte sarcolemma and upregulated in dilated cardiomyopathy: implications for cardiotropic viral infections, *Circulation* 104, (3): 275-280.

Okegawa, T.; Li, Y.; Pong, R. C.; Bergelson, J. M.; Zhou, J. and Hsieh, J. T. (2000): The dual impact of coxsackie and adenovirus receptor expression on human prostate cancer gene therapy, *Cancer Res.* 60, (18): 5031-5036.

Okegawa, T.; Pong, R. C.; Li, Y.; Bergelson, J. M.; Sagalowsky, A. I. and Hsieh, J. T. (2001): The mechanism of the growth-inhibitory effect of coxsackie and adenovirus receptor (CAR) on human bladder cancer: a functional analysis of car protein structure, *Cancer Res.* 61, (17): 6592-6600.

Olson, E. N. and Srivastava, D. (1996): Molecular pathways controlling heart development, *Science* 272, (5262): 671-676.

Oxford, E. M.; Musa, H.; Maass, K.; Coombs, W.; Taffet, S. M. and Delmar, M. (2007): Connexin43 remodeling caused by inhibition of plakophilin-2 expression in cardiac cells, *Circ.Res.* 101, (7): 703-711.

Patrie, K. M.; Drescher, A. J.; Welihinda, A.; Mundel, P. and Margolis, B. (2002): Interaction of two actin-binding proteins, synaptopodin and alpha-actinin-4, with the tight junction protein MAGI-1, *J.Biol.Chem.* 277, (33): 30183-30190.

Pearson, A. S.; Koch, P. E.; Atkinson, N.; Xiong, M.; Finberg, R. W.; Roth, J. A. and Fang, B. (1999): Factors limiting adenovirus-mediated gene transfer into human lung and pancreatic cancer cell lines, *Clin.Cancer Res.* 5, (12): 4208-4213.

Pellegrino, M.; Furmaniak-Kazmierczak, E.; LeBlanc, J. C.; Cho, T.; Cao, K.; Marcovina, S. M.; Boffa, M. B.; Cote, G. P. and Koschinsky, M. L. (2004): The apolipoprotein(a) component of lipoprotein(a) stimulates actin stress fiber formation and loss of cell-cell contact in cultured endothelial cells, *J.Biol.Chem.* 279, (8): 6526-6533.

Peng, J.; Raddatz, K.; Molkentin, J. D.; Wu, Y.; Labeit, S.; Granzier, H. and Gotthardt, M. (2007): Cardiac hypertrophy and reduced contractility in hearts deficient in the titin kinase region, *Circulation* 115, (6): 743-751.

Perriard, J. C.; Hirschy, A. and Ehler, E. (2003): Dilated cardiomyopathy: a disease of the intercalated disc?, *Trends Cardiovasc.Med.* 13, (1): 30-38.

Person, A. D.; Garriock, R. J.; Krieg, P. A.; Runyan, R. B. and Klewer, S. E. (2005): Frzb modulates Wnt-9a-mediated beta-catenin signaling during avian atrioventricular cardiac cushion development, *Dev.Biol.* 278, (1): 35-48.

Peters, N. S. (2006): Gap junctions: clarifying the complexities of connexins and conduction, *Circ.Res.* 99, (11): 1156-1158.

Petrella, J.; Cohen, C. J.; Gaetz, J. and Bergelson, J. M. (2002): A zebrafish coxsackievirus and adenovirus receptor homologue interacts with coxsackie B virus and adenovirus, *J.Virol.* 76, (20): 10503-10506.

Pickles, R. J.; Fahrner, J. A.; Petrella, J. M.; Boucher, R. C. and Bergelson, J. M. (2000): Retargeting the coxsackievirus and adenovirus receptor to the apical surface of polarized epithelial cells reveals the glycocalyx as a barrier to adenovirus-mediated gene transfer, *J.Virol.* 74, (13): 6050-6057.

Pong, R. C.; Lai, Y. J.; Chen, H.; Okegawa, T.; Frenkel, E.; Sagalowsky, A. and Hsieh, J. T. (2003): Epigenetic regulation of coxsackie and adenovirus receptor (CAR) gene promoter in urogenital cancer cells, *Cancer Res.* 63, (24): 8680-8686.

Prota, A. E.; Campbell, J. A.; Schelling, P.; Forrest, J. C.; Watson, M. J.; Peters, T. R.; urrand-Lions, M.; Imhof, B. A.; Dermody, T. S. and Stehle, T. (2003): Crystal structure of human junctional adhesion molecule 1: implications for reovirus binding, *Proc.Natl.Acad.Sci.U.S.A* 100, (9): 5366-5371.

Qin, M.; Chen, S.; Yu, T.; Escuadro, B.; Sharma, S. and Batra, R. K. (2003): Coxsackievirus adenovirus receptor expression predicts the efficiency of adenoviral gene transfer into non-small cell lung cancer xenografts, *Clin.Cancer Res.* 9, (13): 4992-4999.

Raschperger, E.; Engstrom, U.; Pettersson, R. F. and Fuxe, J. (2004): CLMP, a novel member of the CTX family and a new component of epithelial tight junctions, *J.Biol.Chem.* 279, (1): 796-804.

Raschperger, E.; Neve, E. P.; Wernerson, A.; Hultenby, K.; Pettersson, R. F. and Majumdar, A. (2008): The coxsackie and adenovirus receptor (CAR) is required for renal epithelial differentiation within the zebrafish pronephros, *Dev.Biol.* 313, (1): 455-464.

Raschperger, E.; Thyberg, J.; Pettersson, S.; Philipson, L.; Fuxe, J. and Pettersson, R. F. (2006): The coxsackie- and adenovirus receptor (CAR) is an in vivo marker for epithelial tight junctions, with a potential role in regulating permeability and tissue homeostasis, *Exp.Cell Res.* 312, (9): 1566-1580.

Rauen, K. A.; Sudilovsky, D.; Le, J. L.; Chew, K. L.; Hann, B.; Weinberg, V.; Schmitt, L. D. and McCormick, F. (2002): Expression of the coxsackie adenovirus receptor in normal prostate and in primary and metastatic prostate carcinoma: potential relevance to gene therapy, *Cancer Res.* 62, (13): 3812-3818.

Ross, S. A.; Song, X.; Burney, M. W.; Kasai, Y. and Orlicky, D. J. (2003): Efficient adenovirus transduction of 3T3-L1 adipocytes stably expressing coxsackie-adenovirus receptor, *Biochem.Biophys.Res.Commun.* 302, (2): 354-358.

Royer, A.; van Veen, T. A.; Le, Bouter S.; Marionneau, C.; Griol-Charhbili, V.; Leoni, A. L.; Steenman, M.; van Rijen, H. V.; Demolombe, S.; Goddard, C. A.; Richer, C.; Escoubet, B.; Jarry-Guichard, T.; Colledge, W. H.; Gros, D.; de Bakker, J. M.; Grace, A. A.; Escande, D. and Charpentier, F. (2005): Mouse model of SCN5A-linked hereditary Lenegre's disease: age-related conduction slowing and myocardial fibrosis, *Circulation* 111, (14): 1738-1746.

Sachs, M. D.; Rauen, K. A.; Ramamurthy, M.; Dodson, J. L.; De Marzo, A. M.; Putzi, M. J.; Schoenberg, M. P. and Rodriguez, R. (2002): Integrin alpha(v) and coxsackie adenovirus receptor expression in clinical bladder cancer, *Urology* 60, (3): 531-536.

Saffitz, J. E. (2005): Dependence of electrical coupling on mechanical coupling in cardiac myocytes: insights gained from cardiomyopathies caused by defects in cell-cell connections, *Ann.N.Y.Acad.Sci.* 1047: 336-344.

Sah, V. P.; Minamisawa, S.; Tam, S. P.; Wu, T. H.; Dorn, G. W.; Ross, J., Jr.; Chien, K. R. and Brown, J. H. (1999): Cardiac-specific overexpression of RhoA results in sinus and atrioventricular nodal dysfunction and contractile failure, *J.Clin.Invest* 103, (12): 1627-1634.

Salomonsson, S.; Sonesson, S. E.; Ottosson, L.; Muhallab, S.; Olsson, T.; Sunnerhagen, M.; Kuchroo, V. K.; Thoren, P.; Herlenius, E. and Wahren-Herlenius, M. (2005): Ro/SSA autoantibodies directly bind cardiomyocytes, disturb calcium homeostasis, and mediate congenital heart block, *J.Exp.Med.* 201, (1): 11-17.

Sanford, J. L.; Edwards, J. D.; Mays, T. A.; Gong, B.; Merriam, A. P. and Rafael-Fortney, J. A. (2005): Claudin-5 localizes to the lateral membranes of cardiomyocytes and is altered in utrophin/dystrophin-deficient cardiomyopathic mice, *J.Mol.Cell Cardiol.* 38, (2): 323-332.

Sasaki, H.; Matsui, C.; Furuse, K.; Mimori-Kiyosue, Y.; Furuse, M. and Tsukita, S. (2003): Dynamic behavior of paired claudin strands within apposing plasma membranes, *Proc.Natl.Acad.Sci.U.S.A* 100, (7): 3971-3976.

Sato, Y.; Osaku, A.; Koyama, S.; Mizukawa, S.; Onikura, S.; Yagi, H.; Suzuki, T.; Sawada, T.; Uchiyama, T.; Kanmatsuse, K. and . (1989): Complete atrioventricular block associated with regional myocardial scarring in a patient with Coxsackie B2 myocarditis, *Jpn.Heart J.* 30, (6): 935-941.

Scanu, A. M. (2003): Lipoprotein(a) and the atherothrombotic process: mechanistic insights and clinical implications, *Curr.Atheroscler.Rep.* 5, (2): 106-113.

Schmidt, M. R.; Piekos, B.; Cabatingan, M. S. and Woodland, R. T. (2000): Expression of a human coxsackie/adenovirus receptor transgene permits adenovirus infection of primary lymphocytes, *J.Immunol.* 165, (7): 4112-4119.

Shafren, D. R.; Bates, R. C.; Agrez, M. V.; Herd, R. L.; Burns, G. F. and Barry, R. D. (1995): Coxsackieviruses B1, B3, and B5 use decay accelerating factor as a receptor for cell attachment, *J.Virol.* 69, (6): 3873-3877.

Shafren, D. R.; Williams, D. T. and Barry, R. D. (1997): A decay-accelerating factor-binding strain of coxsackievirus B3 requires the coxsackievirus-adenovirus receptor protein to mediate lytic infection of rhabdomyosarcoma cells, *J.Virol.* 71, (12): 9844-9848.

Shieh, J. T. and Bergelson, J. M. (2002): Interaction with decay-accelerating factor facilitates coxsackievirus B infection of polarized epithelial cells, *J.Virol.* 76, (18): 9474-9480.

Shiraishi, I.; Simpson, D. G.; Carver, W.; Price, R.; Hirozane, T.; Terracio, L. and Borg, T. K. (1997): Vinculin is an essential component for normal myofibrillar arrangement in fetal mouse cardiac myocytes, *J.Mol.Cell Cardiol.* 29, (8): 2041-2052.

Simon, A. M.; Goodenough, D. A. and Paul, D. L. (1998): Mice lacking connexin40 have cardiac conduction abnormalities characteristic of atrioventricular block and bundle branch block, *Curr.Biol.* 8, (5): 295-298.

Smith, B. T.; Mussell, J. C.; Fleming, P. A.; Barth, J. L.; Spyropoulos, D. D.; Cooley, M. A.; Drake, C. J. and Argraves, W. S. (2006): Targeted disruption of cubilin reveals essential developmental roles in the structure and function of endoderm and in somite formation, *BMC.Dev.Biol.* 6: 30

Sollerbrant, K.; Raschperger, E.; Mirza, M.; Engstrom, U.; Philipson, L.; Ljungdahl, P. O. and Pettersson, R. F. (2003): The Coxsackievirus and adenovirus receptor (CAR) forms a complex with the PDZ domain-containing protein ligand-of-numb protein-X (LNX), *J.Biol.Chem.* 278, (9): 7439-7444.

Staehelin, L. A. (1973): Further observations on the fine structure of freeze-cleaved tight junctions, *J.Cell Sci.* 13, (3): 763-786.

Steendijk, P.; Staal, E.; Jukema, J. W. and Baan, J. (2001): Hypertonic saline method accurately determines parallel conductance for dual-field conductance catheter, *Am.J.Physiol.Heart Circ.Physiol.* 281, (2): H755-H763.

Sugishita, Y.; Watanabe, M. and Fisher, S. A. (2004): Role of myocardial hypoxia in the remodeling of the embryonic avian cardiac outflow tract, *Dev.Biol.* 267, (2): 294-308.

Sun, J. Z.; Chen, S. J.; Li, G. and Chen, Y. F. (2000): Hypoxia reduces atrial natriuretic peptide clearance receptor gene expression in ANP knockout mice, *Am.J.Physiol Lung Cell Mol.Physiol* 279, (3): L511-L519.

Suzu, S.; Hayashi, Y.; Harumi, T.; Nomaguchi, K.; Yamada, M.; Hayasawa, H. and Motoyoshi, K. (2002): Molecular cloning of a novel immunoglobulin superfamily gene preferentially expressed by brain and testis, *Biochem.Biophys.Res.Commun.* 296, (5): 1215-1221.

Tallone, T.; Malin, S.; Samuelsson, A.; Wilbertz, J.; Miyahara, M.; Okamoto, K.; Poellinger, L.; Philipson, L. and Pettersson, S. (2001): A mouse model for adenovirus gene delivery, *Proc.Natl.Acad.Sci.U.S.A* 98, (14): 7910-7915.

Tamanini, A.; Nicolis, E.; Bonizzato, A.; Bezzerri, V.; Melotti, P.; Assael, B. M. and Cabrini, G. (2006): Interaction of adenovirus type 5 fiber with the coxsackievirus and adenovirus receptor activates inflammatory response in human respiratory cells, *J.Virol.* 80, (22): 11241-11254.

Thoelen, I.; Keyaerts, E.; Lindberg, M. and Van, Ranst M. (2001a): Characterization of a cDNA encoding the bovine coxsackie and adenovirus receptor, *Biochem.Biophys.Res.Commun.* 288, (4): 805-808.

Thoelen, I.; Magnusson, C.; Tagerud, S.; Polacek, C.; Lindberg, M. and Van Ranst, M. (2001b): Identification of alternative splice products encoded by the human coxsackie-adenovirus receptor gene, *Biochem.Biophys.Res.Commun.* 287, (1): 216-222.

Tomko, R. P.; Johansson, C. B.; Totrov, M.; Abagyan, R.; Frisen, J. and Philipson, L. (2000): Expression of the adenovirus receptor and its interaction with the fiber knob, *Exp.Cell Res.* 255, (1): 47-55.

Tomko, R. P.; Xu, R. and Philipson, L. (1997): HCAR and MCAR: the human and mouse cellular receptors for subgroup C adenoviruses and group B coxsackieviruses, *Proc.Natl.Acad.Sci.U.S.A.* 94, (7): 3352-3356.

Toshimori, H.; Toshimori, K.; Oura, C. and Matsuo, H. (1987): Immunohistochemical study of atrial natriuretic polypeptides in the embryonic, fetal and neonatal rat heart, *Cell Tissue Res.* 248, (3): 627-633.

Toyofuku, T.; Yabuki, M.; Otsu, K.; Kuzuya, T.; Hori, M. and Tada, M. (1998): Direct association of the gap junction protein connexin-43 with ZO-1 in cardiac myocytes, *J.Biol.Chem.* 273, (21): 12725-12731.

Tracy, S.; Hofling, K.; Pirruccello, S.; Lane, P. H.; Reyna, S. M. and Gauntt, C. J. (2000): Group B coxsackievirus myocarditis and pancreatitis: connection between viral virulence phenotypes in mice, *J.Med.Virol.* 62, (1): 70-81.

van der Merwe, P. A. and Barclay, A. N. (1994): Transient intercellular adhesion: the importance of weak protein-protein interactions, *Trends Biochem.Sci.* 19, (9): 354-358.

van der Merwe, P. A.; Barclay, A. N.; Mason, D. W.; Davies, E. A.; Morgan, B. P.; Tone, M.; Krishnam, A. K.; Ianelli, C. and Davis, S. J. (1994): Human cell-adhesion molecule CD2 binds CD58 (LFA-3) with a very low affinity and an extremely fast dissociation rate but does not bind CD48 or CD59, *Biochemistry* 33, (33): 10149-10160.

van Raaij, M. J.; Chouin, E.; van der, Zandt H.; Bergelson, J. M. and Cusack, S. (2000): Dimeric structure of the coxsackievirus and adenovirus receptor D1 domain at 1.7 A resolution, *Structure.* 8, (11): 1147-1155.

van't Hof, W. and Crystal, R. G. (2002): Fatty acid modification of the coxsackievirus and adenovirus receptor, *J.Virol.* 76, (12): 6382-6386.

Vincent, T.; Pettersson, R. F.; Crystal, R. G. and Leopold, P. L. (2004): Cytokine-mediated down-regulation of coxsackievirus-adenovirus receptor in endothelial cells, *J.Virol.* 78, (15): 8047-8058.

Walters, R. W.; Freimuth, P.; Moninger, T. O.; Ganske, I.; Zabner, J. and Welsh, M. J. (2002): Adenovirus fiber disrupts CAR-mediated intercellular adhesion allowing virus escape, *Cell* 110, (6): 789-799.

Walters, R. W.; van't, Hof W.; Yi, S. M.; Schroth, M. K.; Zabner, J.; Crystal, R. G. and Welsh, M. J. (2001): Apical localization of the coxsackie-adenovirus receptor by glycosyl-phosphatidylinositol modification is sufficient for adenovirus-mediated gene transfer through the apical surface of human airway epithelia, *J.Virol.* 75, (16): 7703-7711.

Wan, Y. Y.; Leon, R. P.; Marks, R.; Cham, C. M.; Schaack, J.; Gajewski, T. F. and DeGregori, J. (2000): Transgenic expression of the coxsackie/adenovirus receptor enables adenoviral-mediated gene delivery in naive T cells, *Proc.Natl.Acad.Sci.U.S.A* 97, (25): 13784-13789.

Wang, X. and Bergelson, J. M. (1999): Coxsackievirus and adenovirus receptor cytoplasmic and transmembrane domains are not essential for coxsackievirus and adenovirus infection, *J.Virol.* 73, (3): 2559-2562.

Wang, Y.; Wang, S.; Bao, Y.; Ni, C.; Guan, N.; Zhao, J.; Salford, L. G.; Widegren, B. and Fan, X. (2006): Coxsackievirus and adenovirus receptor expression in non-malignant lung tissues and clinical lung cancers, *J.Mol.Histol.* 37, (3-4): 153-160.

Welt, S.; Ritter, G.; Williams, C., Jr.; Cohen, L. S.; John, M.; Jungbluth, A.; Richards, E. A.; Old, L. J. and Kemeny, N. E. (2003): Phase I study of anticolon cancer humanized antibody A33, *Clin.Cancer Res.* 9, (4): 1338-1346.

Wessely, R.; Klingel, K.; Knowlton, K. U. and Kandolf, R. (2001): Cardioselective infection with coxsackievirus B3 requires intact type I interferon signaling: implications for mortality and early viral replication, *Circulation* 103, (5): 756-761.

Westermann, D.; Rutschow, S.; Jager, S.; Linderer, A.; Anker, S.; Riad, A.; Unger, T.; Schultheiss, H. P.; Pauschinger, M. and Tschope, C. (2007): Contributions of inflammation and cardiac matrix metalloproteinase activity to cardiac failure in diabetic cardiomyopathy: the role of angiotensin type 1 receptor antagonism, *Diabetes* 56, (3): 641-646.

Wickham, T. J.; Mathias, P.; Cheresh, D. A. and Nemerow, G. R. (1993): Integrins alpha v beta 3 and alpha v beta 5 promote adenovirus internalization but not virus attachment, *Cell* 73, (2): 309-319.

Wilhelm, M.; Kirste, W.; Kuly, S.; Amann, K.; Neuhuber, W.; Weyand, M.; Daniel, W. G. and Garlichs, C. (2006): Atrial distribution of connexin 40 and 43 in patients with intermittent, persistent, and postoperative atrial fibrillation, *Heart Lung Circ.* 15, (1): 30-37.

Xie, Y.; Zhao, W.; Wang, W.; Zhao, S.; Tang, R.; Ying, K.; Zhou, Z. and Mao, Y. (2001): Identification of a human LNX protein containing multiple PDZ domains, *Biochem.Genet.* 39, (3-4): 117-126.

Xu, R. and Crowell, R. L. (1996): Expression and distribution of the receptors for coxsackievirus B3 during fetal development of the Balb/c mouse and of their brain cells in culture, *Virus Res.* 46, (1-2): 157-170.

Yanagawa, B.; Spiller, O. B.; Proctor, D. G.; Choy, J.; Luo, H.; Zhang, H. M.; Suarez, A.; Yang, D. and McManus, B. M. (2004): Soluble recombinant coxsackievirus and adenovirus receptor abrogates coxsackievirus b3-mediated pancreatitis and myocarditis in mice, *J.Infect.Dis.* 189, (8): 1431-1439.

Zhang, N. H.; Song, L. B.; Wu, X. J.; Li, R. P.; Zeng, M. S.; Zhu, X. F.; Wan, D. S.; Liu, Q.; Zeng, Y. X. and Zhang, X. S. (2008): Proteasome inhibitor MG-132 modifies coxsackie and adenovirus receptor expression in colon cancer cell line lovo, *Cell Cycle* 7, (7): 925-933.

Appendix

Tables of regulated genes in microarray:

Table 12: List of upregulated genes in microarray (KO vs. WT)

symbol	ko_wt_fc	title	function
Ambp	++++	alpha 1 microglobulin/bikunin	transport, endopeptidase inhibitor activity
Fgb	++++	fibrinogen, B beta polypeptide	blood coagulation
Apob	++++	apolipoprotein B	lipid metabolism
Apoa1	++++	apolipoprotein A-I	lipid metabolism
Lum	++++	lumican	unknown
Afp	+++	alpha fetoprotein	ovulation, transport
Slc2a2	+++	solute carrier family 2 (facilitated glucose transporter), member 2	carbohydrate transport
Fgg	+++	fibrinogen, gamma polypeptide	signal transduction
Ttr	+++	transthyretin	thyroid hormone generation, transport
Apom	+++	apolipoprotein M	lipid transporter activity
Postn	+++	periostin, osteoblast specific factor	extracellular matrix organization and biogenesis, cell adhesion
Cubn	+++	cubilin (intrinsic factor-cobalamin receptor)	lipid metabolism, receptor mediated endocytosis
Cdh1	+++	cadherin 1	cell-cell adhesion, protein metabolism
Tmprss2	+++	transmembrane protease, serine 2	serine-type endopeptidase activity
Dkk2	++	dickkopf homolog 2 (Xenopus laevis)	Wnt receptor signaling pathway, development
Paip1	++	polyadenylate binding protein-interacting protein 1	regulation of protein biosynthesis and translation
Lasp1	++	LIM and SH3 protein 1	ion transport, protein binding
Smoc2	++	SPARC related modular calcium binding 2	calcium ion binding
Apoc2	++	apolipoprotein C-II	lipid metabolism
Aldh1a7	+	aldehyde dehydrogenase family 1, subfamily A7	metabolism
Col1a2	+	procollagen, type I, alpha 2	transmembrane receptor protein tyrosine kinase signaling pathway

Table 13: List of downregulated genes in microarray (KO vs. WT)

symbol	ko_wt_fc	title	function
Cxadr	-----	coxsackievirus and adenovirus receptor	heart development, protein binding
Fos	----	FBJ osteosarcoma oncogene	regulation of transcription, DNA-dependent
Egr1	----	early growth response 1	regulation of transcription, DNA-dependent
Ttyh3	----	tweety homolog 3 (Drosophila)	chloride channel activity
Rpo1-4	----	RNA polymerase 1-4	protein binding, transcription
Add3	----	adducin 3 (gamma)	structural molecule activity, calmodulin binding
Mrap	----	melanocortin 2 receptor accessory protein	membrane protein
Rgl1	---	Ral guanine nucleotide dissocia-tion stimulator,-like 1	small GTPase mediated signal transduction
Ly6a	---	lymphocyte antigen 6 complex, locus A	GPI anchor binding
Abcb10	---	ATP-binding cassette, sub-family B (MDR/TAP), member 10	Transport, ATPase activity
Rbm38	---	RNA binding motif protein 38	nucleotide binding
Eraf	---	erythroid associated factor	protein folding, erythrocyte differentiation, hemoglobin metabolism
Il6st	---	interleukin 6 signal transducer	regulation of Notch signaling pathway
Bcl2	--	B-cell leukemia/lymphoma 2	anti-apoptosis
Amph	--	amphiphysin	learning, synaptic vesicle en-docytosis
Tbc1d4	--	TBC1 domain family, member 4	intracellular signaling cascade
Tmem153	--	transmembrane protein 153	unknown
Kcnn4	-	potassium intermediate/small conductance calcium-activated channel, subfamily N, member 4	positive regulation of protein secretion
Slc4a1	-	solute carrier family 4, member 1	anion exchanger
Gja1 (Cx43)	-	gap junction membrane channel protein alpha 1	Gap junction, cell-cell signaling
Socs3	-	suppressor of cytokine signaling 3	regulation of protein amino acid phosphorylation

Table of comparison of all available CAR knockout animal models

Table 14: Comparison of CAR loss of function mutants

	Asher 06/2005	**Dorner** 08/2005	**Chen** 03/2006	**Chen** 03/2006	**Chen** 03/2006	**Lim** 08/2008	**Lim** 08/2008	**Li-sewski** 09/2008	**Li-sewski** 09/2008	**Chen** This thesis
Animal Model	KO	KO	KO	cardiac KO	cardiac KO	KO	cardiac KO	cardiac KO	induci-ble card. KO	KO induci-ble card. KO
Exon	Exon 2	Exon 1[1]	Exon 2	Exon 2	Exon 2	Exon 2	Exon 2	Exon 1	Exon 1	Exon 1
Constitutive	+	+	+[2]			+[3]				+
Conditional				TNTcre	MHC cre		MHC cre	MHC cre		
Inducible									MCM	MCM
Phenotype										
Lethality	E11.5-14.5[4]	E11.5-13.5	E11.5-12.5	Before w4	Embryo 80%	E11.5-12.5	no increase	E11.5-12.5	no increase	E10.5-11.5 neonatal 40%
Ventr. Wall	<	>	>	>	>=	=	=	n.d.	=	>
Apoptosis	+	-	n.d.	n.d.	n.d.	-	-	n.d.	n.d.	n.d.
Fibrosis	n.d.	n.d.	n.d.	n.d.	n.d.	n.d.	+	-	-	-
AV-block	n.d.	n.d.	n.d.	n.d.	n.d.	+	+	n.d.	+	+
Sinus node	n.d.	n.d.	n.d.	n.d.	n.d.	n.d.	n.d.	n.d.	+	-
Car-Function										
Cell Contacts	n.d.	-	+	n.d.	n.d.	n.d.	+	n.d.	+	+
Myofilament	n.d.	+	+	n.d.	n.d.	n.d.	-	n.d.	-	+
Compartment	n.d.	-	n.d.	n.d.	n.d.	n.d.	n.d.	+	+	+
Remodeling	+	-	n.d.	n.d.	n.d.	n.d.	+	n.d.	n.d.	n.d.
Electrophysiol	n.d.	n.d.	n.d.	n.d.	n.d.	+	+	n.d.	+	+
Reference	(Asher et al., 2005b)	(Dorner et al., 2005)	(Chen et al., 2006)	(Chen et al., 2006)	(Chen et al., 2006)	(Lim et al., 2008)	(Lim et al., 2008)	(Li-sewski et al., 2008)	(Li-sewski et al., 2008)	

KO knockout, *w* week, *E* embryonic day, *n.d.* not described; < decreased; > increased; >= slightly increased; = unchanged; + yes; - no

[1] from ATG

[2] converted with Protamine-Cre (PRMcre)

[3] □-gal knock-in

[4] some animals survive to term

Abbreviations

2-D electrophoresis	two-dimensional gel electrophoresis
ANP	atrial natriuretic peptide
AV	atrioventricular
AVB	AV conduction block
B.W.	body weight
BDM	2, 3- butanedione monoxime
ß-ME	ß-mercaptoethanol
BNP	brain natriuretic peptide
bp	base pair
BSA	bovine serum albumin
CAR	Coxsackievirus-Adenovirus-Receptor
cDNA	complementary DNA
CHAPS	3-[(3-Cholamidopropyl)-dimethylammonio]-1-propanesulfonate
CIP	calf intestinal alkaline phosphatase
Cre	causes recombination
C-terminus	carboxy terminus
CVB3	coxsackievirus B3
Cx	connexin
DAF	decay-accelerating factor
DEPC	diethylpyrocarbonate
DIG	digoxigenin
DMEM	Dulbecco's modified Eagle Medium
DNA	deoxyribonucleic acid
DNase	deoxyribonuclease
dNTP	2'-deoxy nucleoside-5'-triphosphate
dP/dt_{max}	the maximum rate of ventricular pressure increase
dP/dt_{min}	the minimum rate of ventricular pressure drop
dpc	dias post coitus
DTT	dithiothreitol
ECG	electrocardiogram
ECL	enhanced chemiluminescence
EDTA	ethylene-diamine-tetraacetic acid
EF	ejection fraction
ES	Embryonic stemcell
FA	formamide
FBS	fetal bovine serum
FCS	fetal calf serum
H&E	hematoxylin and eosin
H_2O_2	hydrogen peroxide
HRP	horse radish peroxidase
HV	his-ventricle
IFN-α	interferon alpha
IFN-β	interferon beta
IFN-γ	interferon gamma
IgG	immunoglobulin G
IL-6	interleukin-6
IL-10	interleukin-10
kb	kilobase
kDa	kilo Dalton
KO	knockout
LCK	lymphocyte protein tyrosine kinase
MCM	MerCreMer transgenics
mRNA	messenger-RNA

NBT	nitroblue-tetrazolium salt
NEAA	None-essential amino acids
NP-40	Nonidet P-40 Substitute, Nonylphenyl-polyethylene glycol
N-terminus	amino terminus
o/n	overnight
OD	optical density
PAGE	polyacrylamide gel electrophoresis
PBS	phosphate buffered saline
PCR	polymerase chain reaction
PFA	paraformaldehyde
pfu	plaque-forming unit
pI	isoelectric point
pIpC	polyinosinic-polycytidylic ribonucleic acid
P_{max}	maximum P-wave duration
P_{min}	minimum P-wave duration
PMSF	phenylmethanesulfonyl fluoride
P/S	Penicillin/Streptomycin
RNA	ribonucleic acid
RNase	ribonuclease
rpm	rotations per minute
RT	room temperature
SDS	sodium-dodecylsulfate
TAE	tris-acetate-EDTA
Tam	Tamoxifen
Taq	thermus aquaticus
TBS	tris buffered saline
TE	tris-EDTA-buffer
TEMED	N, N, N`, N´-Tetramethylethylendiamin
TNFα	Tumor necrosis factor-alpha
Tris	tris(hydroxymethyl)-aminomethane
Triton X-100	polyethylene glycol octylphenol ether
U	unit
UTP	uridine triphosphate
V	volt
VP1	major capsid protein
WT	wildtype
ZO-1	zonula occludens-1

List of tables

List of figures

Acknowledgements

Life is a long journey, and this thesis should be a milestone of the end of pursuing a PhD degree and a new start point of my future life. I am lucky enough that in every period of my life journey, I am not always travelling alone. There are many people helped me made the journey much easier and I would like to unreservedly express my immense gratitude to them.

First, I have to appreciate my supervisor Prof. Dr. Michael Gotthardt deeply. He not only gave me the opportunity to work on this project, but also offered a very good working condition and freedom to do the research. He helped me to establish scientific thinking and encouraged my pursuit of truth, which are precious for my future career.

I am grateful to the help of the whole "Gotthardt-lab" members and their kindness and friendship. Especially to Dr. Yu Shi, who guided me and introduced me into this project, from whom I gained a lot of animal experiences and embryonic stem cell culture and differentiation techniques. I can discuss the very detailed problems with him about the project. I thank to Beate Goldbrich and Sandra Bundschuh for expert technical assistance, Mandy Terne, Carolin Schmidt and Melannie Manzke for part of DNA preparation and PCR genotyping. Dr. Michael Radke generated CAR knockout targeting vectors and I learned adult mouse cardiomyocytes isolation from him. Dr. Steffi Weinert taught me the embryo preparation. To the others that I did not mention your name, we together are real "Gottles" team, thank you for the pleasant atmosphere and frequent discussions towards the technical details.

This is a very well cooperated project. Without the cooperation of those partners, some critical data could not be achieved. I am extremely grateful to the support of Prof. Dr. Karin Klingel and Dr. Martina Sauter for the CVB3 infection and *in situ* hybridization. I

thank Dr. Rene Jüttner for his support with the dye coupling experiment. I would also like to acknowledge Dr. Dirk Westermann for the hemodynamic measurements and Dr. Robert Fischer for the surface ECG studies gratefully.

I have to express heartfelt gratitude to my doctor father Prof. Dr. Harald Saumweber and the PhD committee members Prof. Dr. Fritz Rathjen, Dr. Armin Rehm and Prof. Dr. Bernd Dörken for their most valuable suggestions.

I am also very grateful to Ms Sylvia Sibilak, Ms Verona Kuhle, Ms Brunhilde Poppe and Ms Sylvia Olbrich for their help in dealing with public relations and my daily life.

As a member of the International PhD Program “Molecular Cell Biology”, I thank Max-Delbrück-Center for Molecular Medicine for financial support and equipment support.

When I meet any obstacles either in research or in daily life, so many good friends are always available and ready to help and encouraged me, regardless where they are. I am indebted to them. You are the ones that I can also share joys with, and you will never let me down!

Last but not least, I will address my deepest appreciation to my parents. I do not know how to thank them. They are my oldest and longest friends who never asked for return. Because of their guidance, tolerances, patience, supports and understandings, I have grown up and become who I am now. My heart is full of endless gratitude to them and I hope I can make them proud.

Publikationsliste

1. Shi Y*, **Chen C***, Lisewski U, Wrackmeyer U, Radke M, Westermann D, Sauter M, Tschöpe C, Poller W, Klingel K, Gotthardt M. Cardiac deletion of the coxsackievirus- adenovirus-receptor abolishes coxsackievirus B3 infection and prevents myocarditis in vivo. *J Am Coll Cardiol.*, 2009. 53(14): 1219-26 *contribute equally
2. Lisewski U, Shi Y, Wrackmeyer U, Fischer R, **Chen C**, Schirdewan A, Jüttner R, Rathjen F, Poller W, Radke MH, Gotthardt M. The tight junction protein CAR regulates cardiac conduction and cell-cell communication. *J Exp Med.*, 2008. 205(10):2369-79.
3. **Chen C***, Wang H*, Song X, Chen J, Zhen Y, Sun K, Hui R. Mef2c is an essential regulatory element required for unique expression of the cardiac-specific CARK gene. *J Cell Mol Med.*, 2008. 12(1):304-15. *contribute equally
4. Chen J, Han Y, Lin C, Zhen Y, Song X, Teng S, **Chen C**, Chen Y, Zhang Y, Hui R. PDGF-D contributes to neointimal hyperplasia in rat model of vessel injury. *Biochem Biophys Res Commun.*, 2005. 329(3):976-83.
5. **Chen C,** Hui R. The regulatory roles of cardiac specific transcription factors in heart development. *Chin Mol Cardiol.*, 2005. 5(3):561-567
6. Liu Y, Zhen Y**, Chen C**, Hui R. Effect of CARK on NFκB during Cardiac Hypertrophy. *Chin Mol Cardiol.*, 2004. 4(2):89-93.
7. **Chen C**, Genomic bioinformatics—current and future perspectives. *Chin Mol Cardiol.*, 2003. 3(5):286-295.

Eidesstattliche Erklärung

Hiermit erkläre ich, dass ich die vorgelegte Dissertationsschrift mit dem Thema: "Evaluation of the Coxsackievirus and Adenovirus Receptor (CAR) as a therapeutic target in cardiac disease" selbst verfasst und keine anderen als die angegebenen Quellen und Hilfsmittel benutzt habe und ohne die Hilfe Dritter verfasst und auch in Teilen keine Kopien anderer Arbeiten dargestellt habe.

Außerdem erkläre ich hiermit, dass ich mich nicht anderweitig um einen entsprechenden Doktorgrad beworben habe.

Die Promotionsordnung der Mathematisch-Naturwissenschaftlichen Fakultät I der Humboldt-Universität zu Berlin habe ich gelesen und akzeptiert.

Chen Chen

Berlin, März, 2009